Obliquity Variations of Stars and Planets

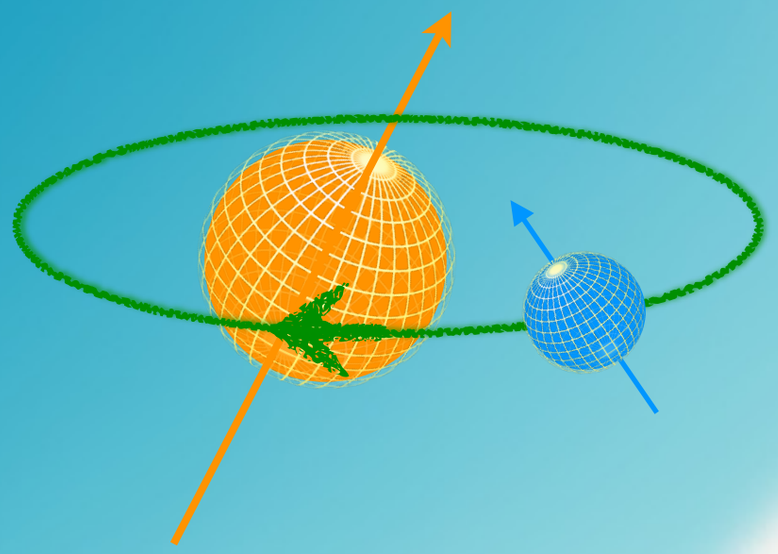

Gongjie Li (Harvard)

Main Collaborators: Avi Loeb (Harvard), Smadar Naoz (UCLA), Konstantin Batygin (Caltech), Josh Winn (Princeton), Matt Holman (Harvard), Bence Kocsis (IAS/Eotvos), Jason Steffen (UNLV)

RESCEU Summer School, 2016

Obliquity Variations of Stars and Planets

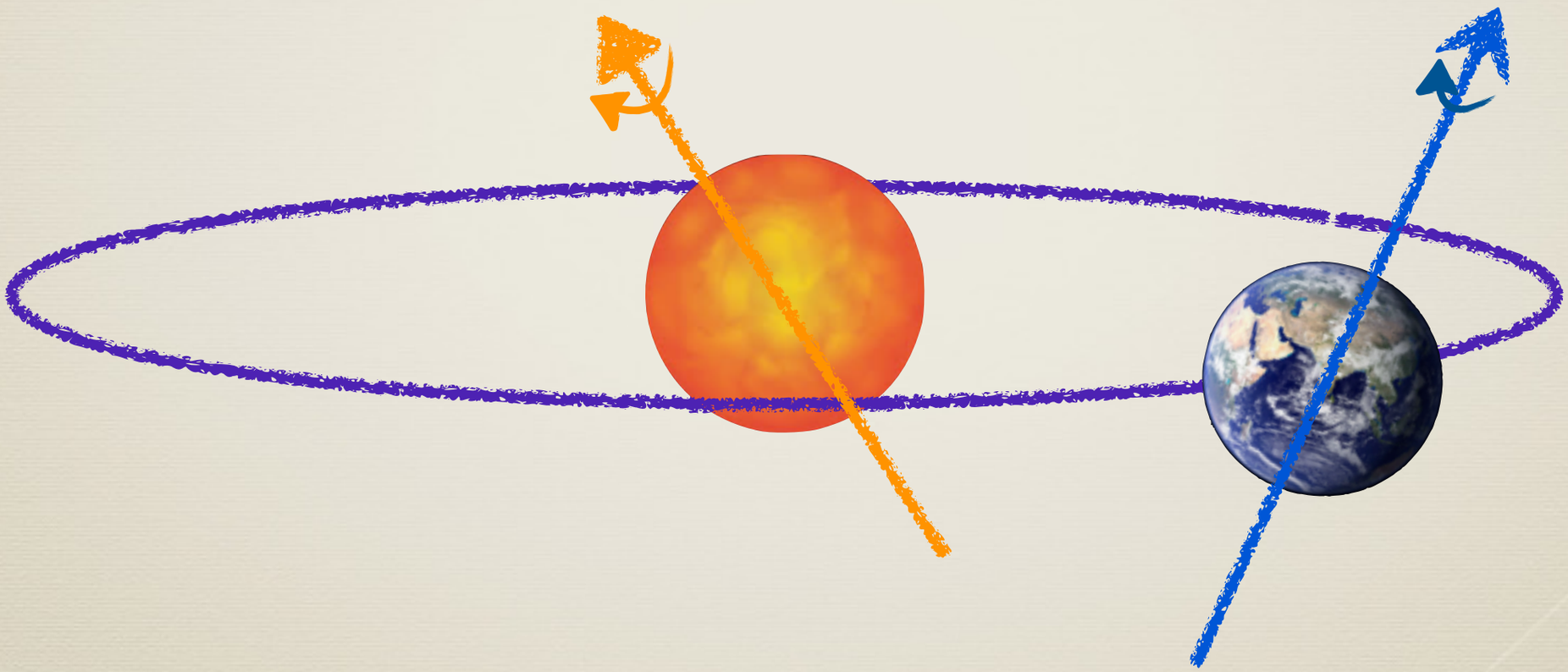

Obliquity Variations of Stars and Planets

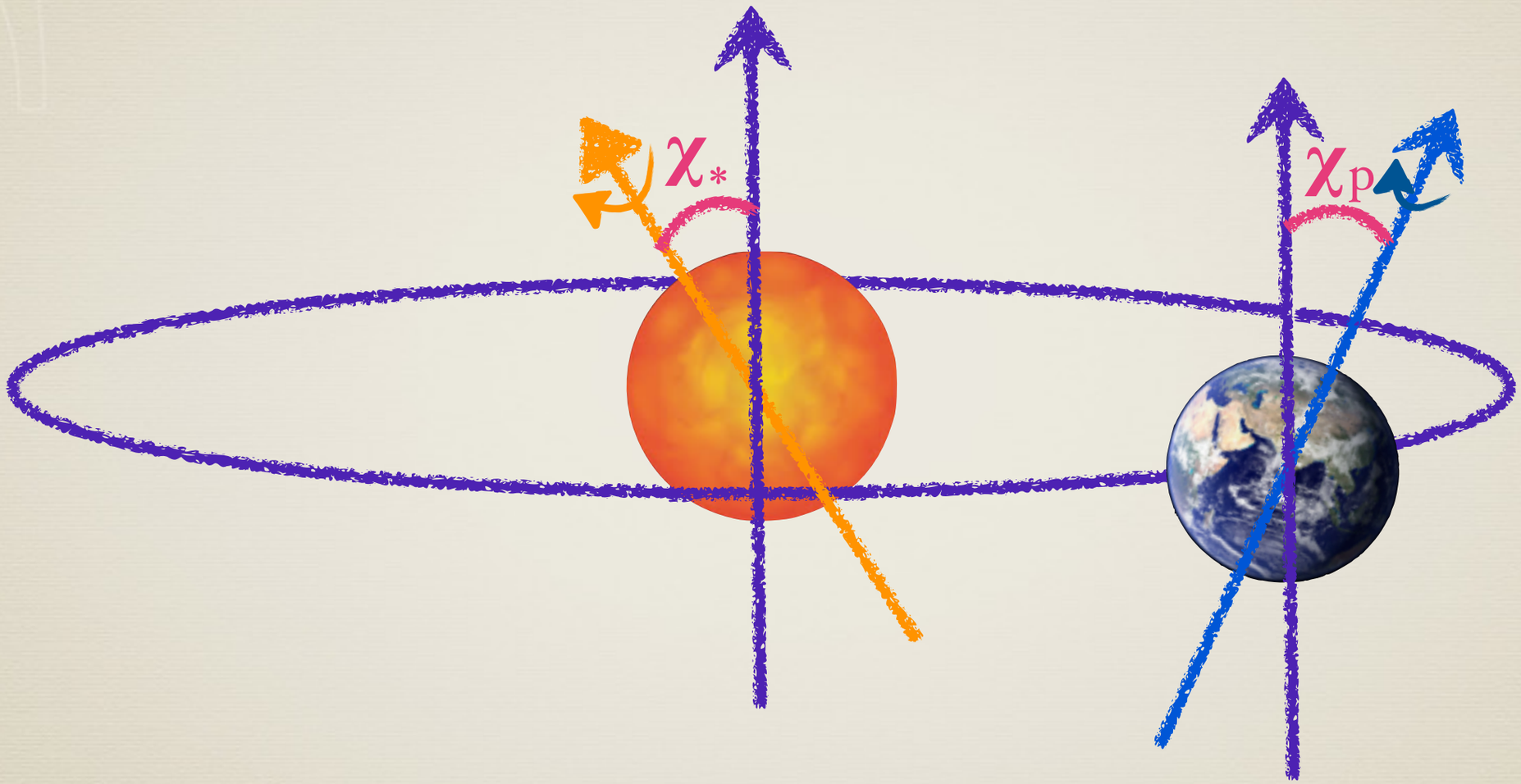

The star/planet's obliquity (χ_*/χ_p) is the angle between the spin axis of the star/planet and the orbit of star/planet.

Outline

- Stellar obliquity variations in extra solar planetary systems
  - Due to hierarchical three-body dynamics
  - Tidal re-alignment of the stellar obliquity
- Planetary obliquity variation

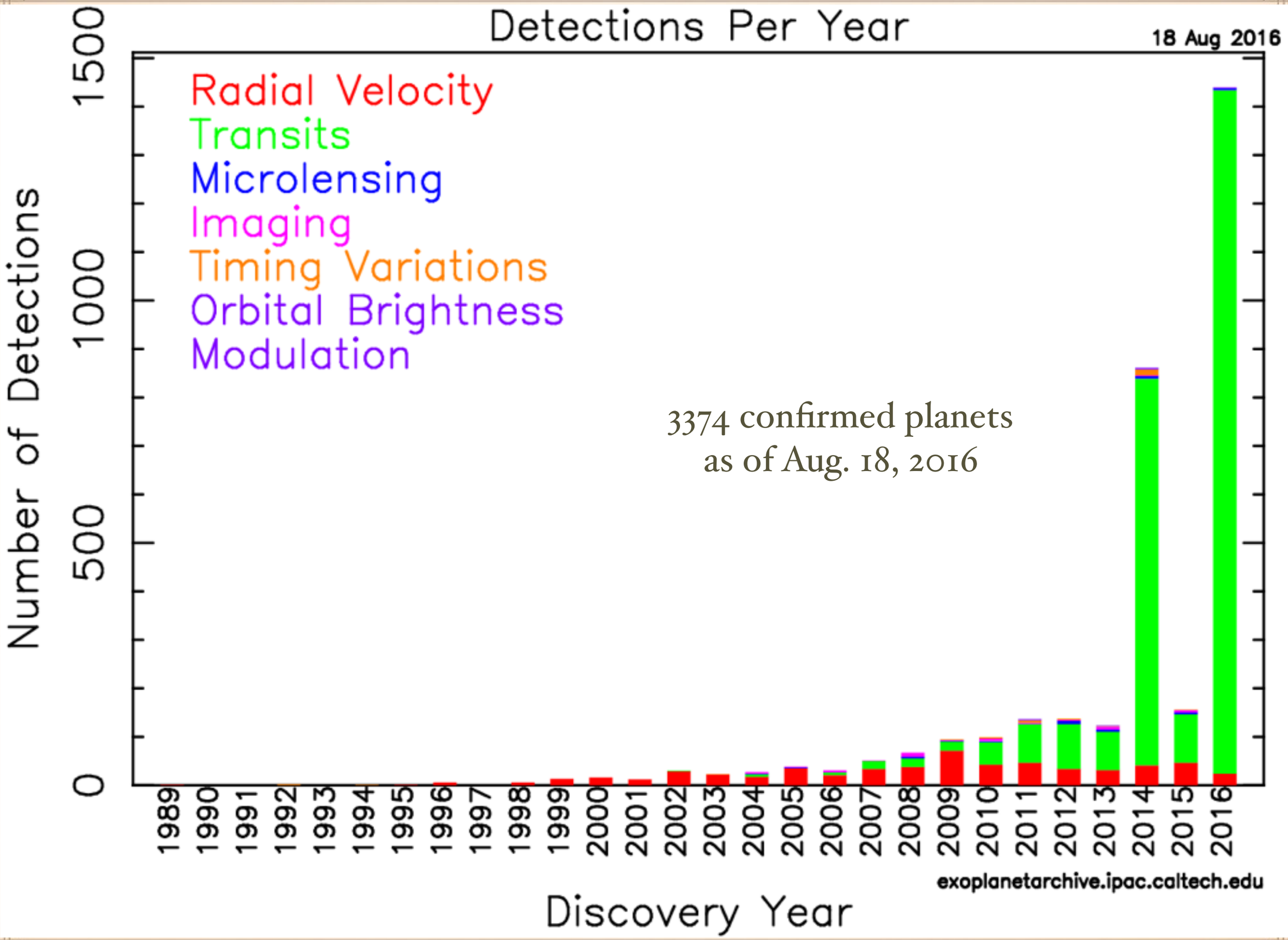
Detections Per Year
18 Aug 2016
Radial Velocity
Transits
Microlensing
Imaging
Timing Variations
Orbital Brightness
Modulation
3374 confirmed planets
as of Aug. 18, 2016
Number of Detections
0
500
1000
1500
1989
1990
1991
1992
1993
1994
1995
1996
1997
1998
1999
2000
2001
2002
2003
2004
2005
2006
2007
2008
2009
2010
2011
2012
2013
2014
2015
2016
exoplanetarchive.ipac.caltech.edu
Discovery Year

Mass – Period Distribution

18 Aug 2016

Hot Jupiters

Mass [Jupiter Masses]

0.01 0.1 1 10 100

Radial Velocity
Transits
Microlensing
Imaging
Timing Variations
Orbital Brightness Modulation

0.1 1 10 100 1000 10^4 10^5 10^6 10^7 10^8

Period [days]

exoplanetarchive.ipac.caltech.edu

ROSSITER-MCLAUGHLIN METHOD (SPIN-ORBIT MISALIGNMENT)

Stellar-spin planetary orbit aligned case:

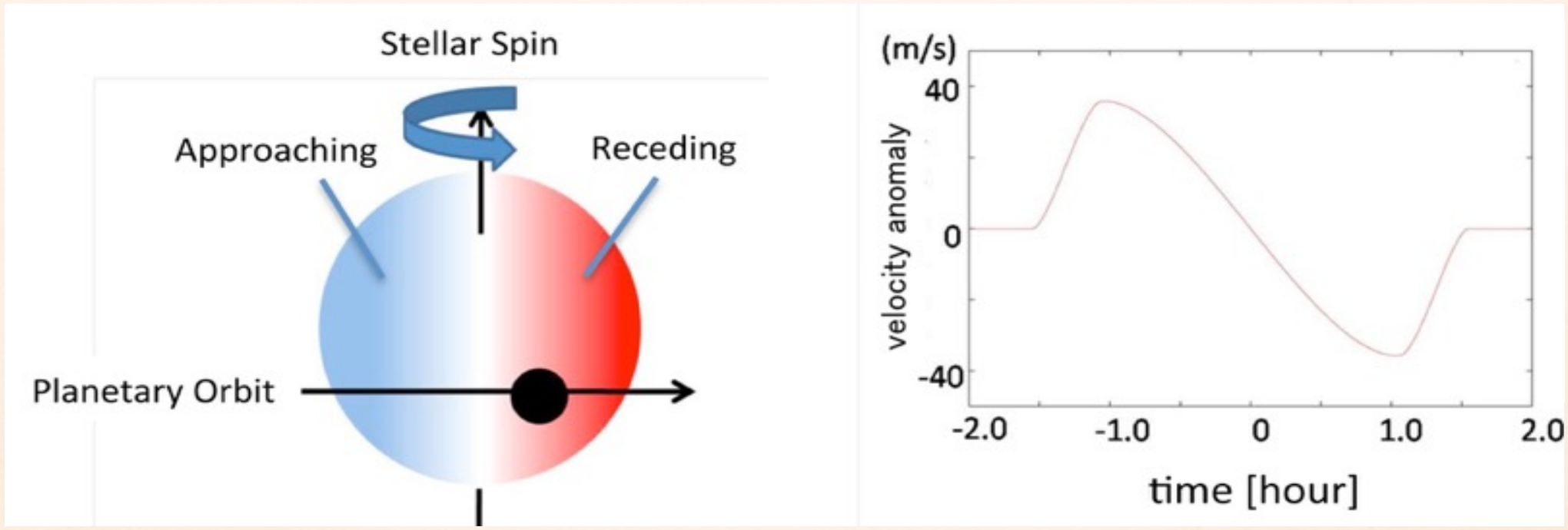

e.g., Ohta et al. 2005, Winn 2006

ROSSITER-MCLAUGHLIN METHOD (SPIN-ORBIT MISALIGNMENT)

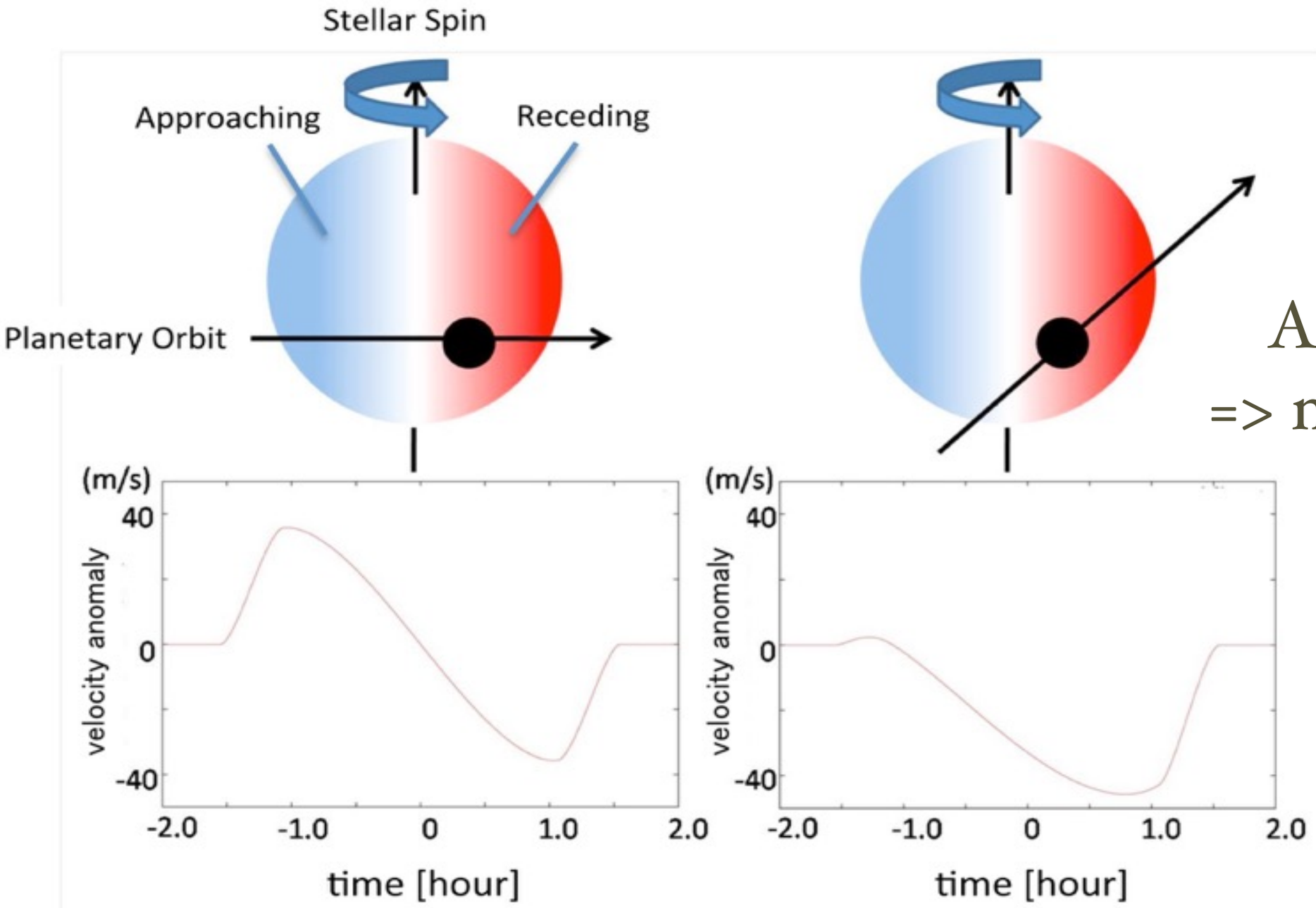

Asymmetric
=> misalignment

e.g., Ohta et al. 2005, Winn 2006

ROSSITER-MCLAUGHLIN METHOD (SPIN-ORBIT MISALIGNMENT)

- HD 209458 (Ohta et al. 2005)

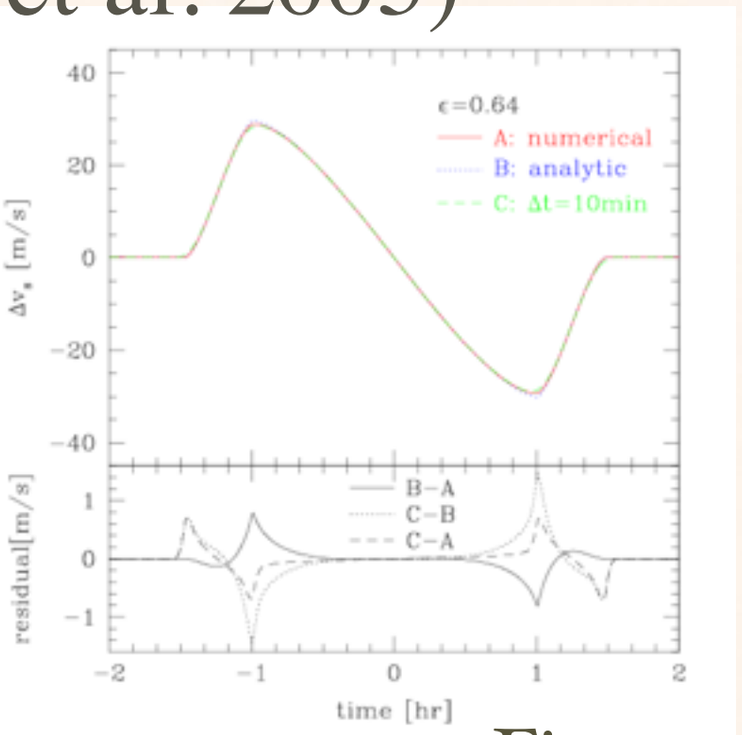

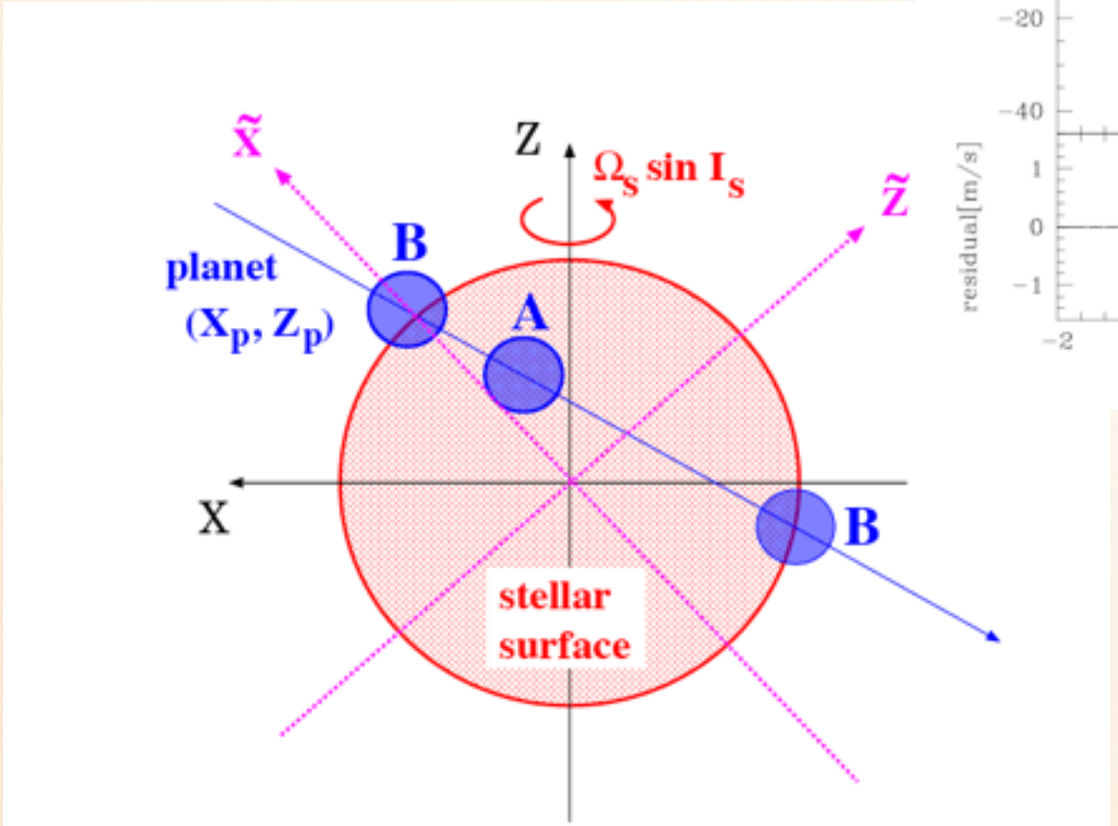

First stellar spin-planetary orbit misalignment measurement using MR effect.

λ~ -24.7 to 21.7 degree

OBSERVED SPIN-ORBIT MISALIGNMENT

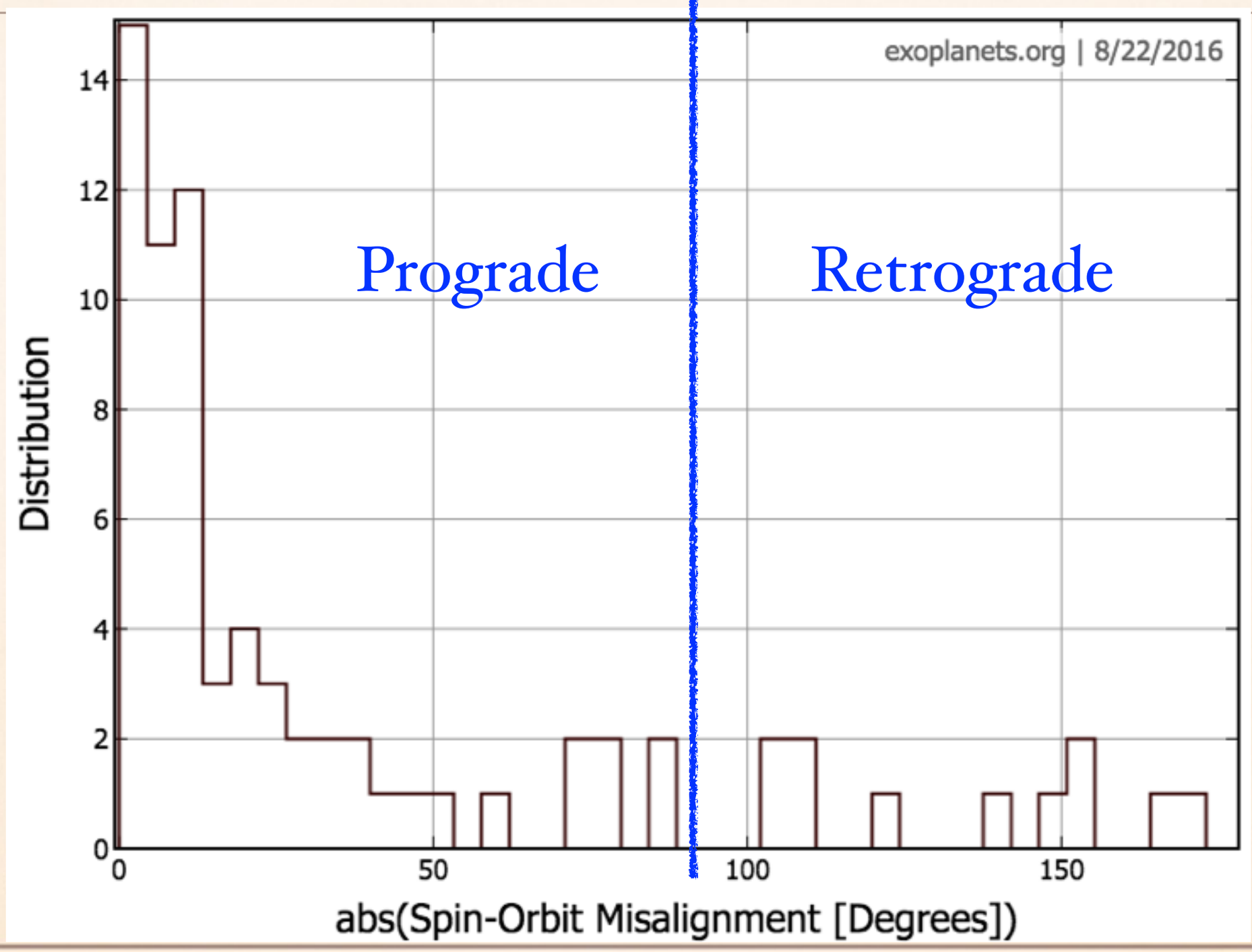

CHALLENGES CLASSICAL PLANETARY FORMATION THEORIES

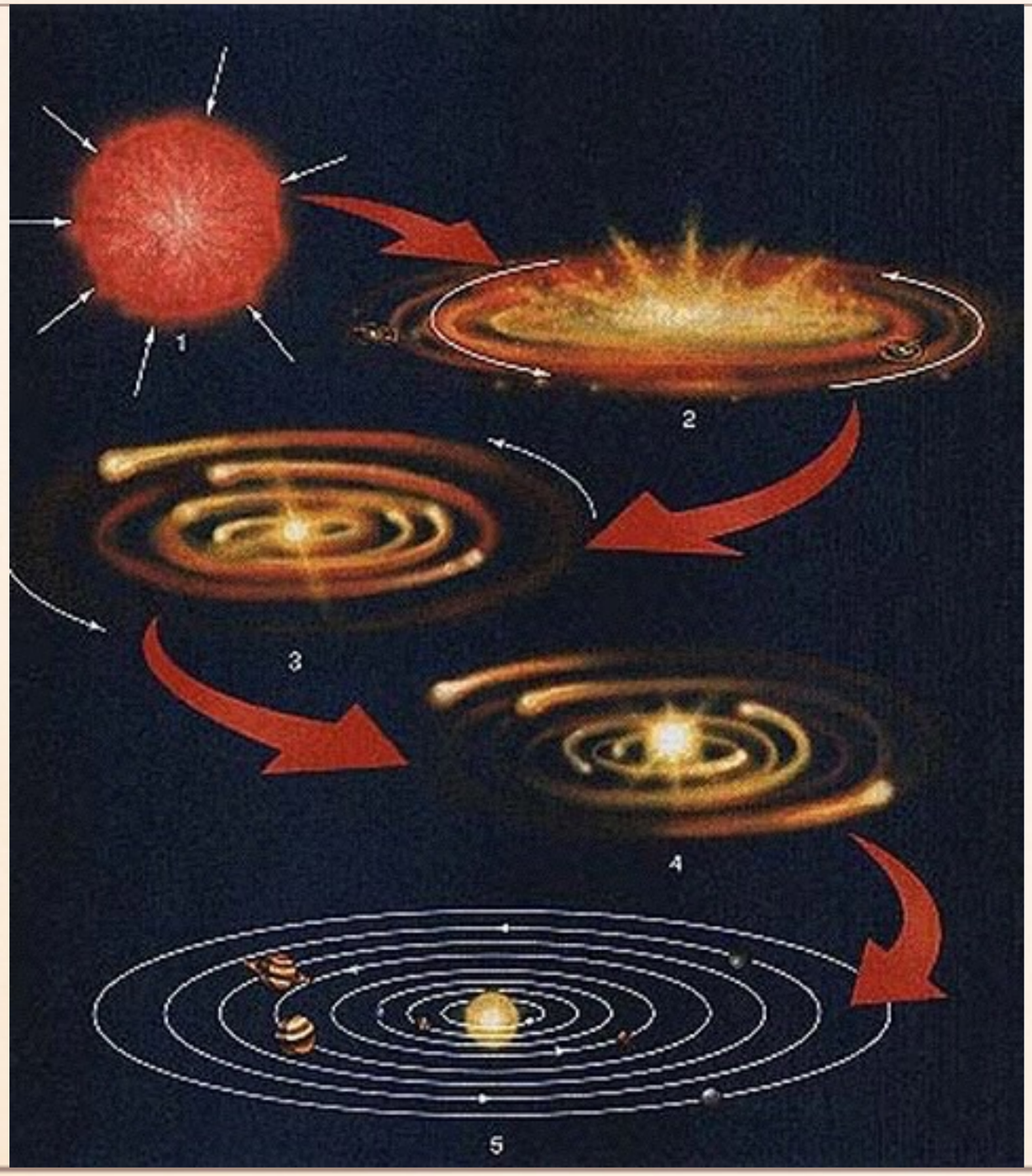

Classical planetary formation theory:

Star and planets form in a molecular cloud, and share the same direction of rotation.

CHALLENGES CLASSICAL PLANETARY FORMATION THEORIES

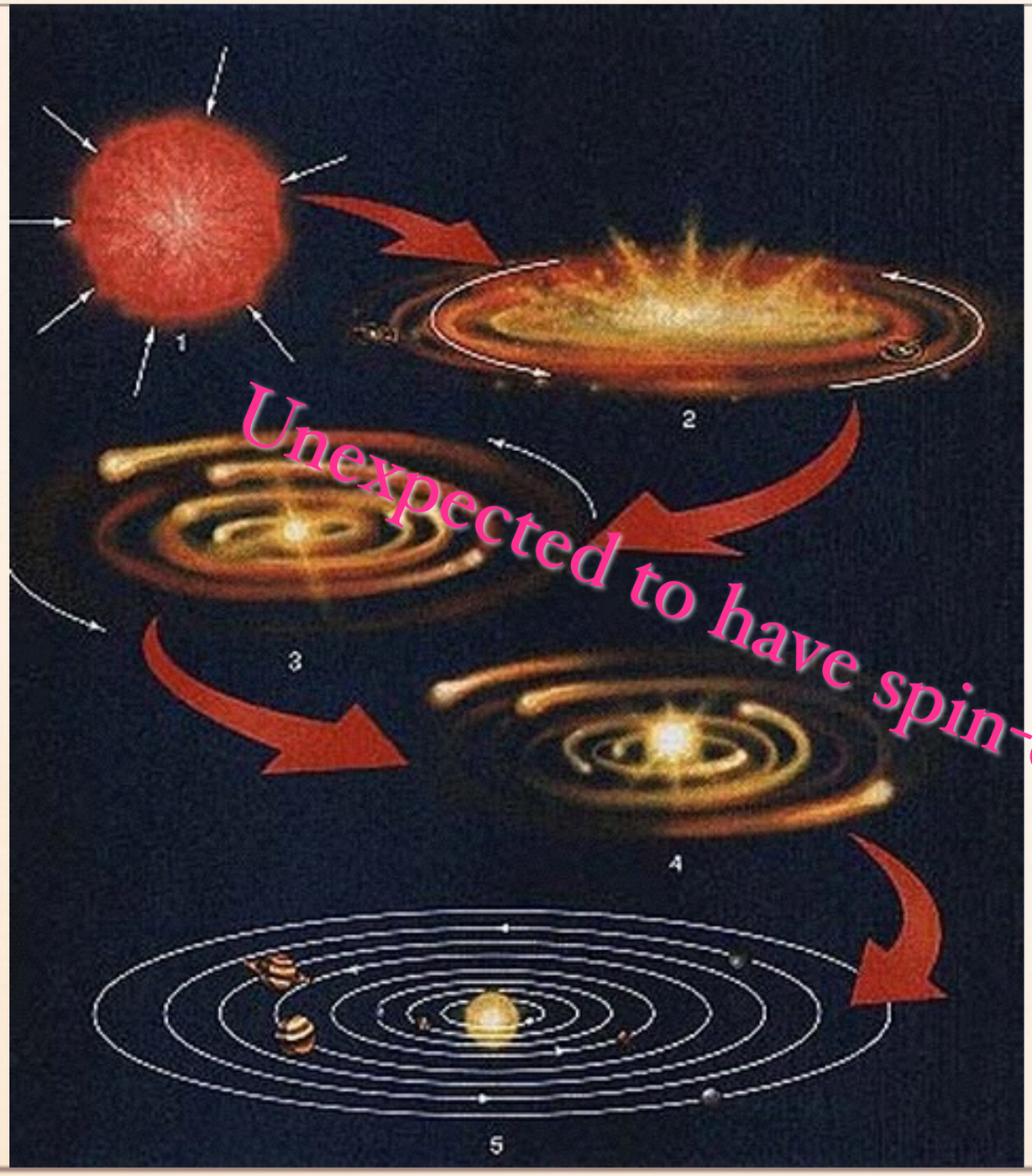

Unexpected to have spin-orbit misalignment!

Classical planetary formation theory:

Star and planets form in a molecular cloud, and share the same direction of rotation.

ORIGIN OF SPIN-ORBIT MISALIGNMENT

* **Smooth Migration:** planets move close due to interaction with proto-planetary disk.

Star tilts through magnetic interaction

(Lai et al. 2011)

or stellar oscillation effects

(Rogers et al. 2012, 2013)

Disk tilts through inhomogeneous collapse of the molecular cloud

(Bate et al. 2010; Thies et al. 2011; Fielding et al. 2015)

or the torque from nearby stars.

(Tremaine 1989; Batygin 2012; Xiang-Gruess & Papaloizou 2013)

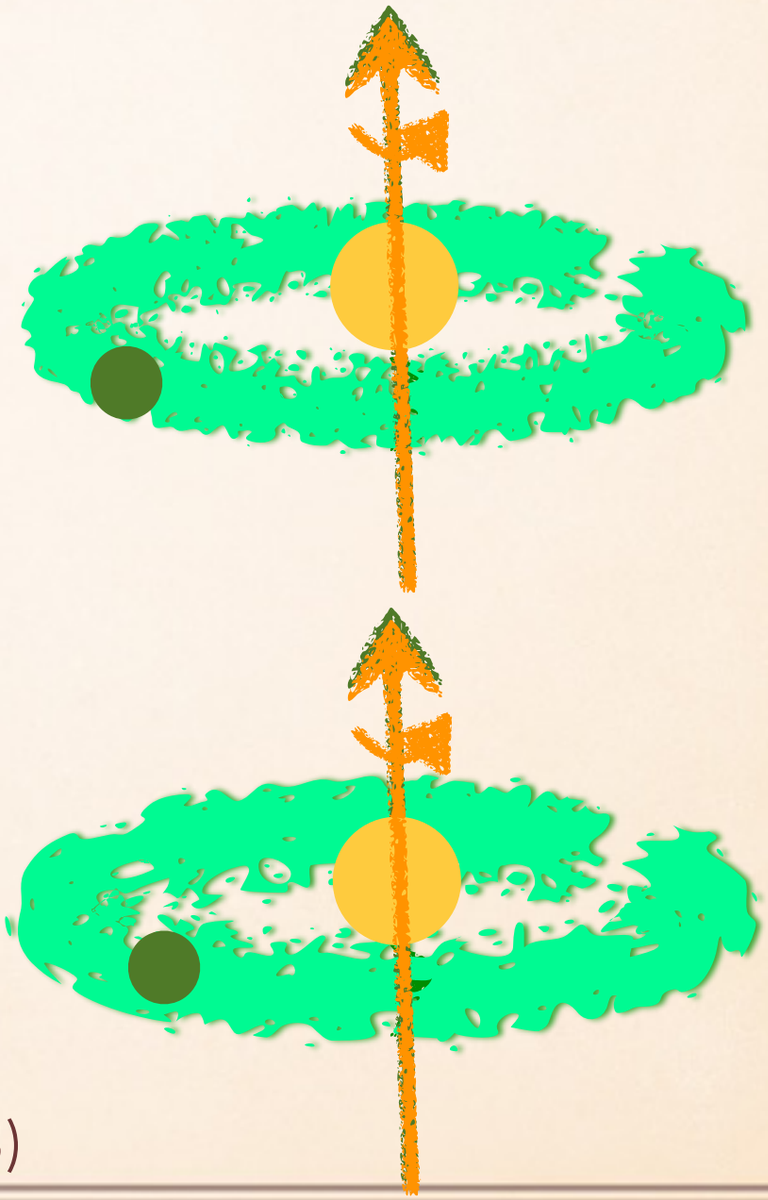

ORIGIN OF SPIN-ORBIT MISALIGNMENT

- **Violent Migration (Dynamical Origin):** planets move close due to interactions with companion stars/planets.

Planetary orbit tilts under planet-planet scattering

(e.g., Chatterjee et al. 2008, Petrovich 2014)

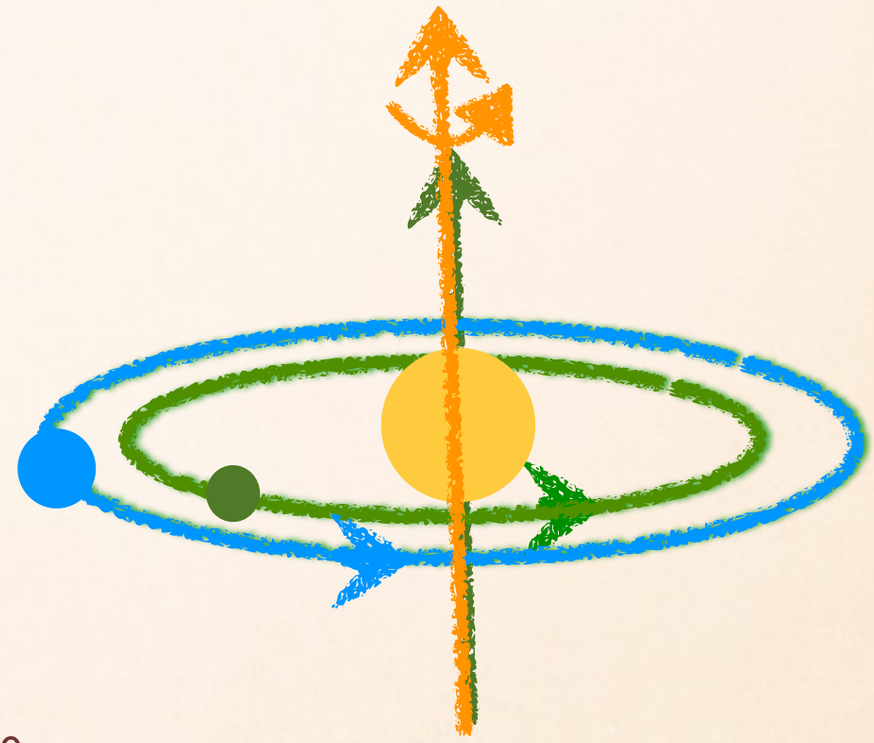

or long-term secular dynamical effects between planets or stellar companion.

(e.g., Fabrycky and Tremaine 2007; Nagasawa et al. 2008; Naoz et al. 2011, 2012; Wu and Lithwick 2011; Li et al. 2014; Valsecchi and Rasio 2014)

ORIGIN OF SPIN-ORBIT MISALIGNMENT

- **Smooth Migration:** planets move close due to interaction with proto-planetary disk.

v.s.

- **Violent Migration (Dynamical Origin):** planets move close due to interactions with companion stars/planets.

Next:
Range of stellar obliquity achieved in violent migration (dynamics of hierarchical three-body interactions)

CONFIGURATION OF HIERARCHICAL 3-BODY SYSTEM

Hierarchical: $a_1 << a_2$ ($\epsilon = \frac{a_1}{a_2}\frac{e_2}{1-e_2^2}$ *hierarchical parameter*)

CONFIGURATION OF HIERARCHICAL 3-BODY SYSTEM

System is stationary and can be thought of as interaction between two orbital wires (secular approximation):

- Inner wires (1): formed by m_1 and m_J.
- Outer wires (2): m_2 orbits the center mass of m_1 and m_J.
- $\mathcal{J}_{1/2}$: Specific orbital angular momentum of inner/outer wire.
- i: inclination between the two orbits.

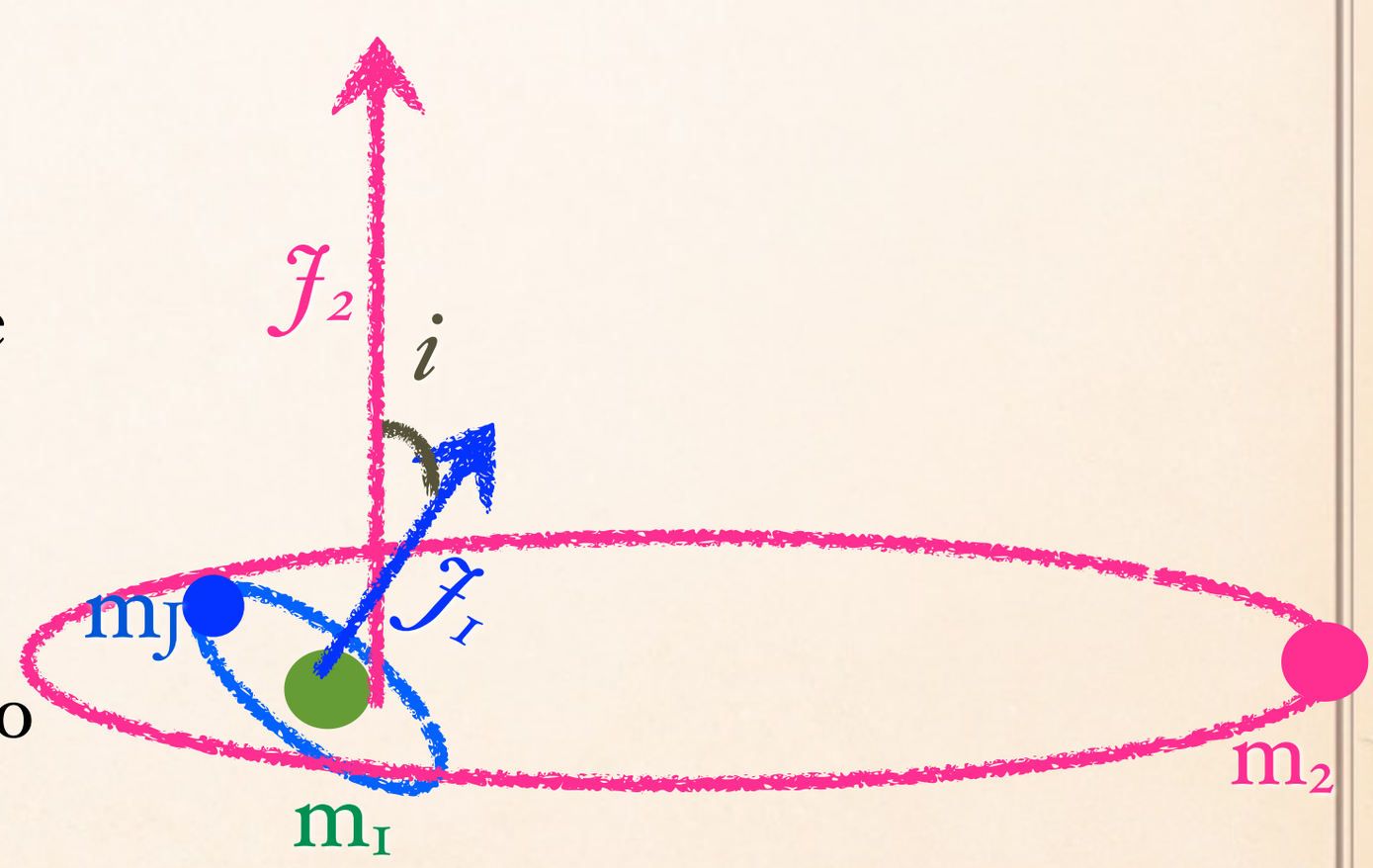

KOZAI-LIDOV MECHANISM

Kozai-Lidov Mechanism

($e_2 = 0$, $m_J \rightarrow 0$)

(*Kozai 1962; Lidov 1962: Solar system objects*)

- Octupole level $O((a_1/a_2)^3)$ is zero.
- Quadrupole level $O((a_1/a_2)^2)$:

=> $Jz = \sqrt{1-e_1^2}\cos i_1$ conserved
(axi-symmetric potential).

=> when i>40°, e_1 and i oscillate with large amplitude.

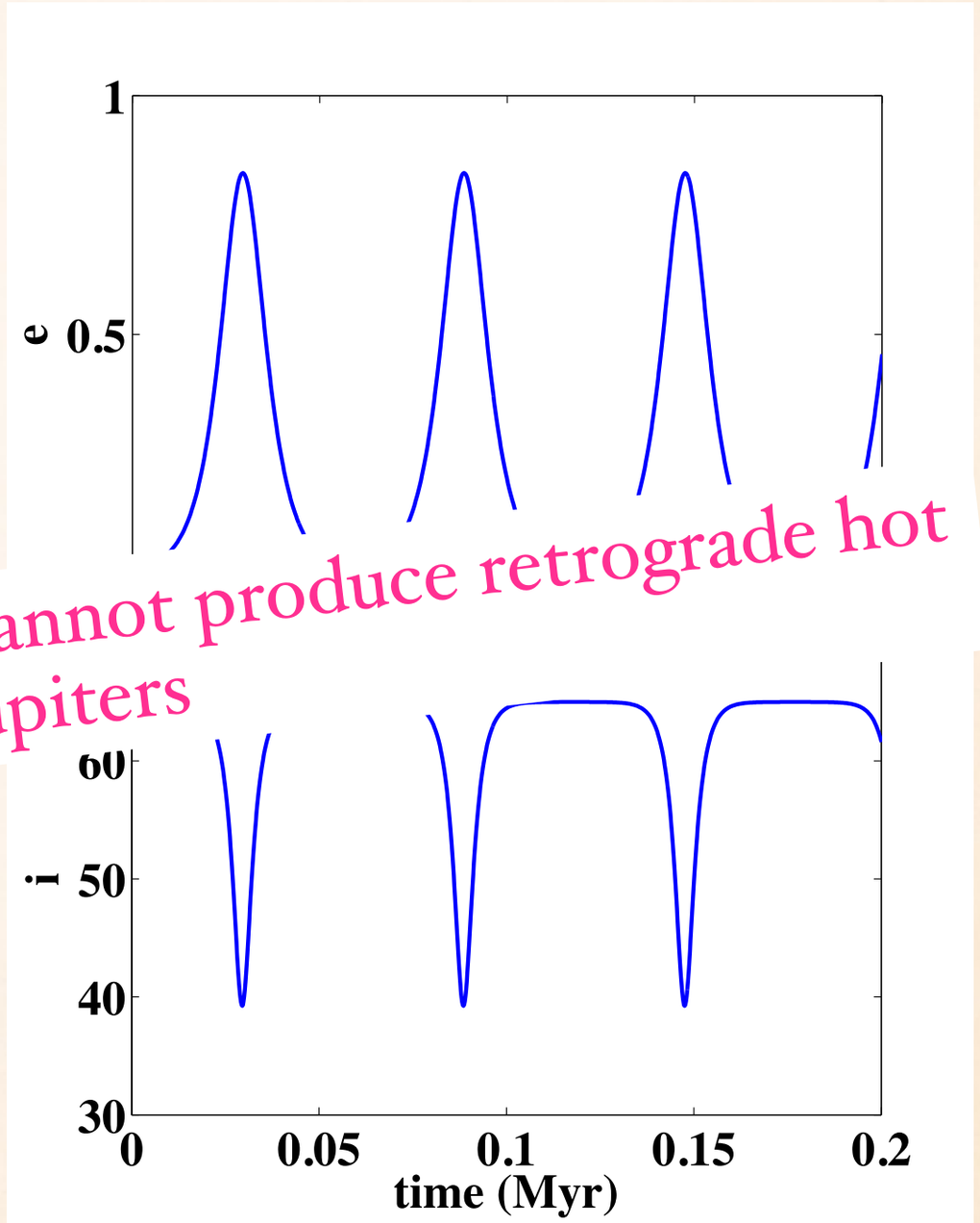

Example of Kozai-Lidov Mechanism.

OCTUPOLE KOZAI-LIDOV MECHANISM

$e_2 \neq 0$ (Eccentric Kozai-Lidov Mechanism) or $m_J \neq 0$:

(e.g., *Naoz et al. 2011, 2013, test particle case: Katz et al. 2011, Lithwick & Naoz 2011*):

- Jz NOT constant, octupole ≠ 0.

- when i>40°: $e_1 \rightarrow 1$.
- when i>40°: i crosses 90°

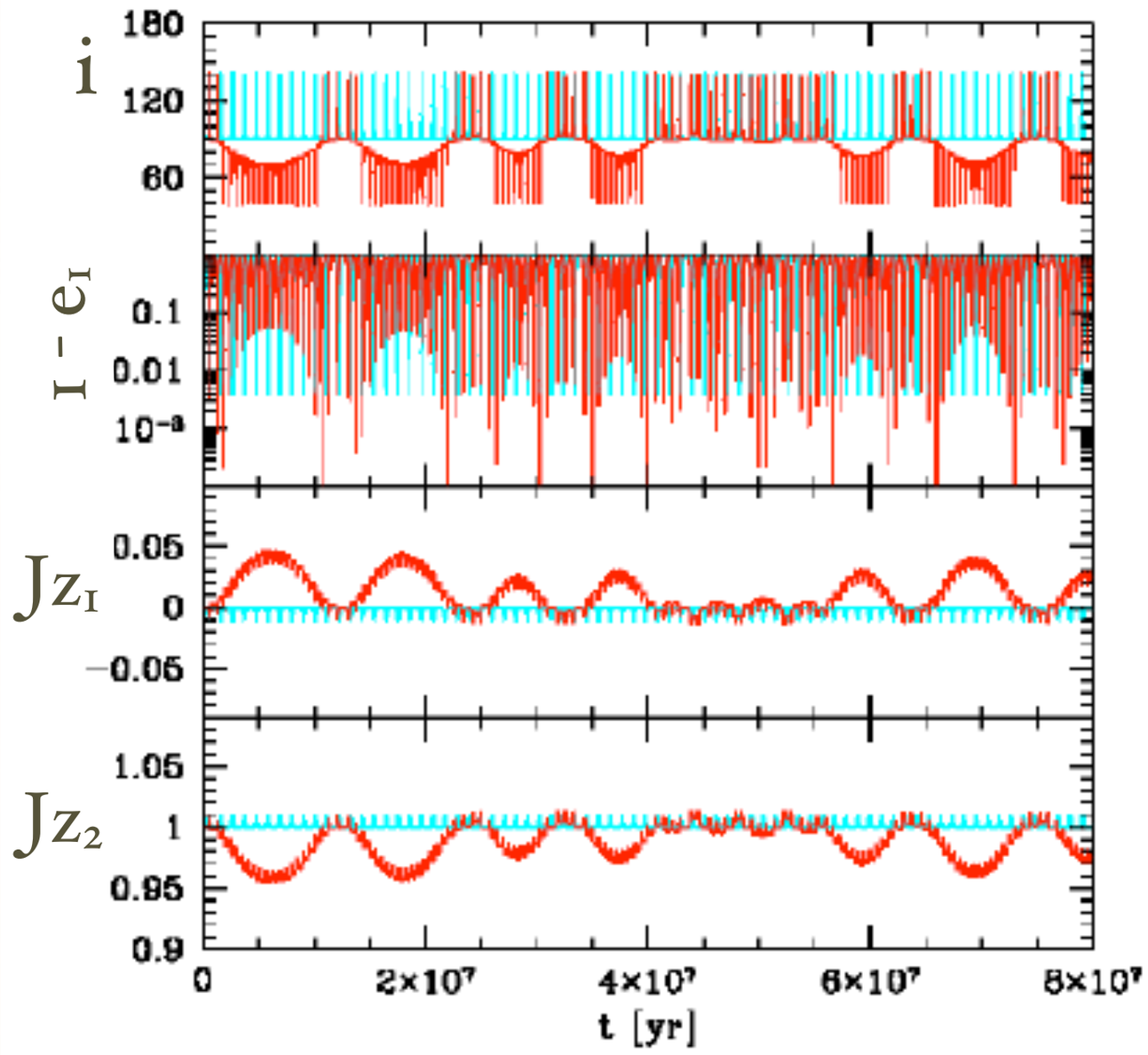

Produce retrograde hot Jupiters

Cyan: quadrupole only.
Red: quadrupole + octupole. Naoz et al 2013

COPLANAR FLIP

- Starting with $i \approx 0$, $e_1 \geq 0.6$, $e_2 \neq 0$:

  $e_1 \rightarrow 1$, i flips by $\approx 180°$ (*Li et al. 2014a*).

=> Produces counter orbiting hot Jupiters.

=> Enhance tidal disruption rates (*Li et al. 2015*).

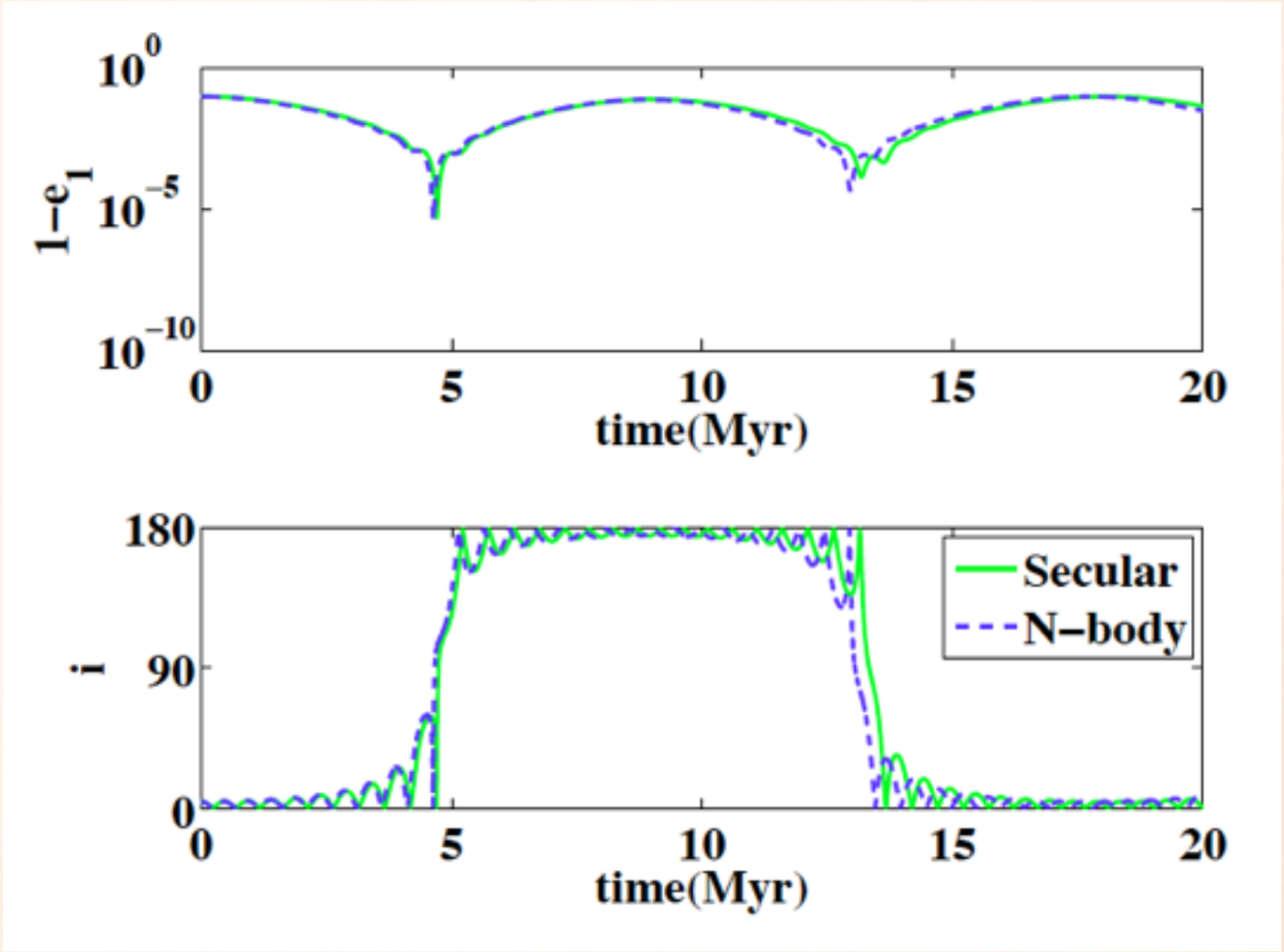

(Li et al. 2014a)

DIFFERENCES BETWEEN HIGH/LOW I FLIP

- Low inclination flip

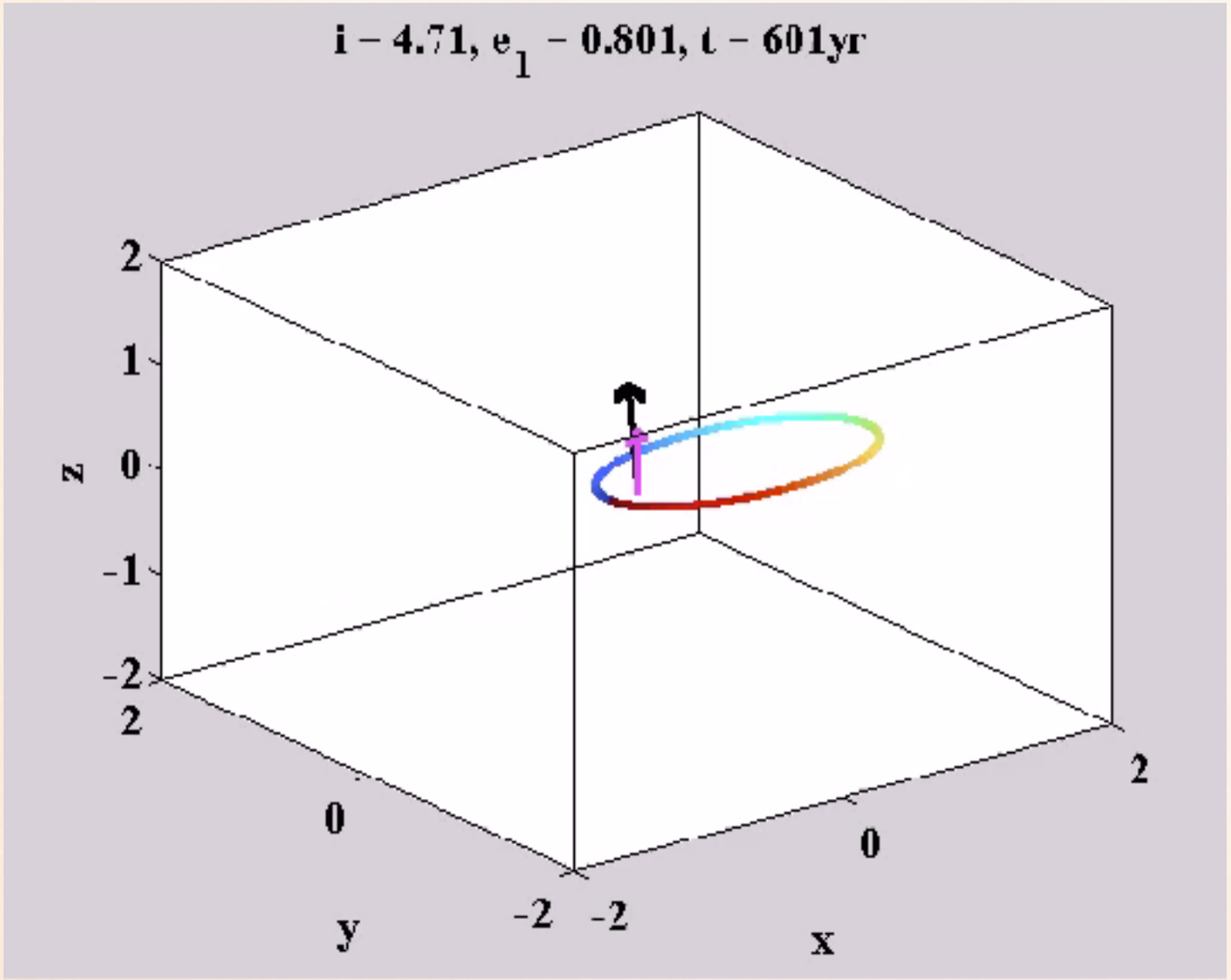

- For simplicity:

take $m_j \rightarrow 0$ => outer orbit stationary.

- z direction: angular momentum of the outer orbit.

- ⬆: direction of J_I.
- ⬆: Jz_I => indicates flip.
- Colored ring: inner orbit. Color: mean anomaly.

Li et al. 2014a

DIFFERENCES BETWEEN HIGH/LOW I FLIP

- High inclination flip

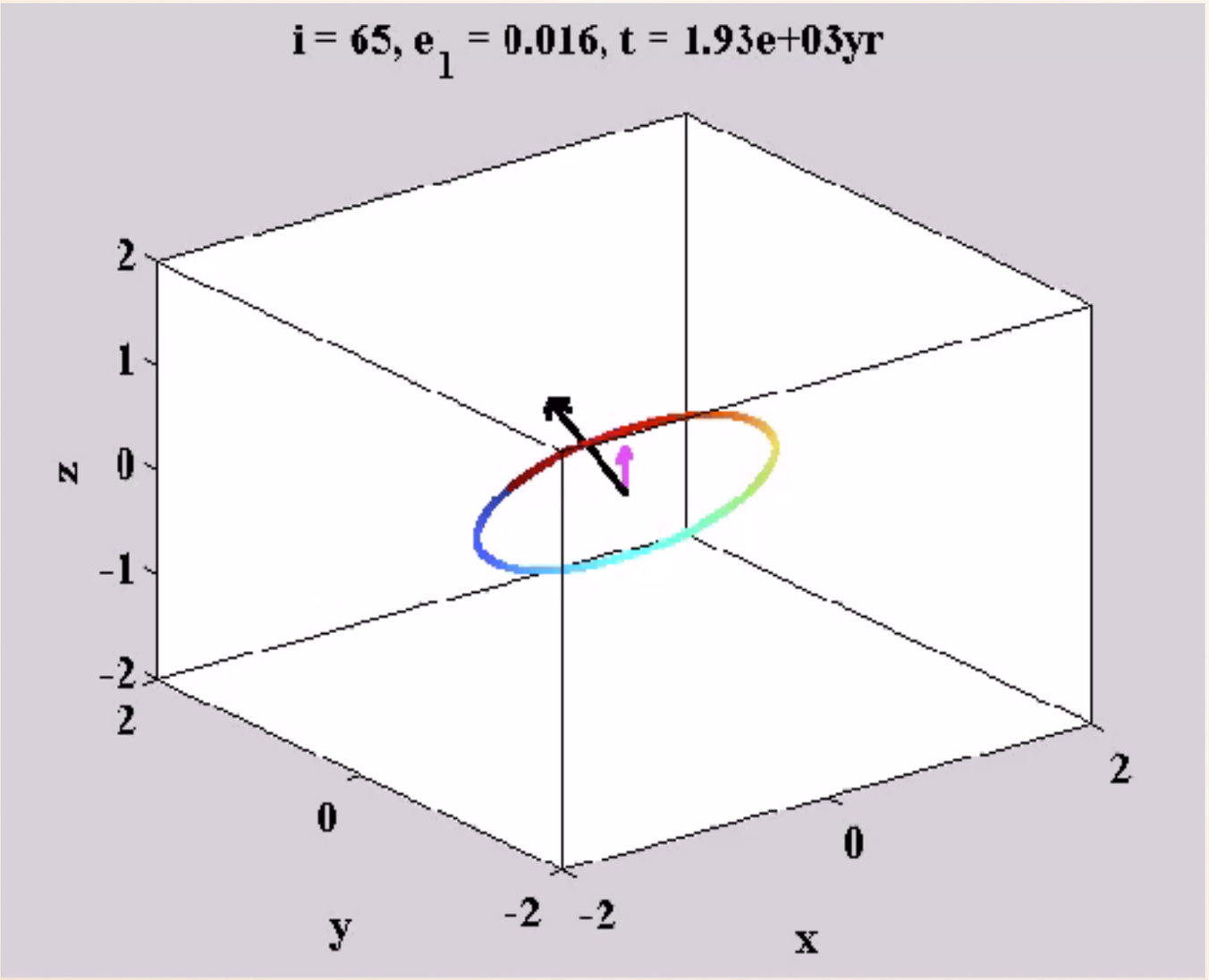

- For simplicity:

take $m_j \rightarrow 0$ => outer orbit stationary.

- z direction: angular momentum of the outer orbit.

- ⬆: direction of J_I.
- ⬆: Jz_I => indicates flip.
- Colored ring: inner orbit. Color: mean anomaly.

Li et al. 2014a

CO-PLANAR FLIP CRITERION

- Hamiltonian (at O(i)):
  - Evolution of e_1 only due to octupole terms:

    => e_1 does not oscillate before flip

  - Depend on only J_1 and $\varpi_1=\omega_1+\Omega_1$

    => System is integrable.

    => e_1(t) can be solved.

    => The flip timescale can be derived.

    => The flip criterion can be derived.

$$\varepsilon > \frac{8}{5}\frac{1-e_1^2}{7-e_1\left(4+3e_1^2\right)\cos\left(\omega_1+\Omega_1\right)}$$

Li et al. 2014a

ANALYTICAL RESULTS V.S. NUMERICAL RESULTS

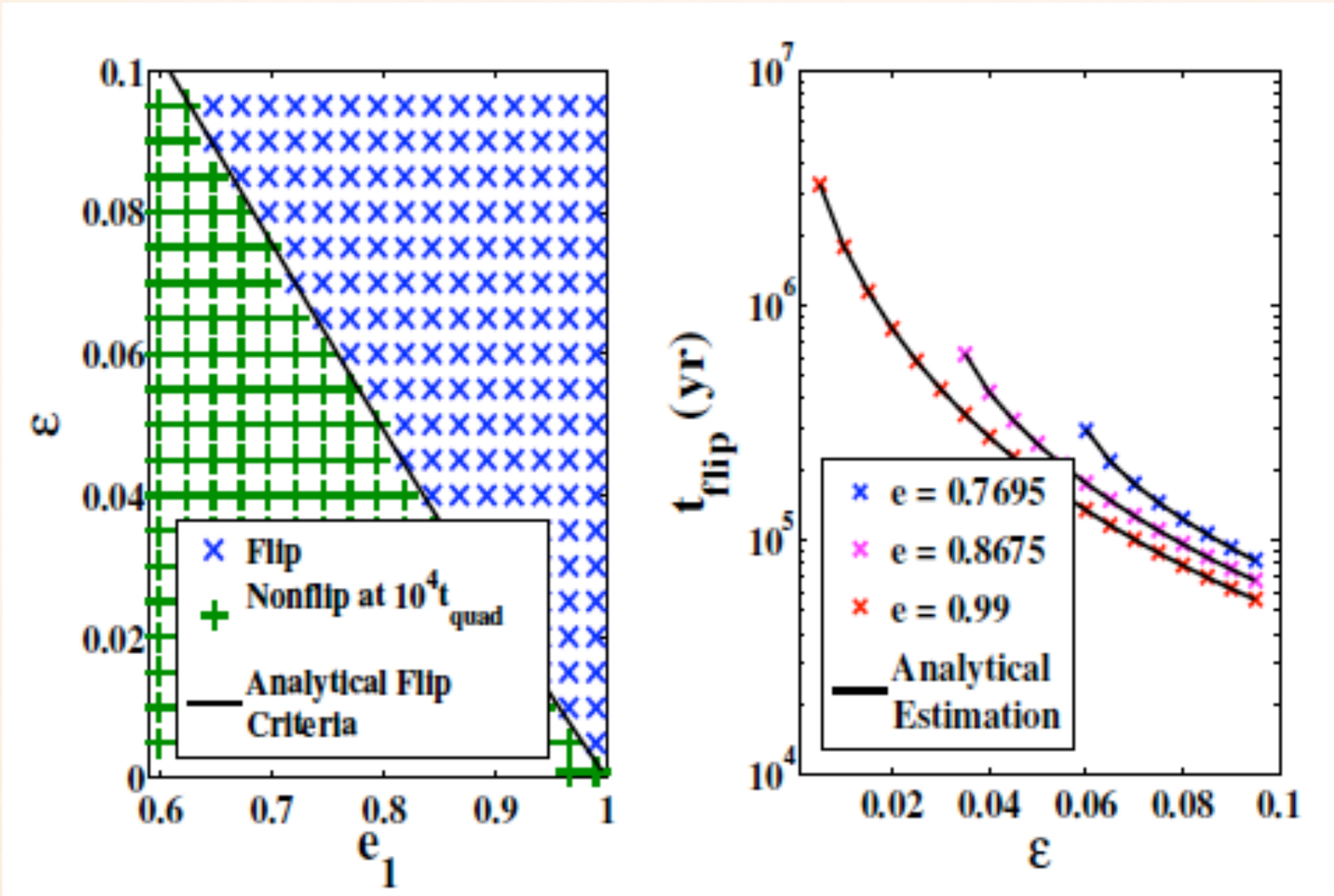

IC: i=5°.

- The flip criterion and the flip timescale from secular integration are consistent with the analytical results.

Li et al. 2014a

FORMATION OF MISALIGNED HOT JUPITERS (KL + TIDE)

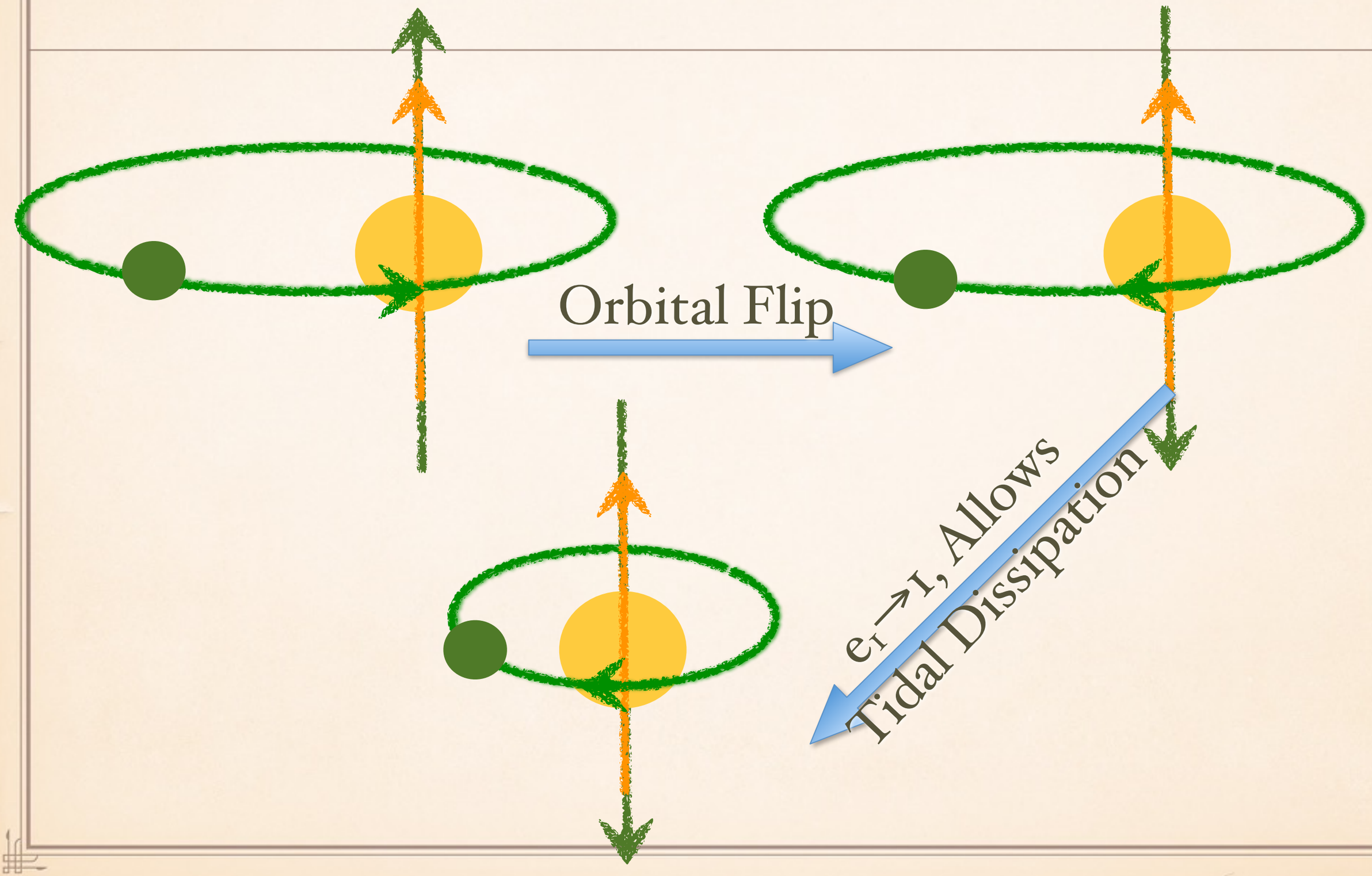

FORMATION OF COUNTER ORBITING HOT JUPITERS (KL + TIDE)

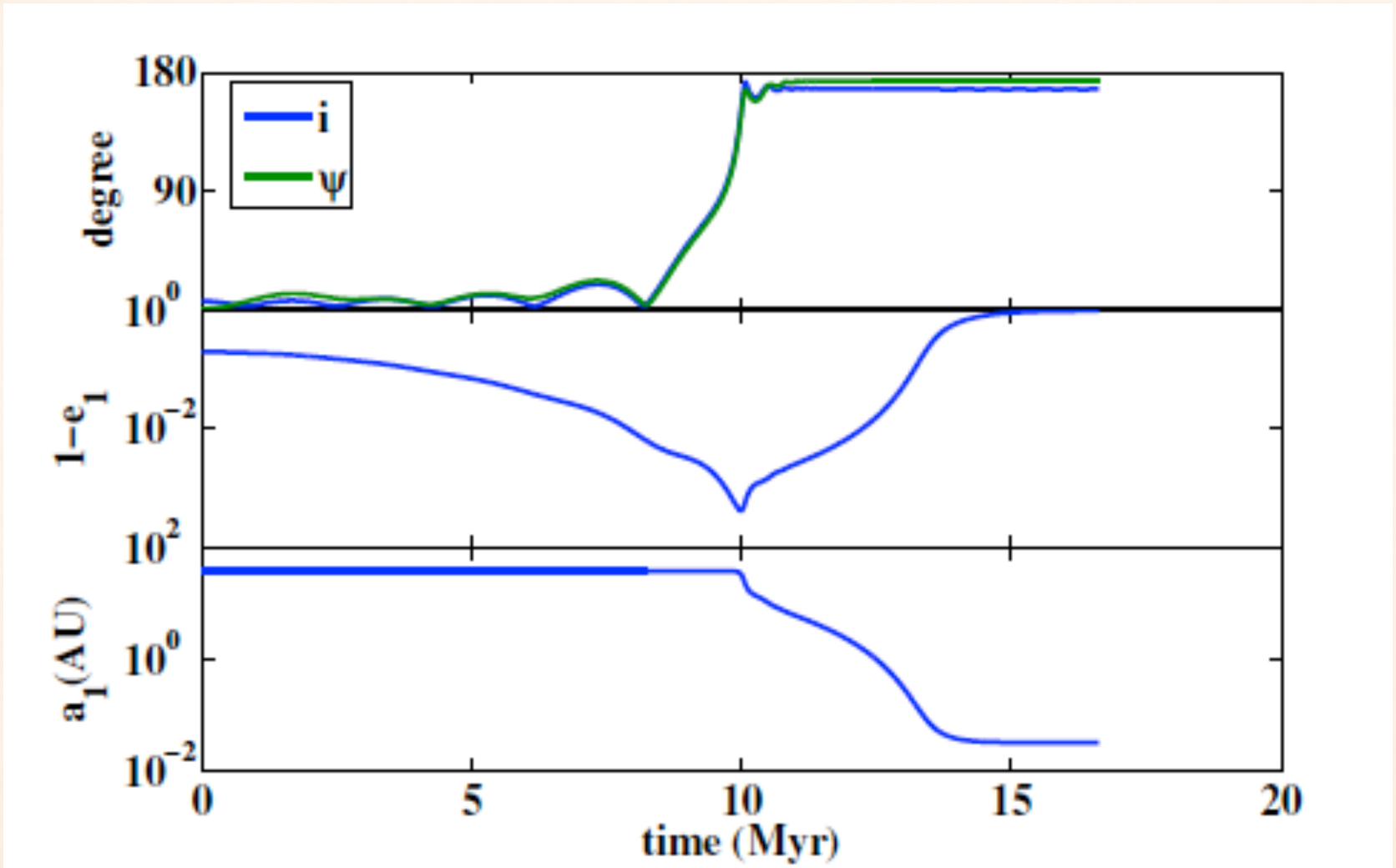

$e_I \rightarrow 1$ during the flip

=> $r_p \downarrow$, tide dominates.

=> $e_I \rightarrow 0$, $a_I \downarrow$, i, $\psi \approx 180^o$.

Li et al. 2014a

DIFFICULTY IN THE FORMATION OF COUNTER-ORBITING HOT JUPITERS

Numerical simulations including short range forces.

Most systems are tidally disrupted and a small fraction turn out to be prograde.

The formation of counter-orbiting HJs in a very restricted parameter region.

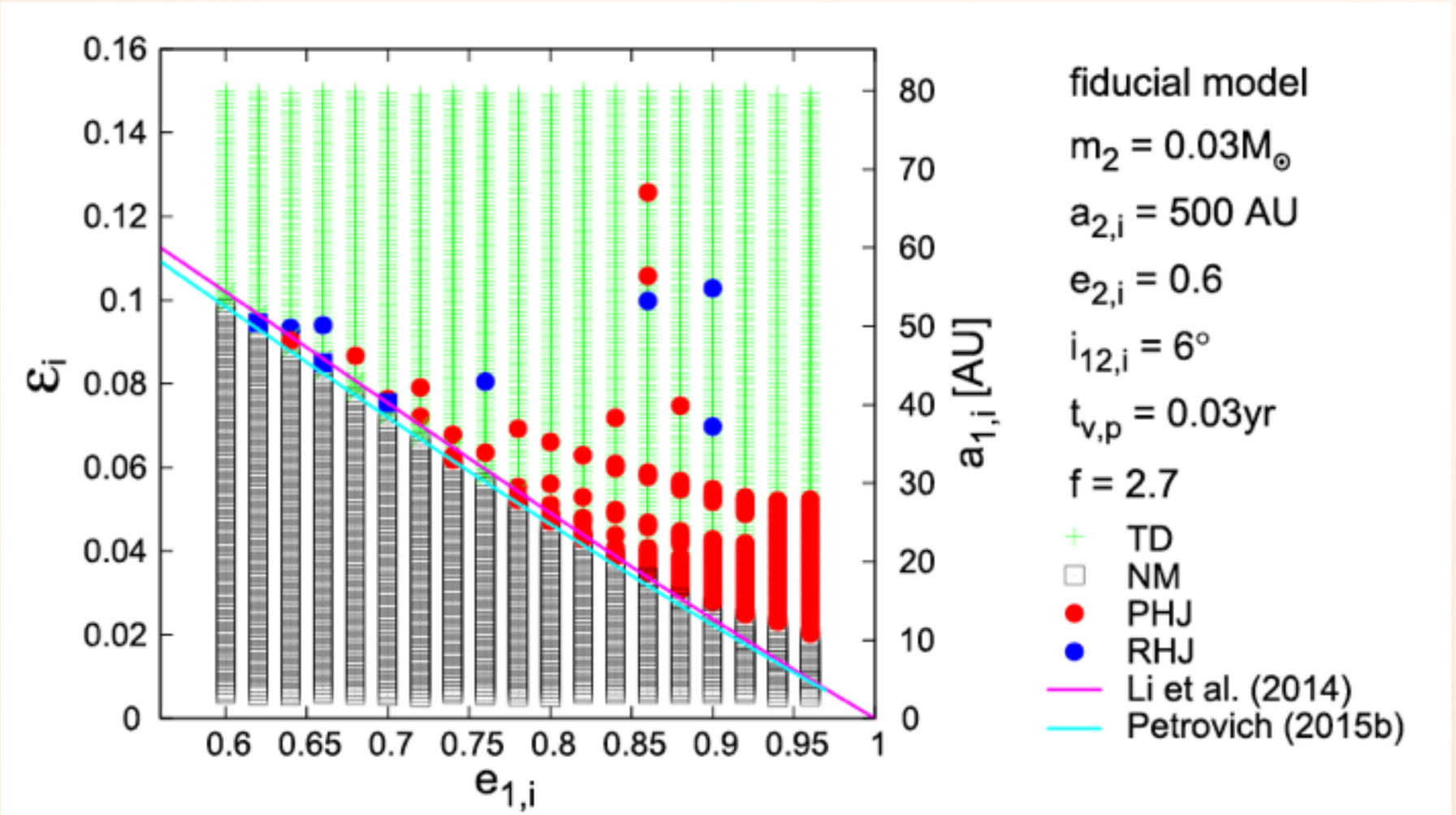

Xue & Suto 2016

FORMATION OF MISALIGNED HOT JUPITERS (KL + TIDE) BY POPULATION SYNTHESIS

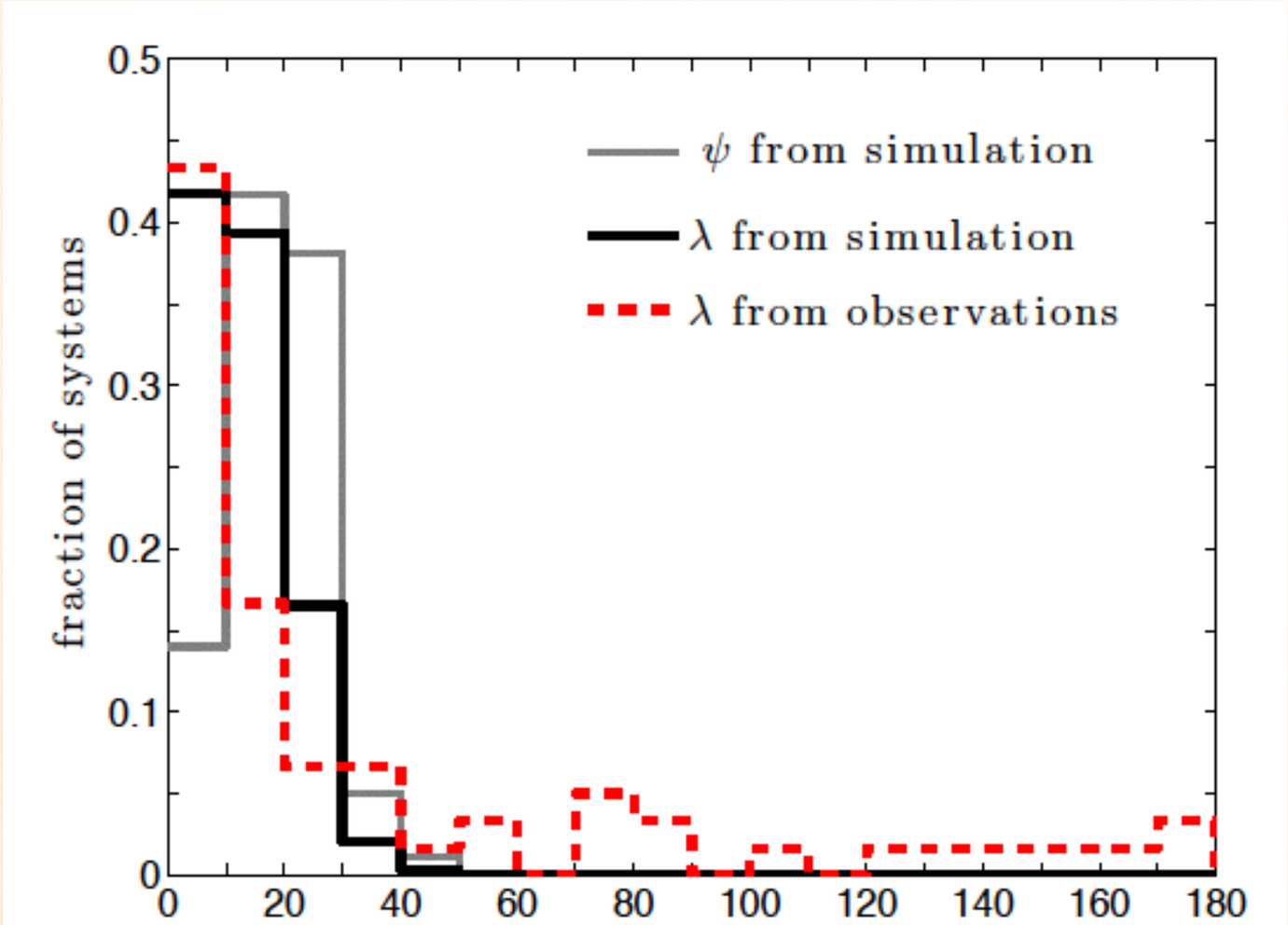

Petrovich 2015

Population synthesis study of interaction of two giant planets.

=> a different mechanism is needed (Petrovich 2015)

FORMATION OF MISALIGNED HOT JUPITERS (KL + STELLAR OBLATENESS + TIDE)

$M_p < 3\ M_J$

=> bimodal

$M_p \sim 5M_J$

=> low misalignment (solar-type stars)

=> higher misalignment (more massive stars)

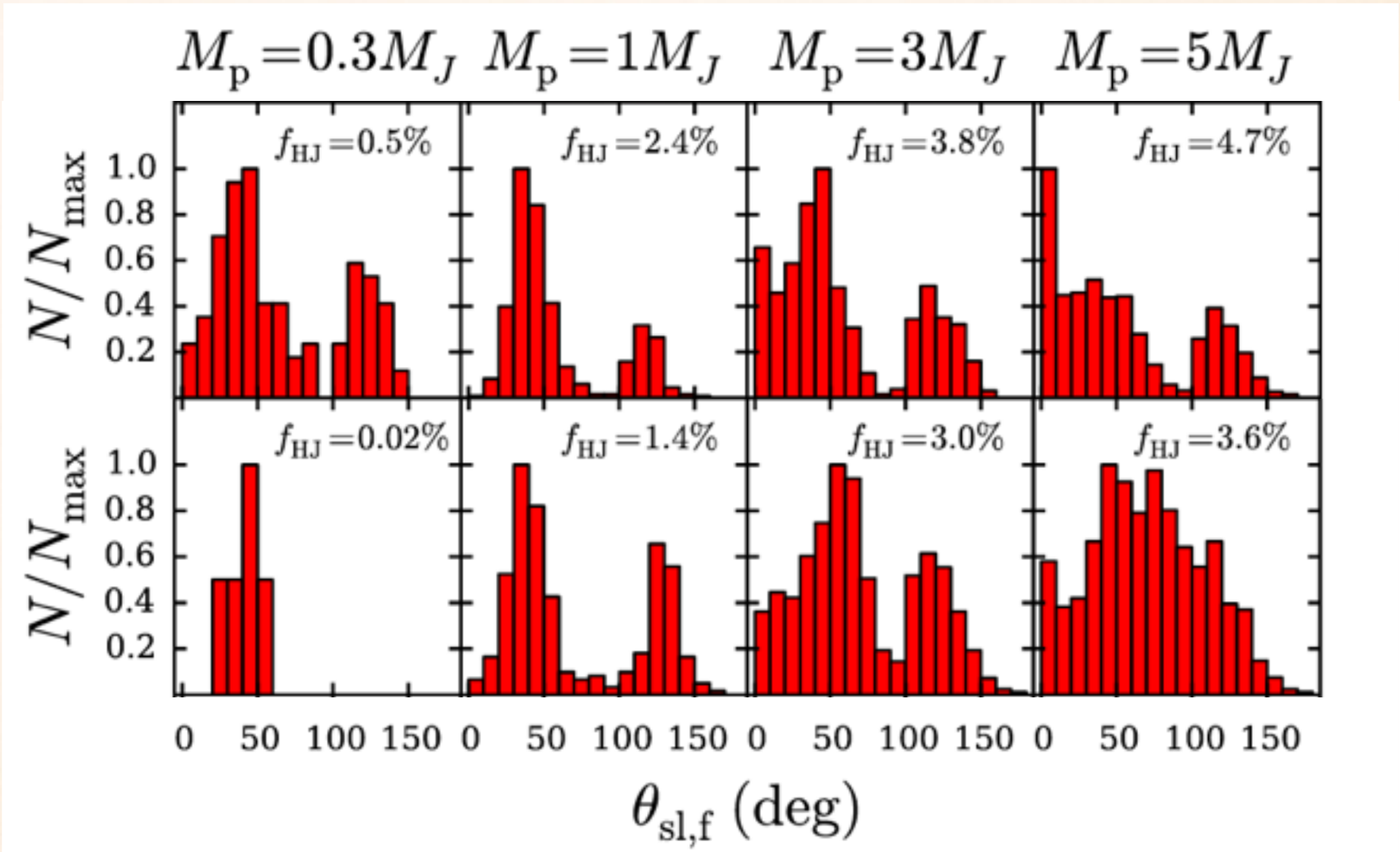

Anderson et al. 2016

Stellar Obliquity v.s. Stellar Temperature

Sky-projected stellar obliquity as a function of stellar effective temperature for hot Jupiters. Obliquity small when T<6100K. (Winn et al. 2010)

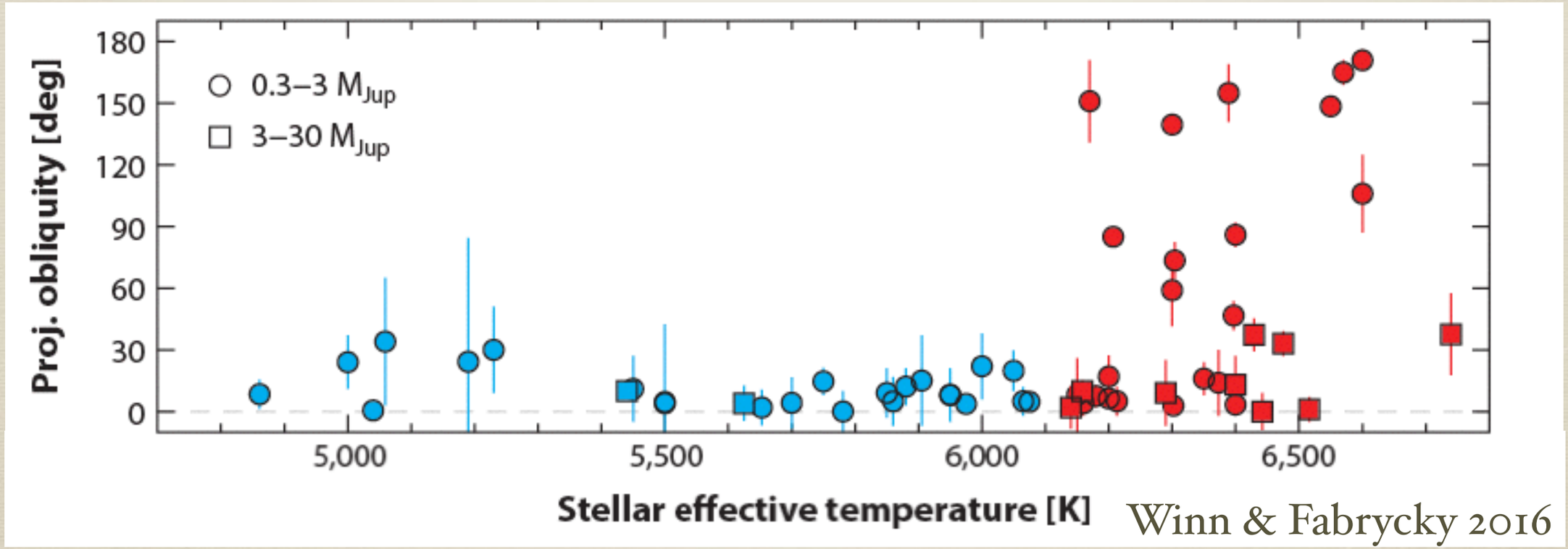

Winn & Fabrycky 2016

Spin-Orbit Alignment

- Tides from close-in planet
  - preference for cool stars with thick convective envelope

(e.g., Winn et al. 2010, Lai 2012,Dawson 2014, Xue et al. 2014)

- Internal gravity waves in radiative zone tilt the star spin axis only for hot stars (Rogers et al. 2012)

- Ingestion from close-in planet (Matsakos & Konigl 2015)

- Star/disk magnetic torques (Spalding & Batygin 2015)

Tidal Realignment? —Challenges

* $t_{decay} \sim t_{align}$ => Cannot align stellar spin before orbital decay (Winn et al. 2010)

* Tidal coupling and alignment of a thin shell of the star (Winn et al. 2010 & Dawson 2014).

* Inertial wave of the (1, 0) component allows $t_{decay} > t_{align}$ (Lai 2012)

=> PROBLEM: Retrograde configurations are driven to 90 or 180 degrees instead of 0 degrees (Rogers & Lin 2013).

Tidal Realignment

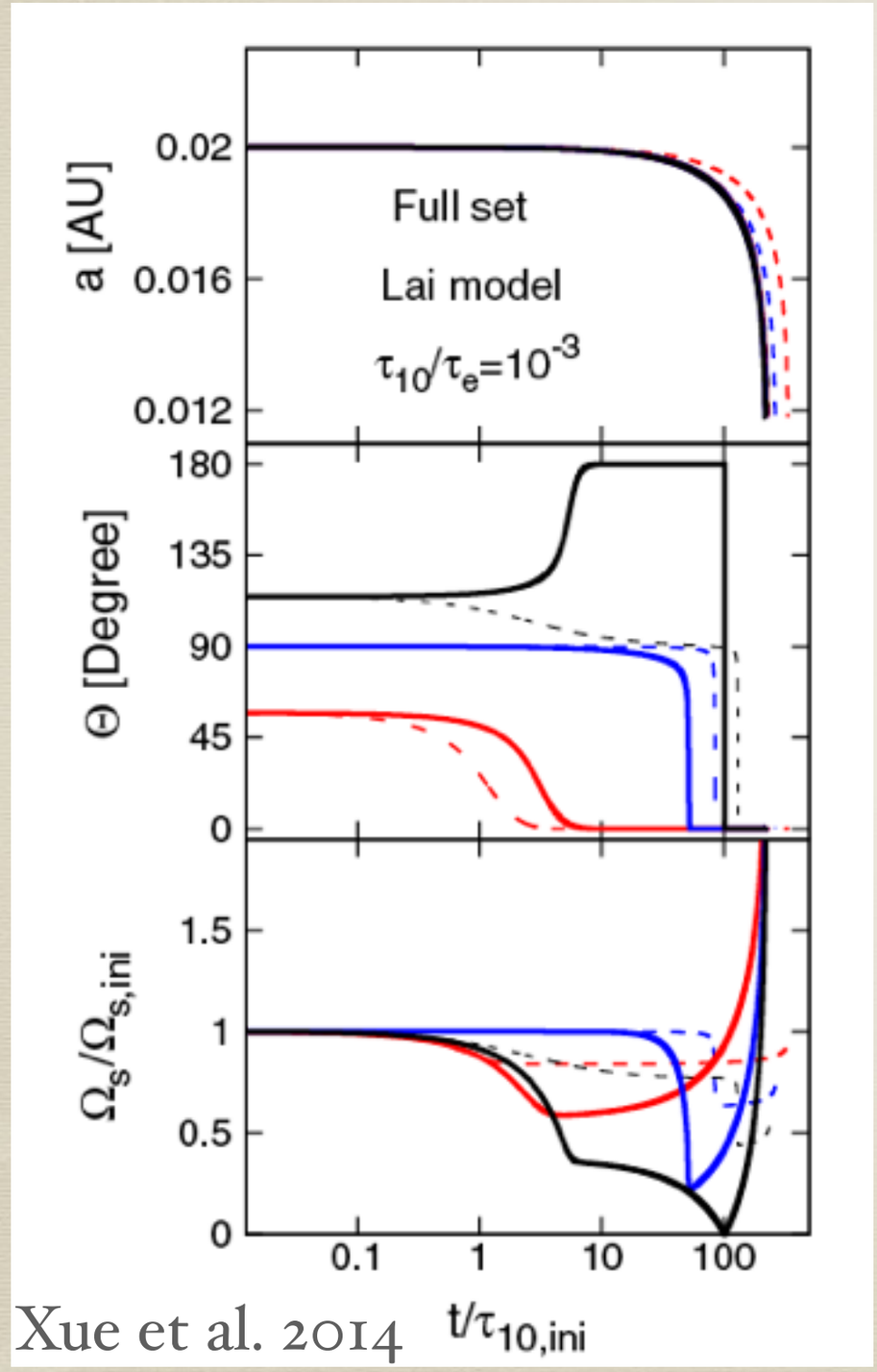

Xue et al. 2014

* Including both inertial wave dissipation and equilibrium tides, obliquity can be aligned from a retrograde configuration before engulfment (Xue et al. 2014).

Tidal Realignment

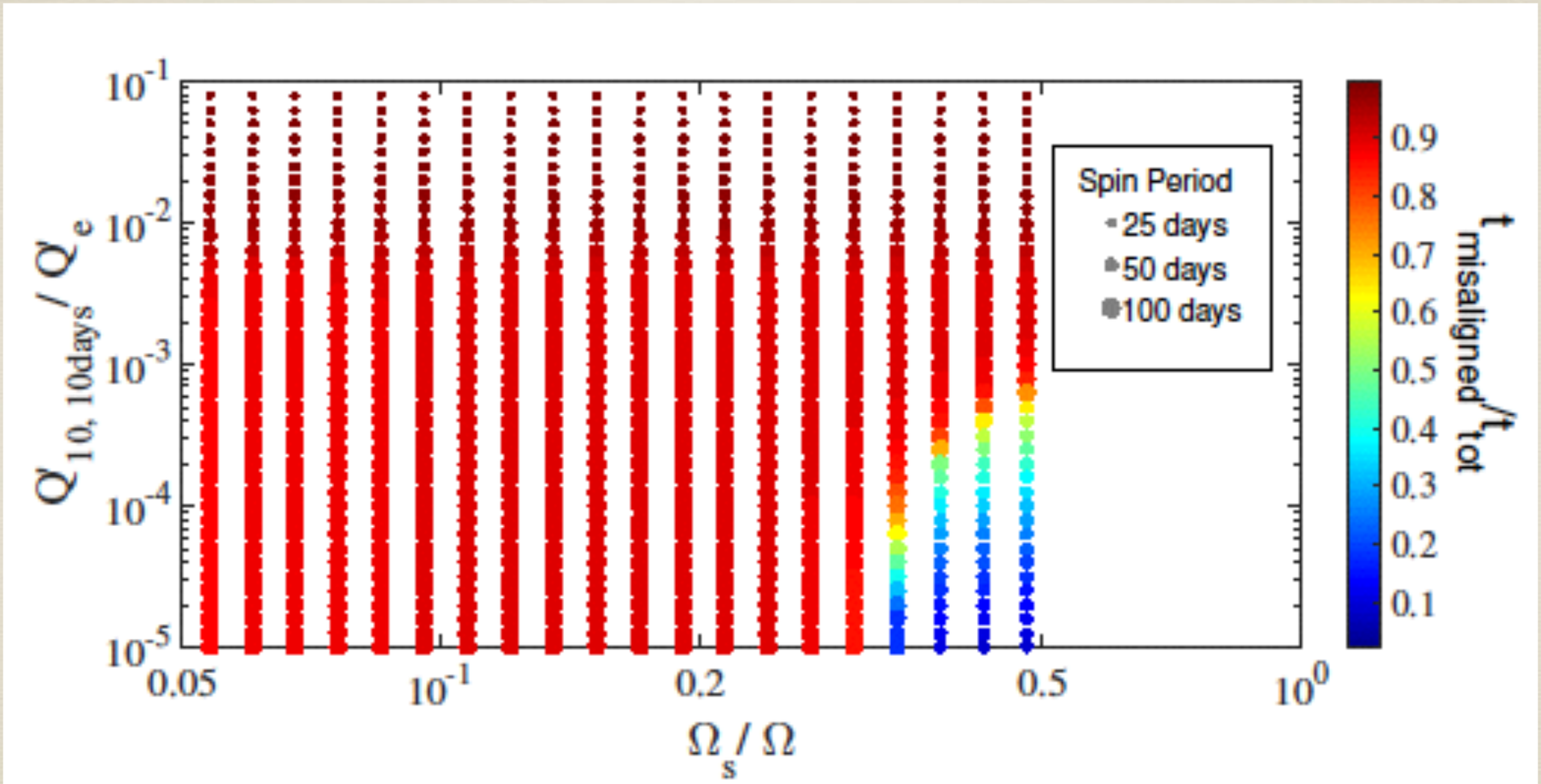

* Spin axis can be aligned before engulfment for high spin rate and low Q value for the (1, 0) component of inertial wave dissipation.

Li & Winn 2016

Probe of Spin-Orbit Misalignment — Photometric Variability

* Photometric Variability due to rotating starspots depends on line of sight inclination ($i_\star$) of the stellar spin axis. (Method introduced by Mazeh et al. 2015)

$\sin(i_\star) = 1$

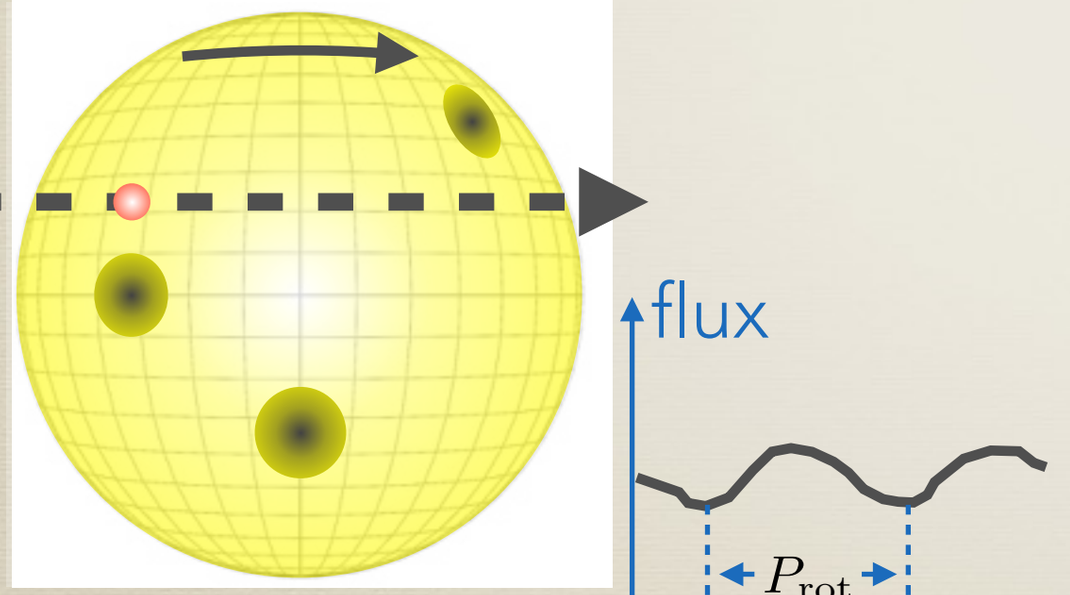

$\sin(i_\star) = 0.5$

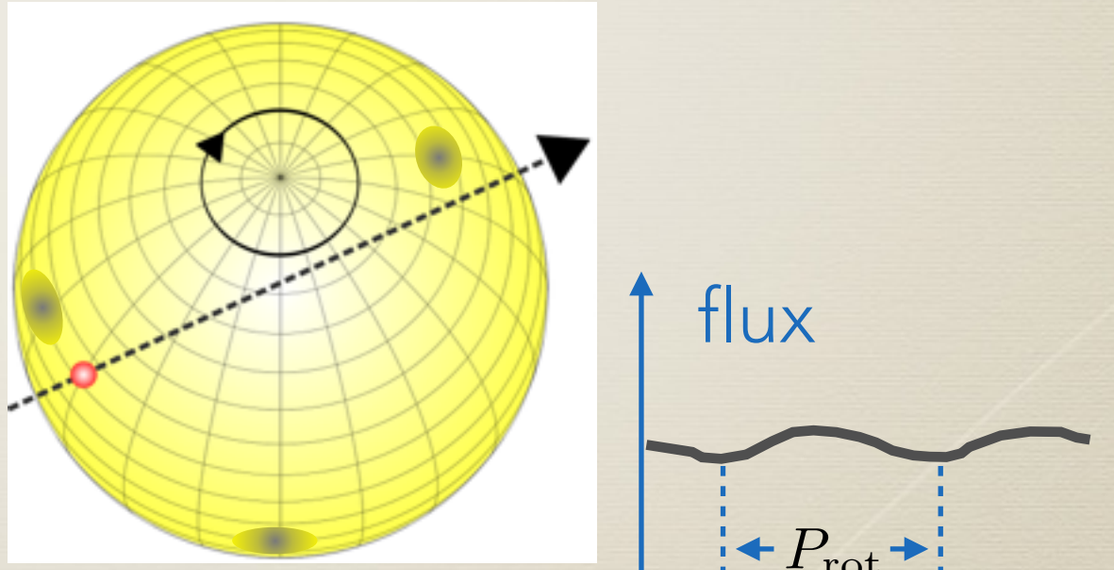

$$R_{\rm var} \propto \sin(i_\star)$$

Probe of Spin-Orbit Misalignment — Photometric Variability

* Photometric Variability depends on line of sight inclination ($i_\star$) of the stellar spin axis.

$$R_{var} \propto \sin(i_\star)$$

* For stellar host of KOIs, the planetary orbit direction perpendicular to the line of sight.

(Method introduced by Mazeh et al. 2015)

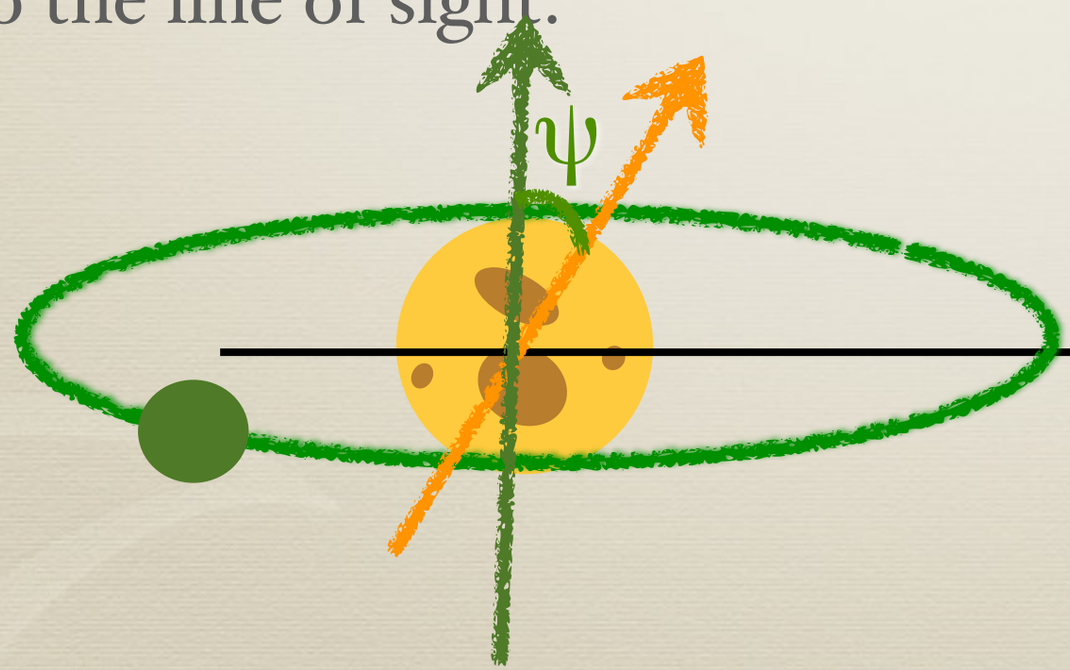

$$\cos(i_\star) = \sin(\psi)\cos(\phi)$$

* $R_{var} \uparrow \Rightarrow \psi \downarrow$

Cool KOI v.s. Hot KOI

* Photometric variability indicates that cool stars tend to be aligned.

  (Mazeh et al. 2015)

* Consistent with results by Rossiter-McLaughlin effects.

  (Schlaufman 2010; Winn et al. 2010; Albrecht et al. 2012.)

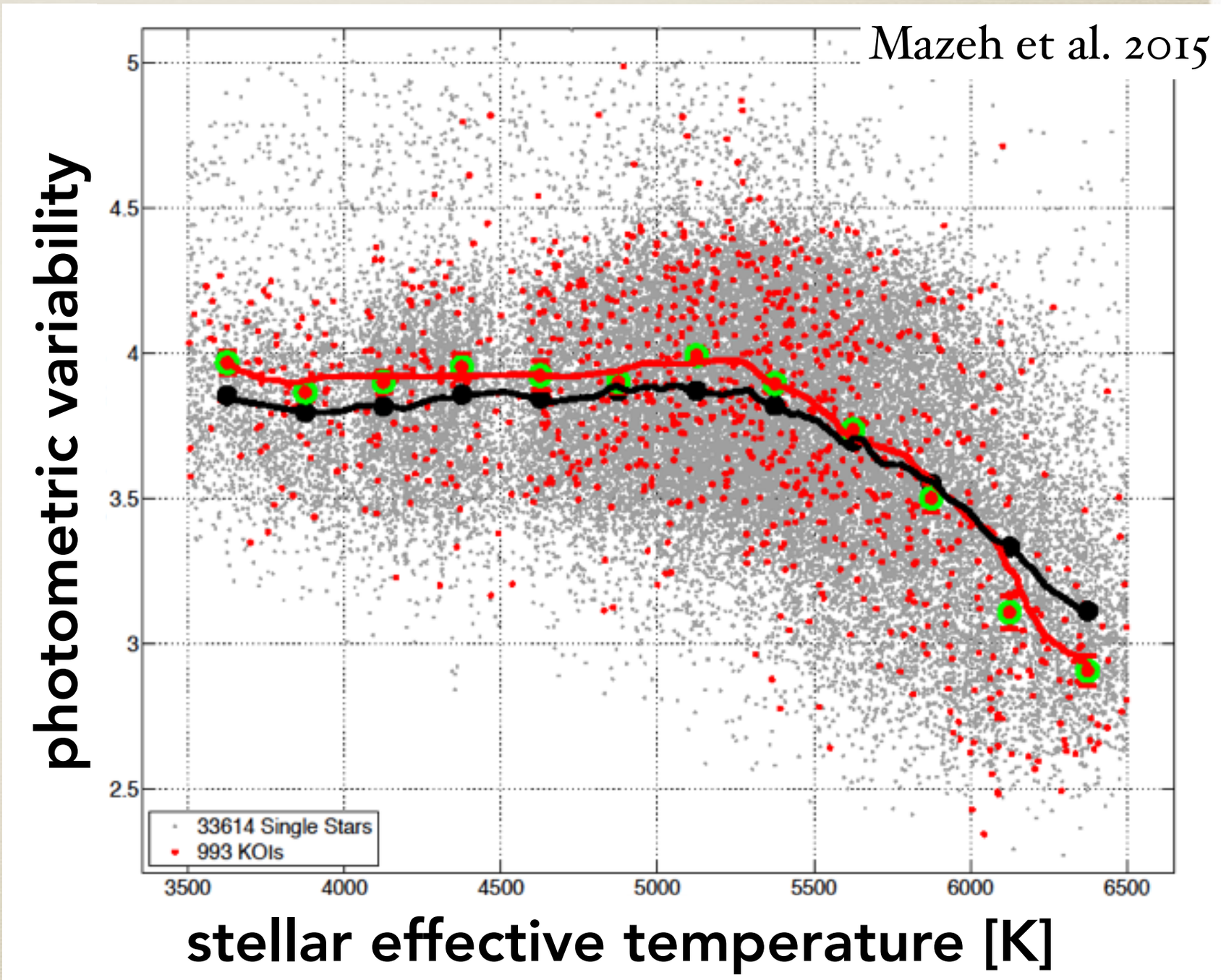

Re-examine Period Dependence

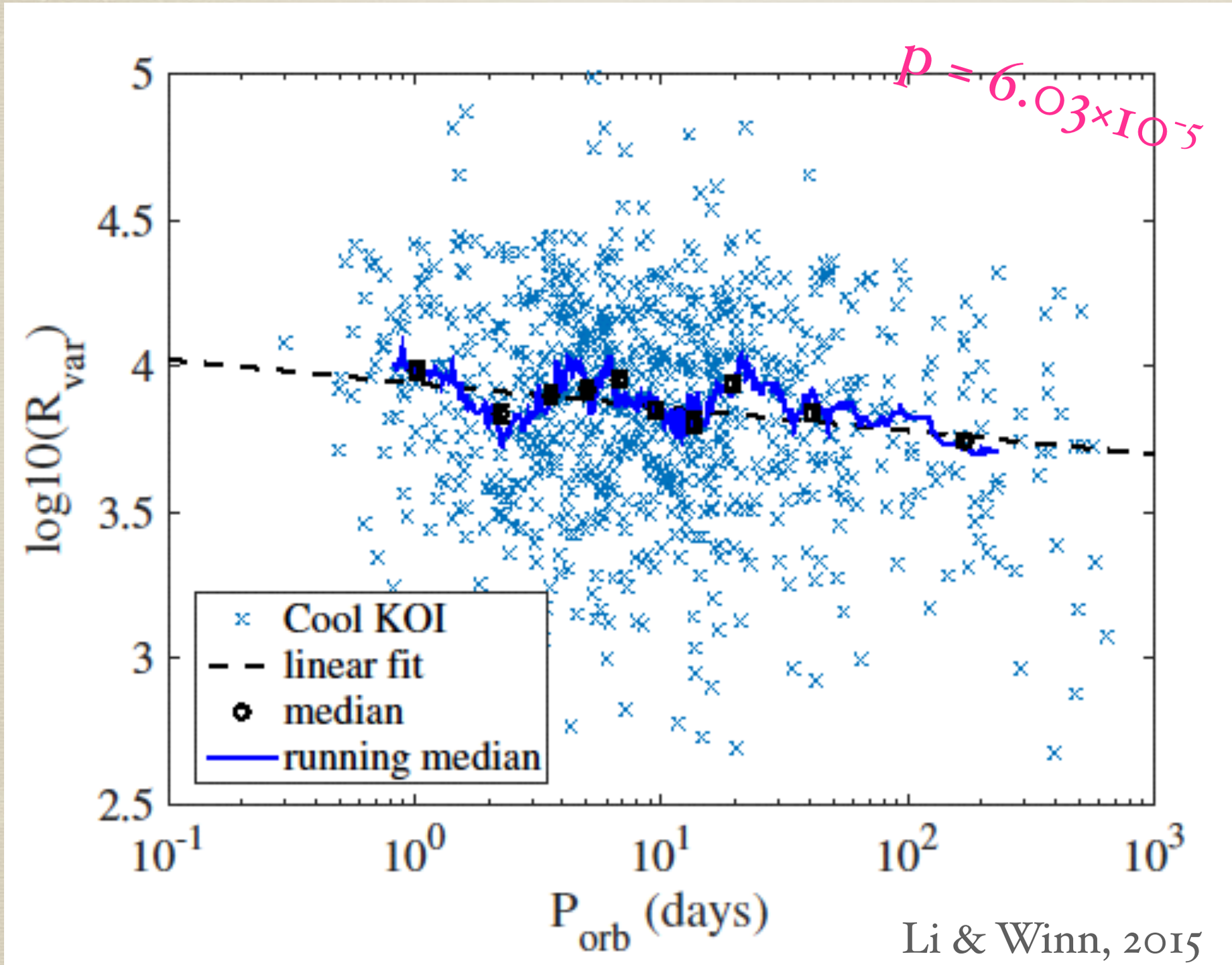

Li & Winn, 2015

* There is a statistically significant linear relationship between R_{var} & P_{orb}.
* Kendall's τ p-value = 0.002
* Spearman's ϱ p-value = 0.002

Period Dependence — Step function vs. Linear relation

Step function motivated by tidal model:
Tidal effects depends sensitively on orbital separation ($t_{tide} \propto P^{10/3}$)

$$\log R_{\rm var} = \beta_0' + \beta_1' I_{<P_{\rm orb,c}}(P_{\rm orb}) + \beta_2' \log P_{\rm orb} + \epsilon.$$

Linear relation fits better than step function

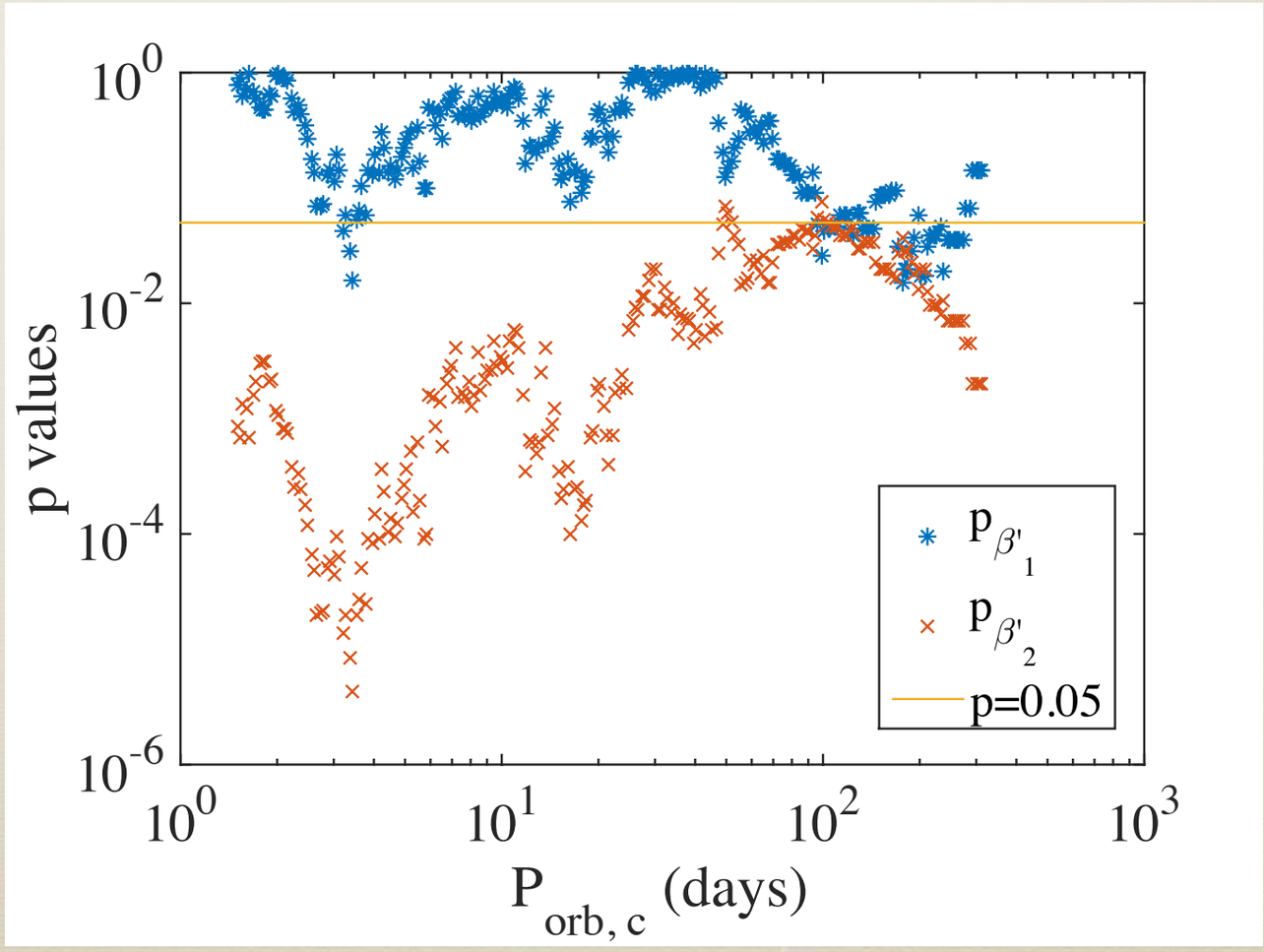

p<0.05 significant dependence

Li & Winn, 2015

Are Tidal Effects Responsible For Spin-Orbit Alignment?

* The statistically significant correlation between the photometric variability (R_{var}) and the orbital period of cool KOIs (P_{orb}) *qualitatively agrees* with tidal re-alignment.
* Linear fit *posts challenges* on the tidal model.
* Other mechanisms need to be involved to produce the overall period dependence.

ON THE OBLIQUITY OF PLANETS

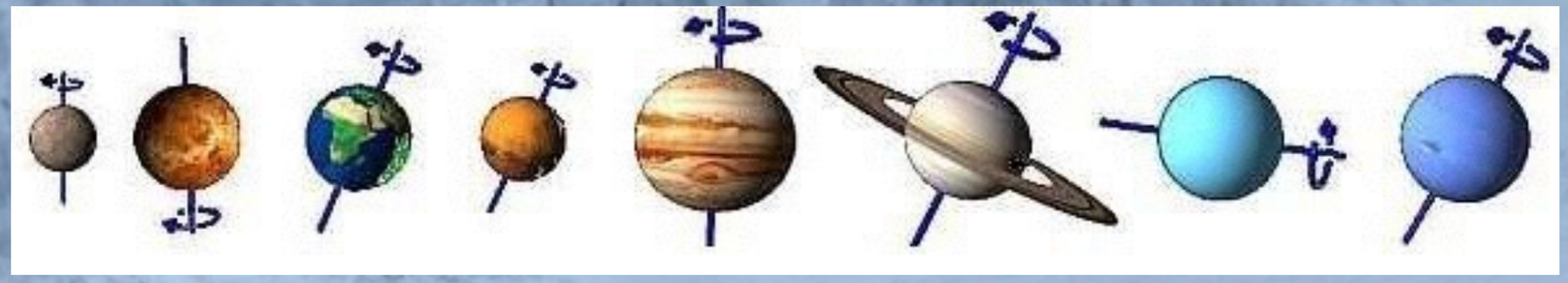

Planet's Obliquity

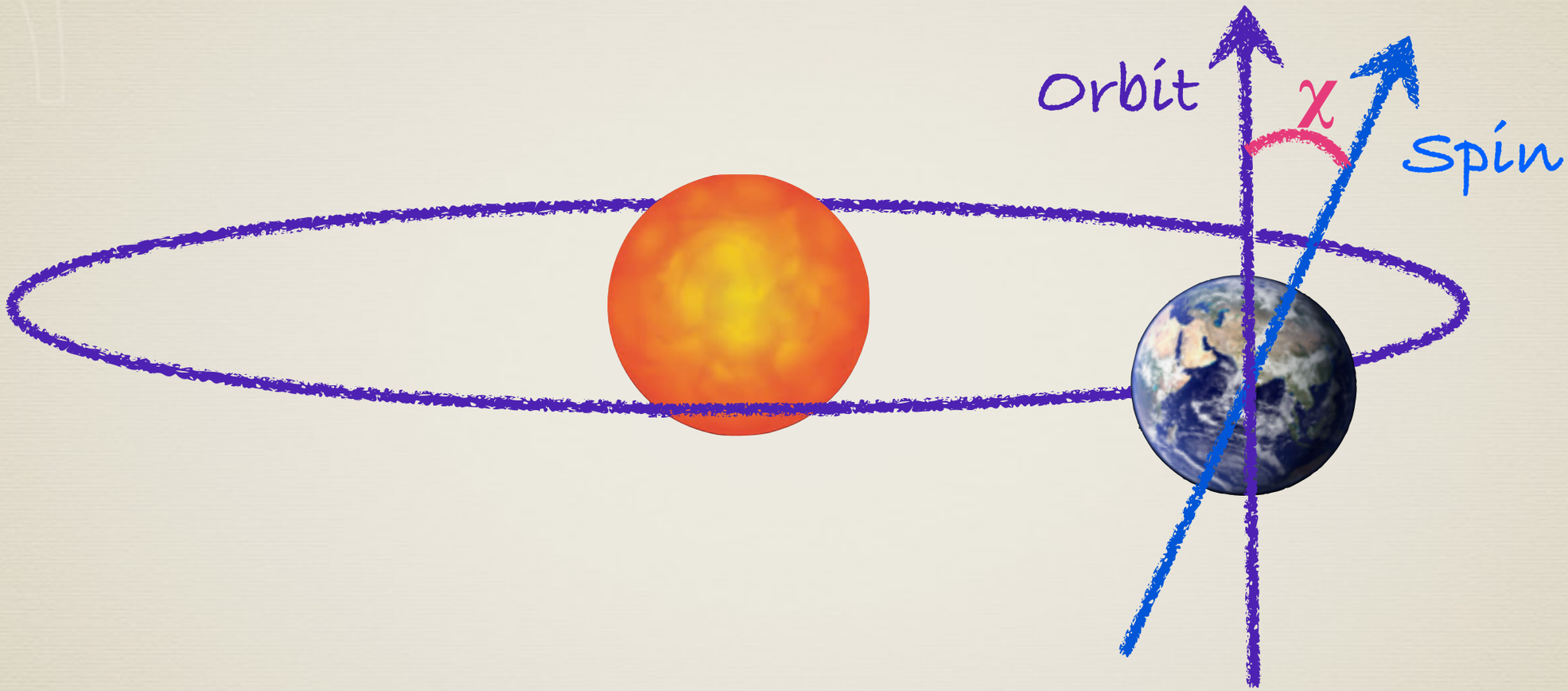

The Earth's obliquity (χ) is the angle between the spin axis of the Earth and the orbit of Earth.

Connection to Climate

- Obliquity variation is very important for the climate of a planet (e.g., Armstrong et al. 2014).
  - obliquity changes affect the latitudinal distribution of stellar radiation.

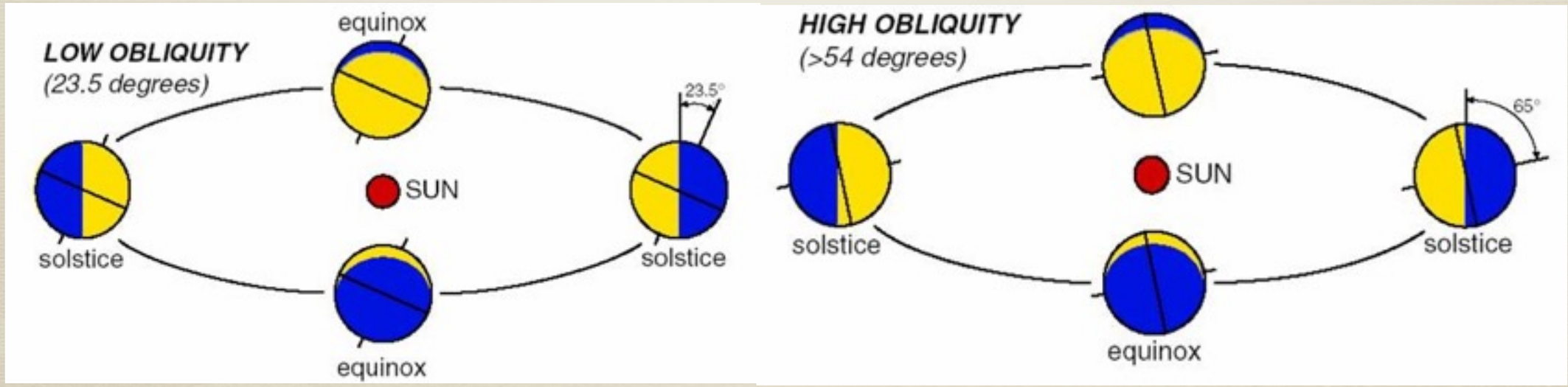

Obliquity Variation of Earth

- Obliquity varies from 22.1-24.5°
- Period ~ 41000yrs

- Milankovitch Cycles: changes in Earth's orbital and orientation parameters affect the climate (e.g., Imbrie 1982)

- Dated evidence:
  - oxygen isotopic ratio in calcite shells or ice cores.

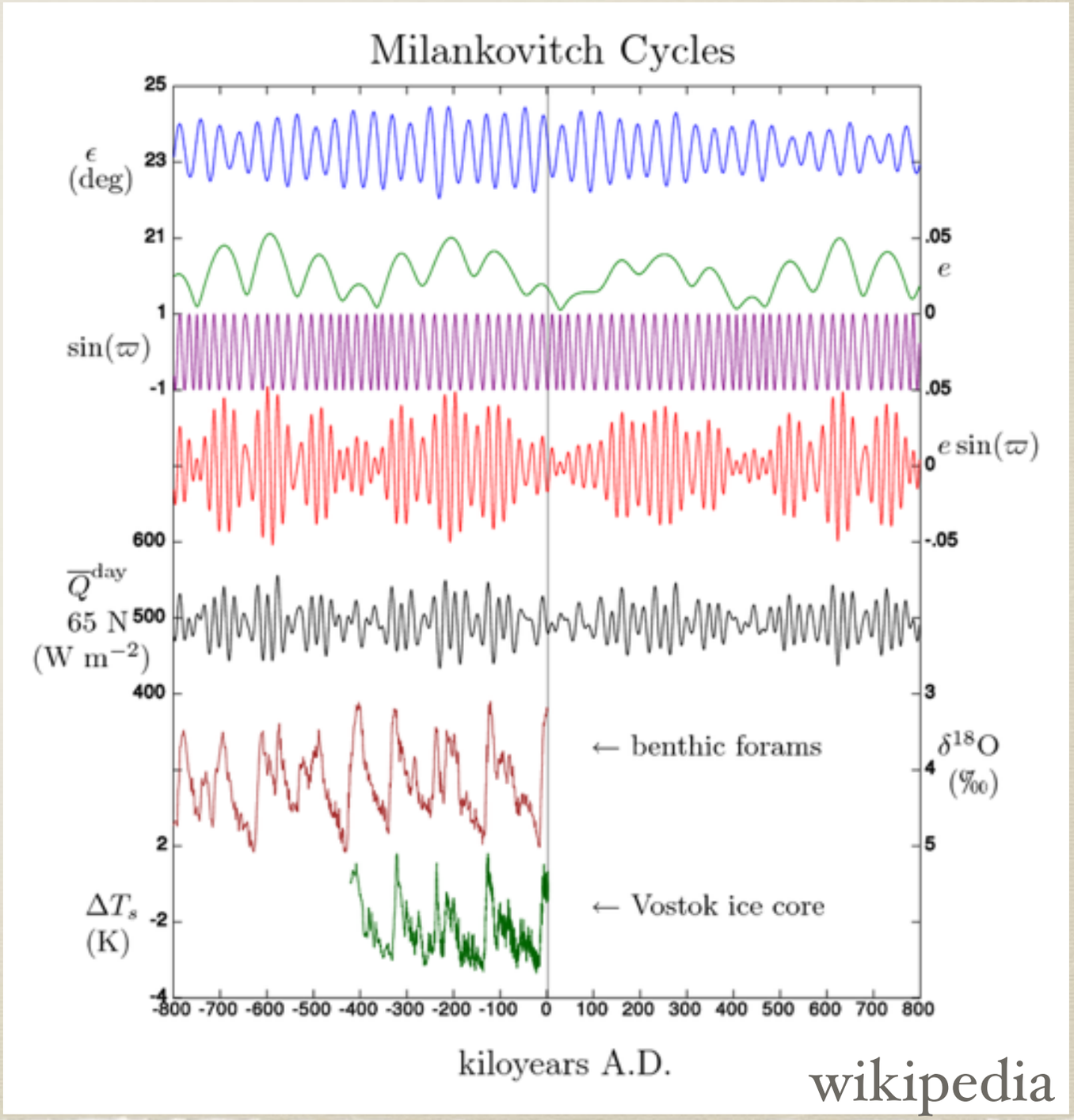

wikipedia

Obliquity Variation of Mars

- Chaotic from 0-60°
- Mars obliquity variation may cause the collapse of atmosphere (Toon et al. 1980, Nakamura & Tajika 2003, Soto et al. 2012)
- Atmosphere precipitation origin of glacierlike landforms at obliquity of 45° ~Myr ago (Forget et al. 2006).

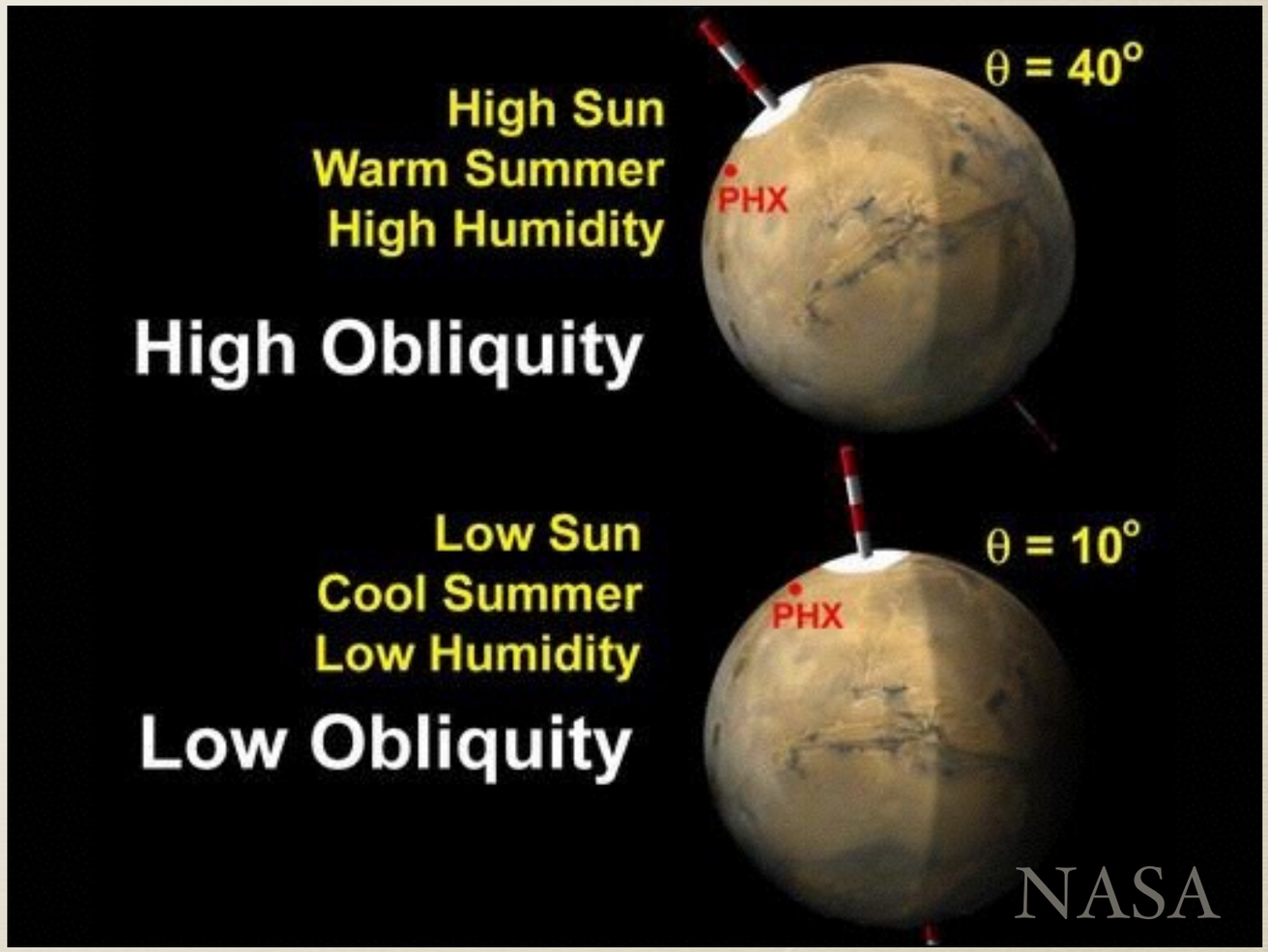

Obliquity Variation of a Moonless Earth

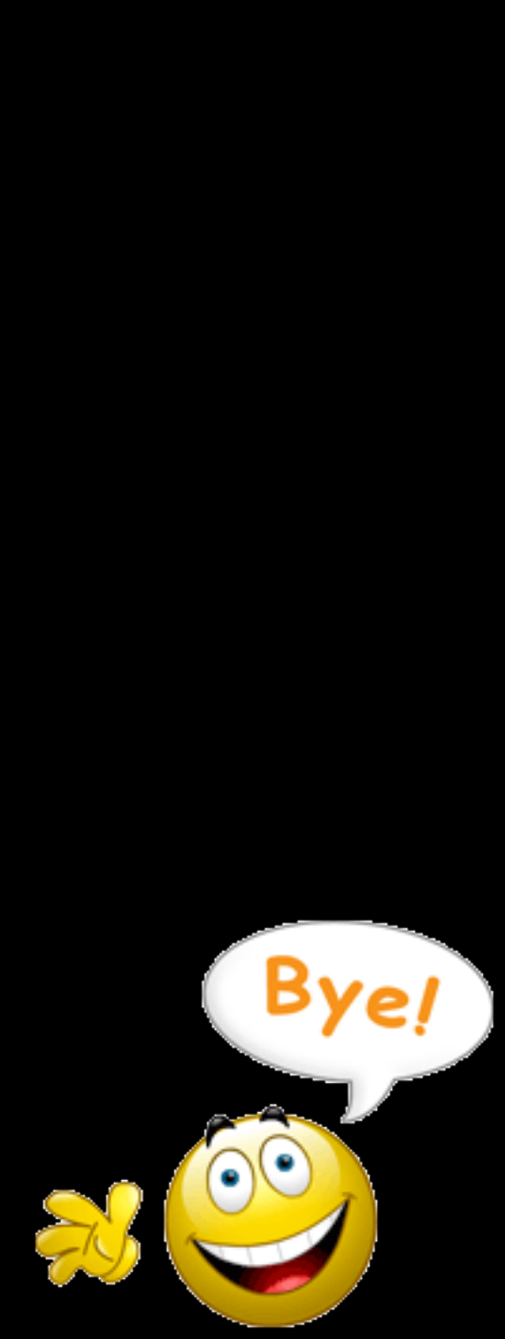

Puzzle of the Obliquity of a Moonless Earth

- Without the Moon, the Earth's obliquity is Chaotic between 0° to ~85° (Laskar et al. 1993) .

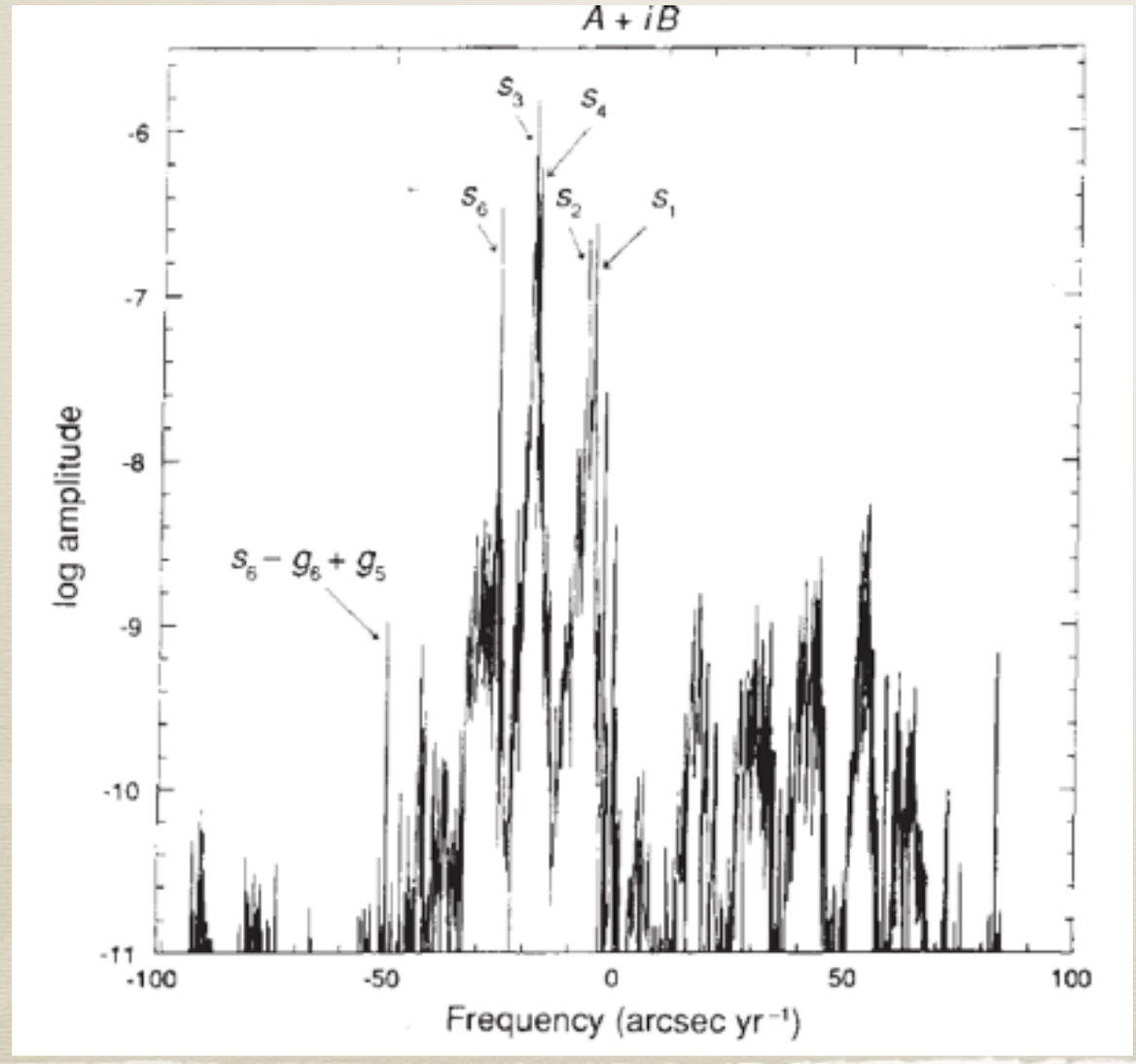

Results from frequency analysis

ε > 54°, climatic zonation would be reversed, low to equatorial latitudes would be glaciated (Williams 1993)

Puzzle of the Obliquity of a Moonless Earth

- Without the Moon, the Earth's obliquity is Chaotic between 0° to ~85° (Laskar et al. 1993) .

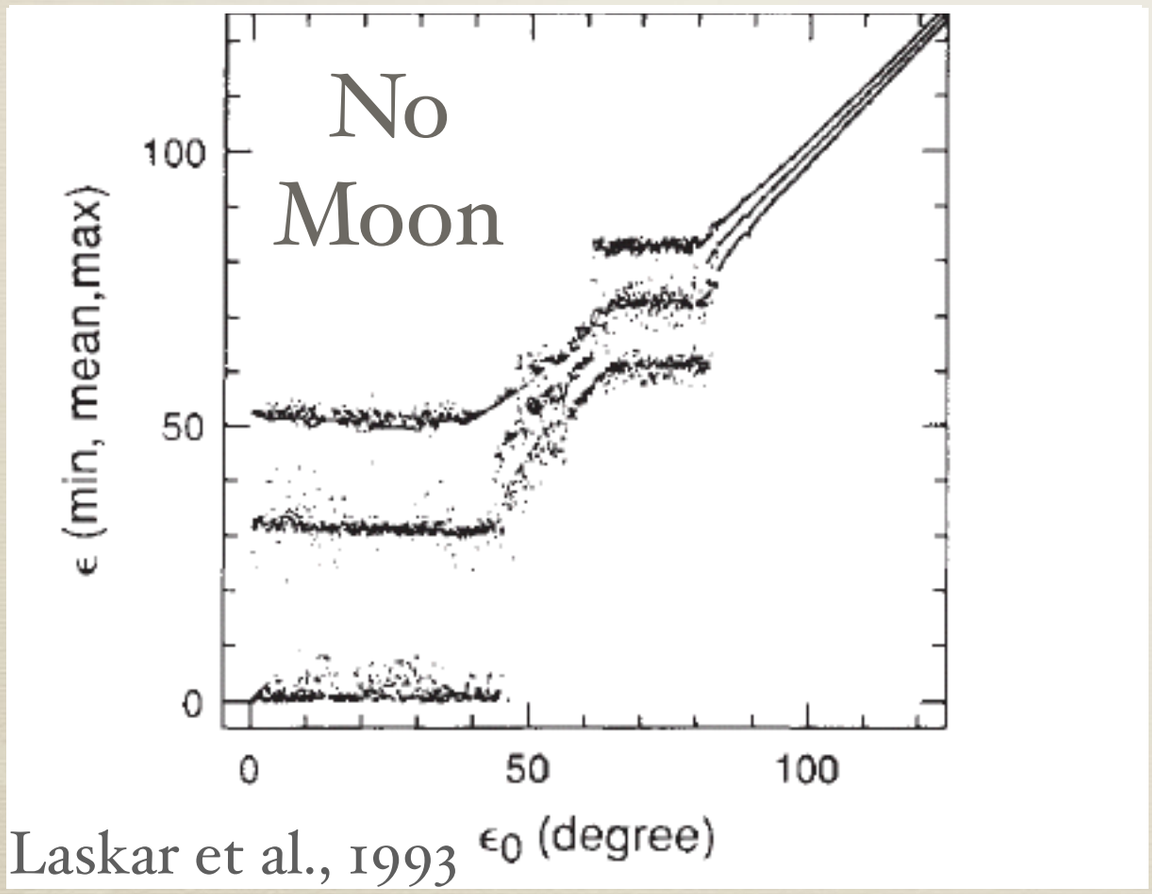

Laskar et al., 1993

Obliquity variation large at ~20 degree without the Moon

Chaotic from 0 to 85 degree

Puzzle of the Obliquity of a Moonless Earth

- Without the Moon, the Earth's obliquity is Chaotic between 0° to ~85° (Laskar et al. 1993) .

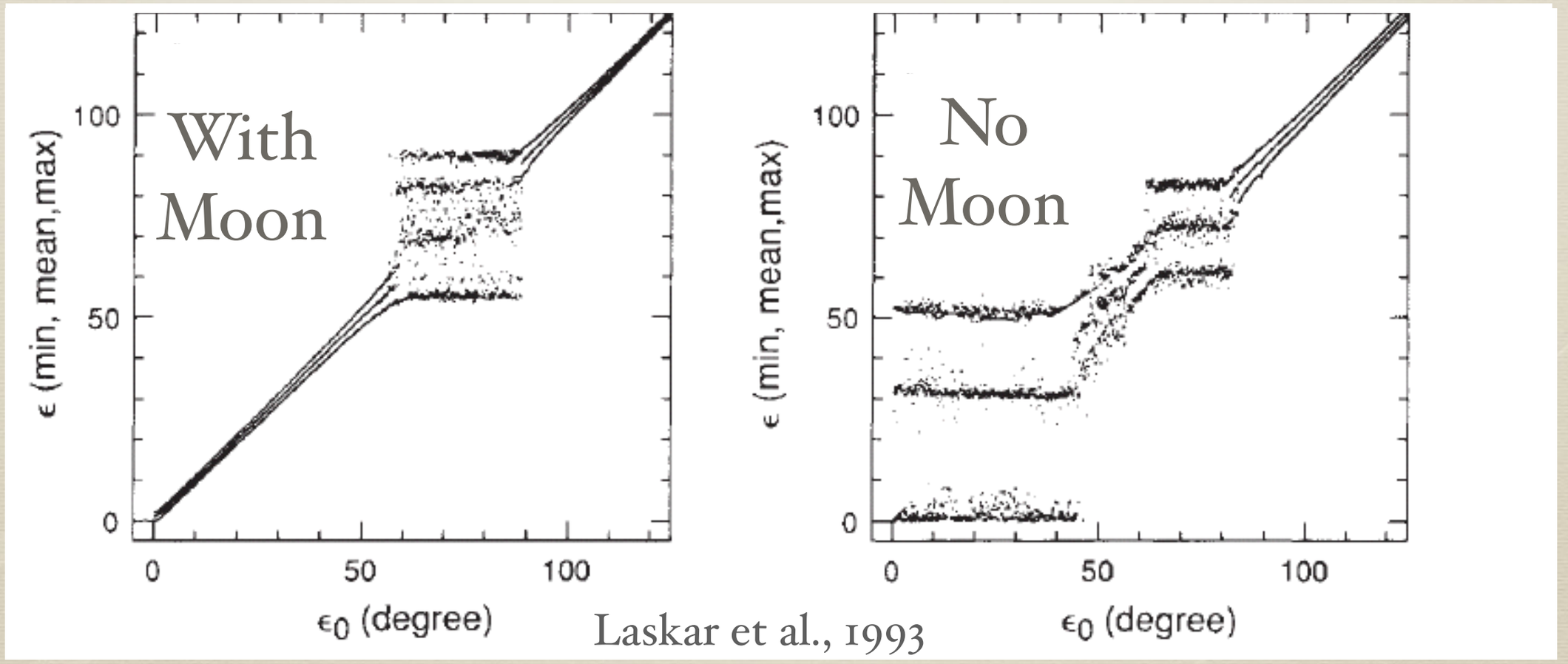

Laskar et al., 1993

Puzzle of the Obliquity of a Moonless Earth

- Without the Moon, the Earth's obliquity is Chaotic between 0° to ~85° (Laskar et al. 1993) .

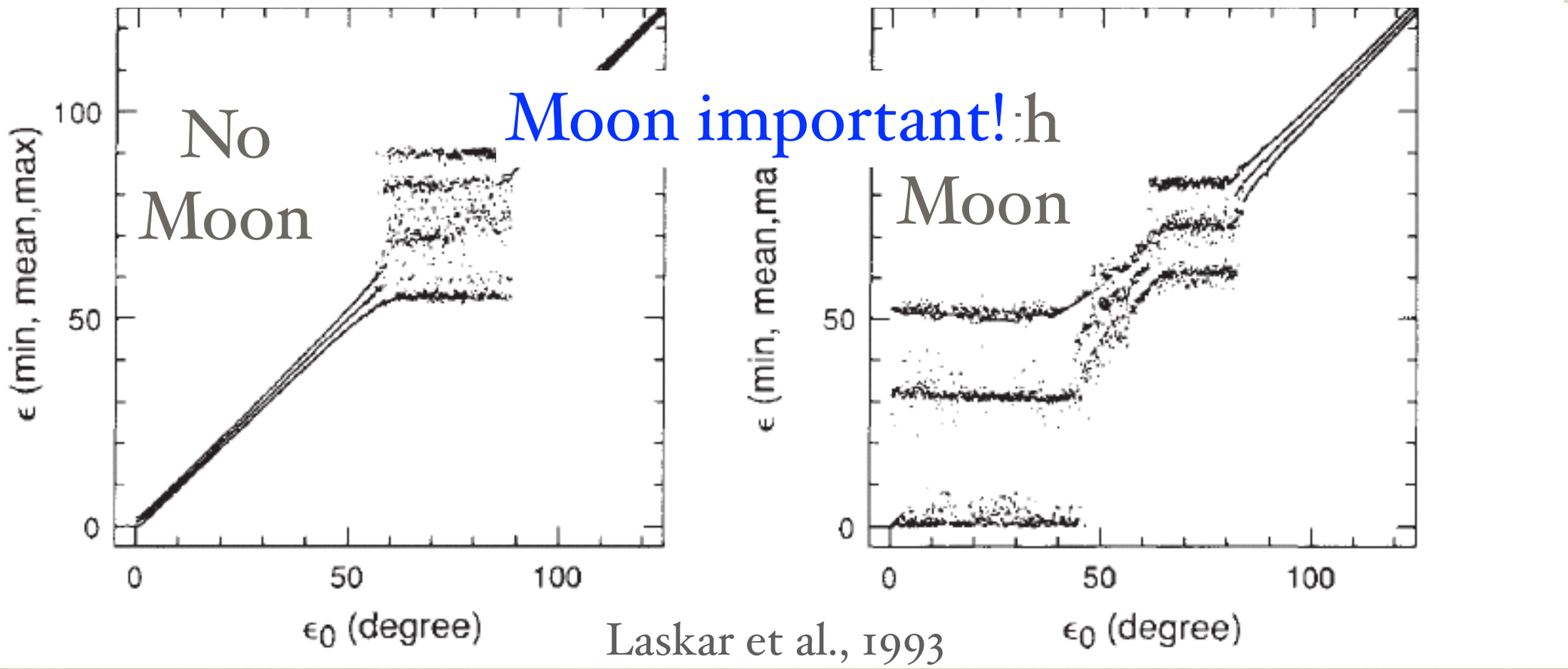

Laskar et al., 1993

Puzzle of the Obliquity of a Moonless Earth

- Recently, N-body simulations show that over ~4Billion years, obliquity constrained between 0-~45° (Lissauer et al. 2012).

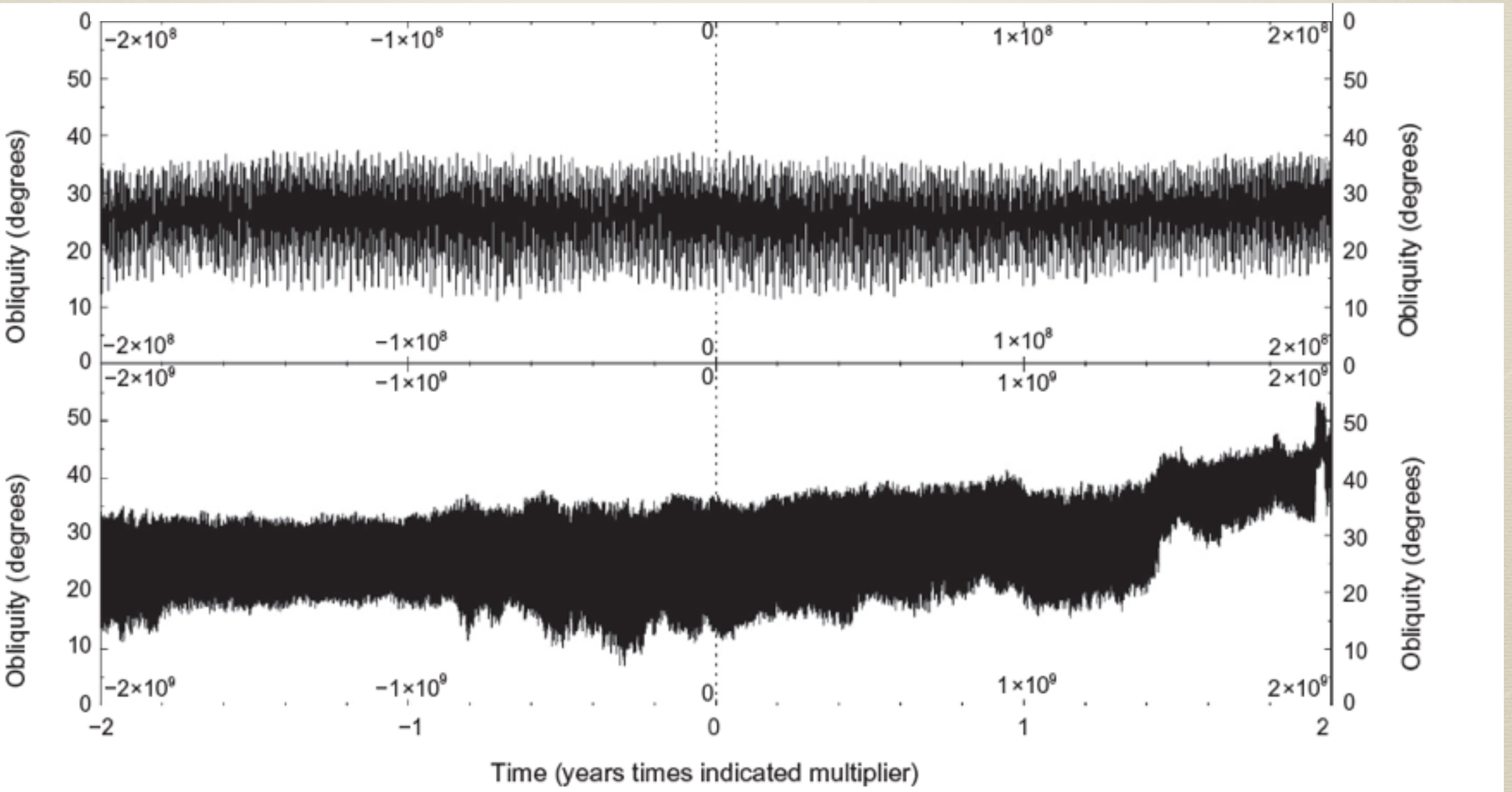

Puzzle of the Obliquity of a Moonless Earth

- Recently, N-body simulations show that over ~4Billion years, obliquity constrained between 0-~45° (Lissauer et al. 2012).

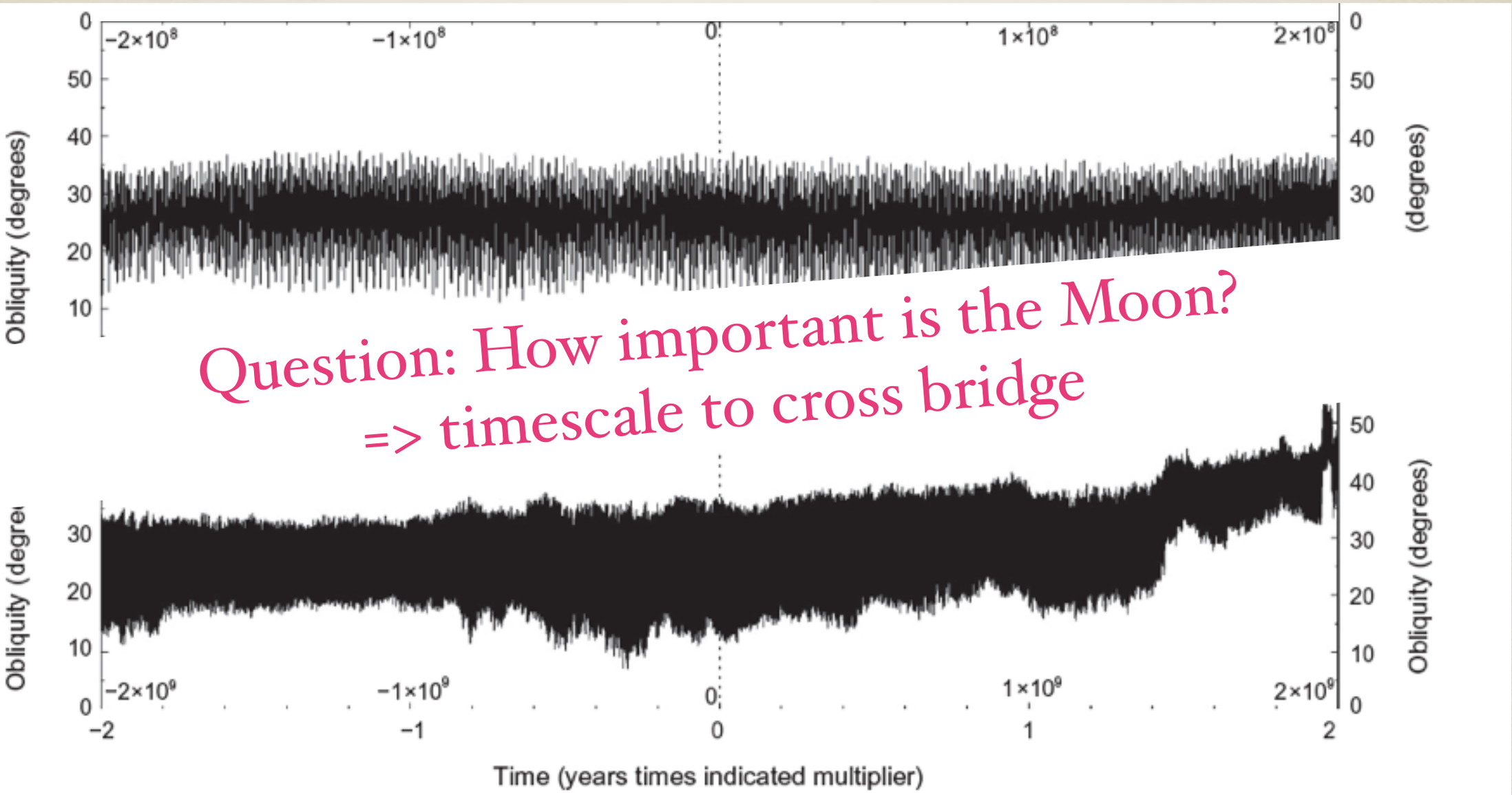

Physical Picture

- The Sun torques the Earth's quadrupole moment:

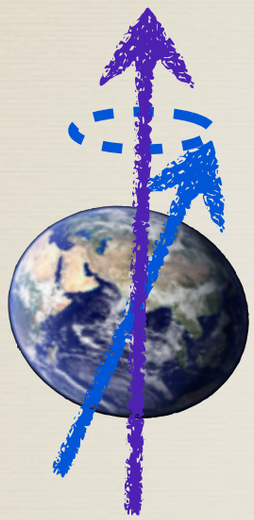

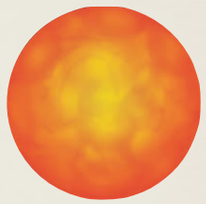

Physical Picture

- The Sun torques the Earth's quadrupole moment:

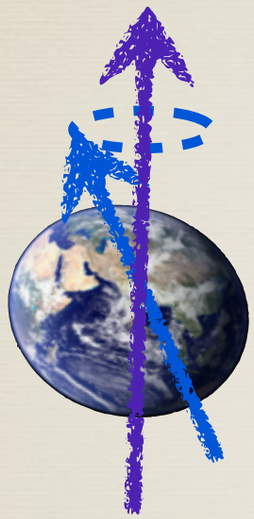

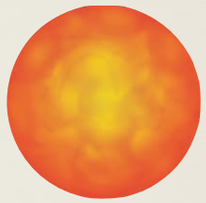

- Spin precession rate: α cos(ε). (ε: obliquity)

$$\alpha = \frac{3G}{2\omega}\left[\frac{m_\odot}{(a_\odot\sqrt{1-e_\odot^2})^3} + \frac{m_M}{(a_M\sqrt{1-e_M^2})^3}(1-\frac{3}{2}\sin^2 i_M)\right]E_d$$

ω: Earth spin,
E_d: Dynamical ellipticity ($E_d \propto \omega^2$).

Precession ↑:
Earth spin (ω)↑, $m_\odot$ ↑, $a_\odot$ ↓

Physical Picture

- The other planets perturb the Earth's orbit:

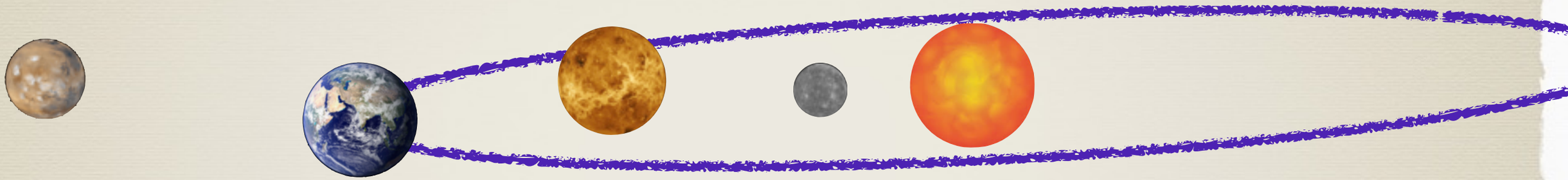

- Earth orbital variation:

$$i\cos\Omega = \sum i_k \cos(s_k t + \gamma_k),$$
$$i\sin\Omega = \sum i_k \sin(s_k t + \gamma_k).$$

s_k: frequencies of the modes due to the perturbation.

Physical Picture

- Hamiltonian:

$$H(\chi,\psi,t) = \frac{1}{2}\alpha\chi^2 + \sqrt{1-\chi^2} \times (A(t)\sin\psi + B(t)\cos\psi))$$

(Laskar et al. 1993)

χ: cos(ε);

ψ: longitude of the spin axis.

α: precession coefficient;

A(t), B(t): depends on the Earth inclination.

Resonances Arise if Frequencies Match (spin precession rate & Earth's inclination variation frequency)
=> Cause Large Obliquity Variation

Physical Picture

- Hamiltonian:

$$H(\chi,\psi,t) = \frac{1}{2}\alpha\chi^2 + \sqrt{1-\chi^2} \times (A(t)\sin\psi + B(t)\cos\psi))$$

χ: cos(ε);

ψ: longitude of the spin

α: precession co

A(t), B(t) ds on the Earth inclination.

Not always require a moon.

Resonances Arise if Frequencies Match (spin precession rate & Earth's inclination variation frequency)
=> Cause Large Obliquity Variation

Numerical Results

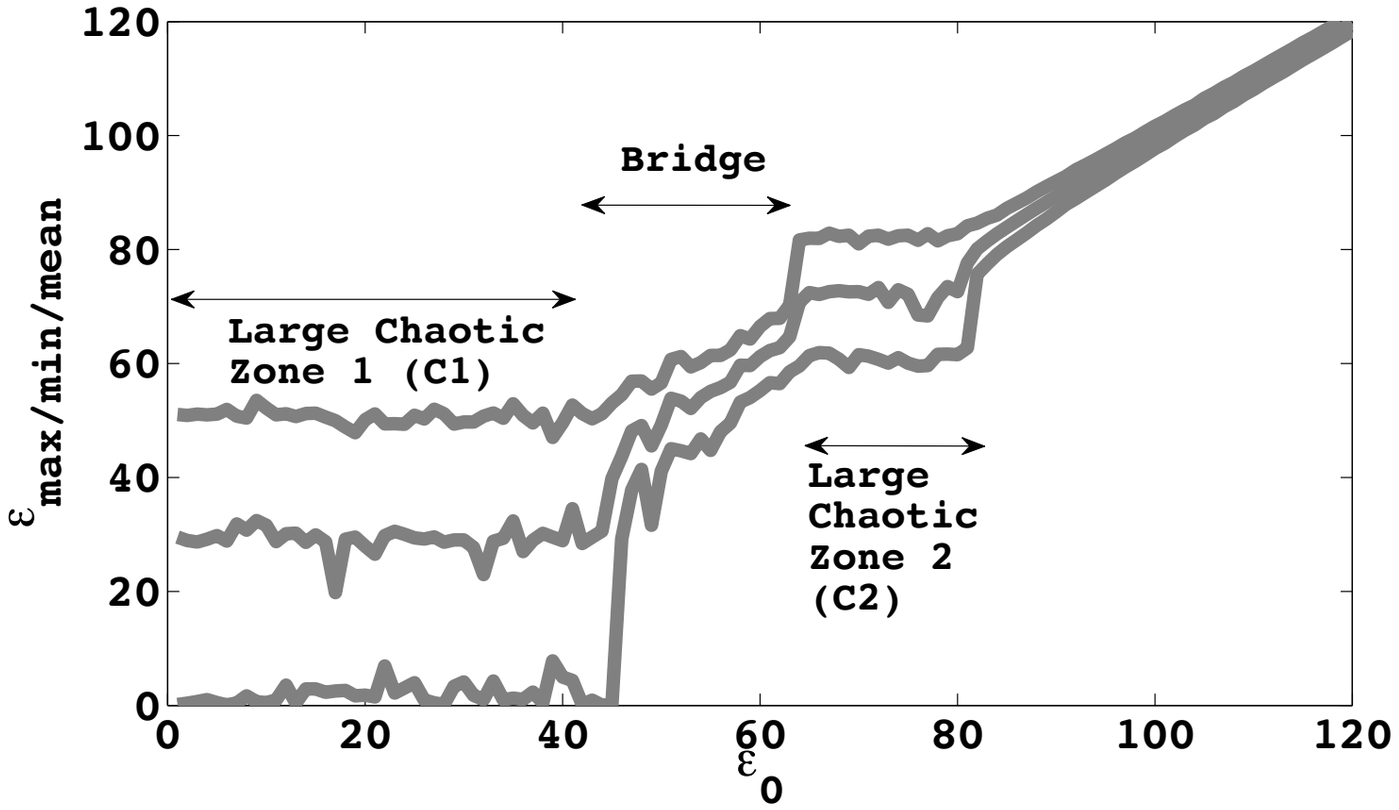

Obliquity variation in ~10Myr, starting with different initial obliquity.

- Two chaotic zones connected with a chaotic bridge (Laskar et al. 1993, Morbidelli 2000).

Numerical Results

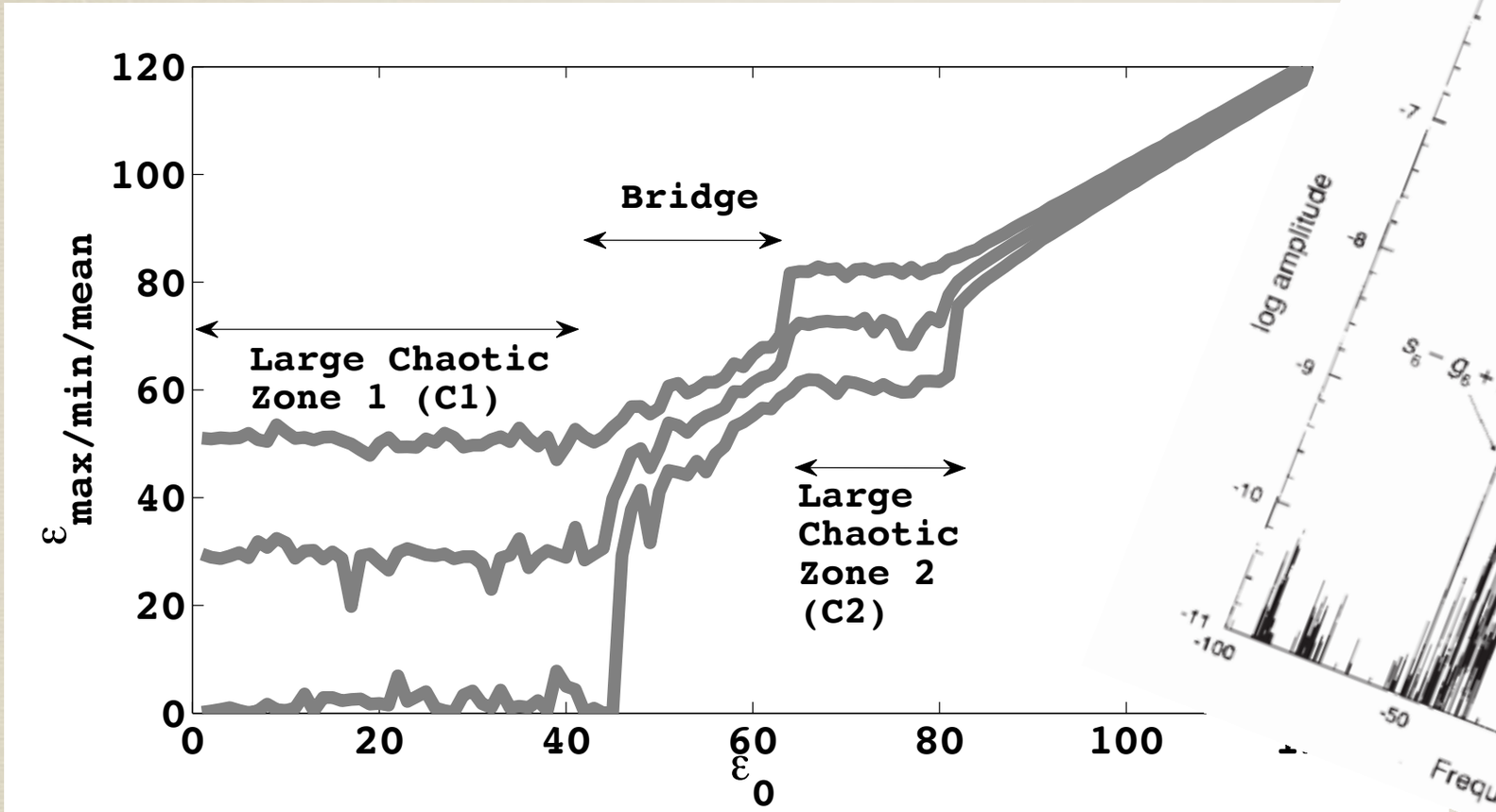

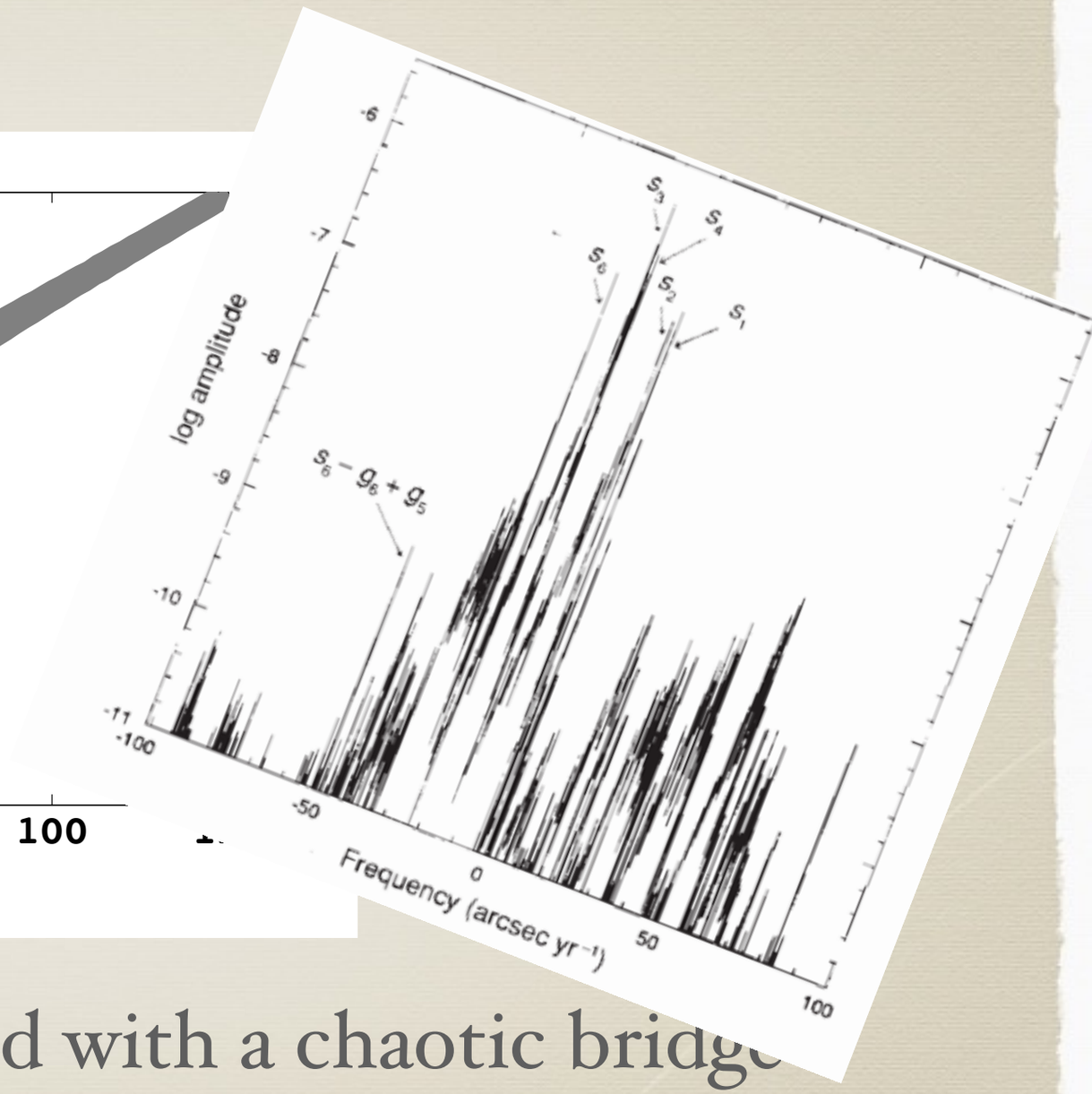

- Two chaotic zones connected with a chaotic bridge (Laskar et al. 1993, Morbidelli 2000).

Numerical Results

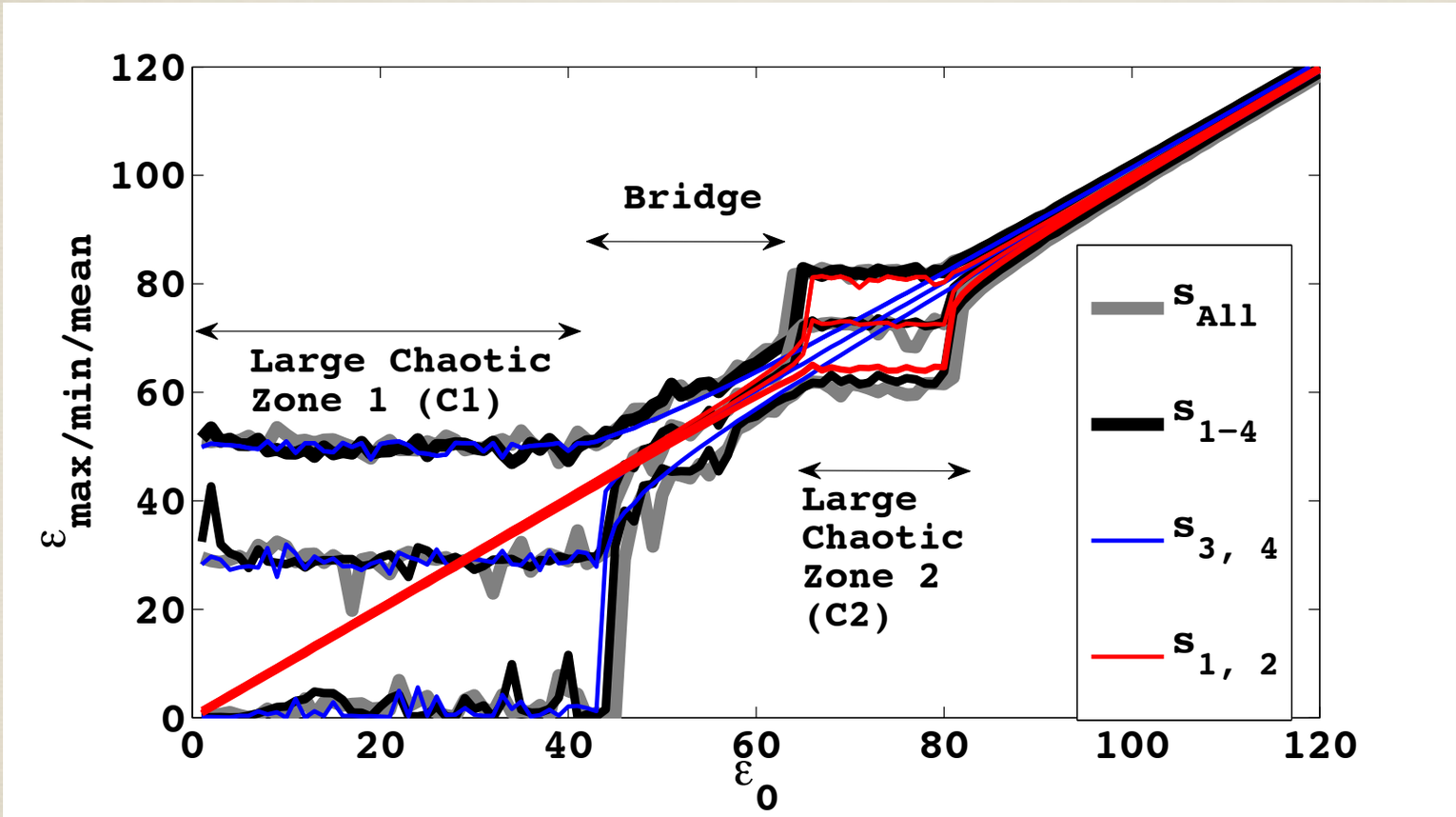

- Two chaotic zones connected with a chaotic bridge (Laskar et al. 1993, Morbidelli 2000)
- C1: caused by s3, s4; C2: caused by s1, s2

Numerical Results

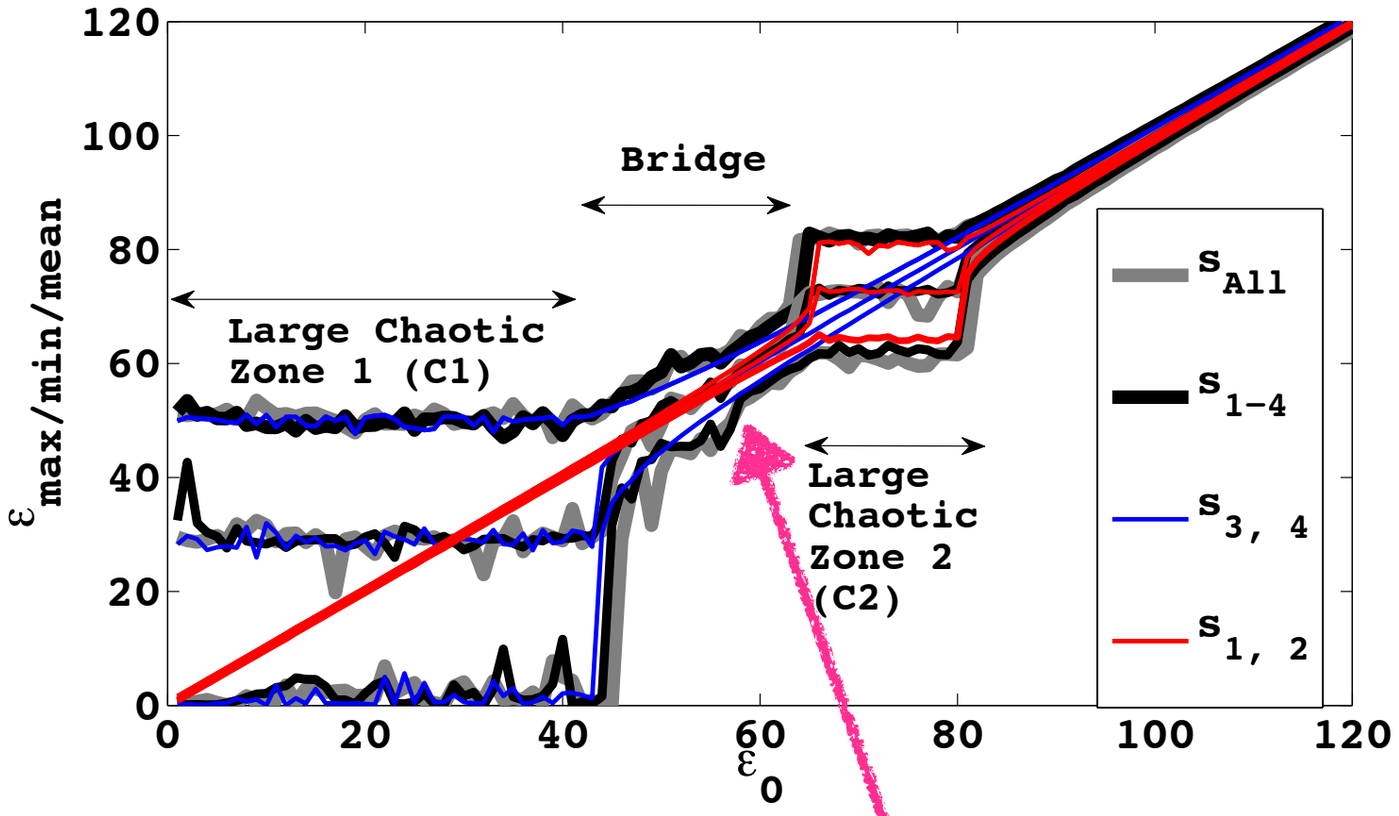

Obliquity variation in ~10Myr, starting with different initial obliquity.

Need to understand the diffusion in the bridge

Resonances

- Averaging the Hamiltonian over the primary resonances with canonical transformation to obtain the secondary resonances.

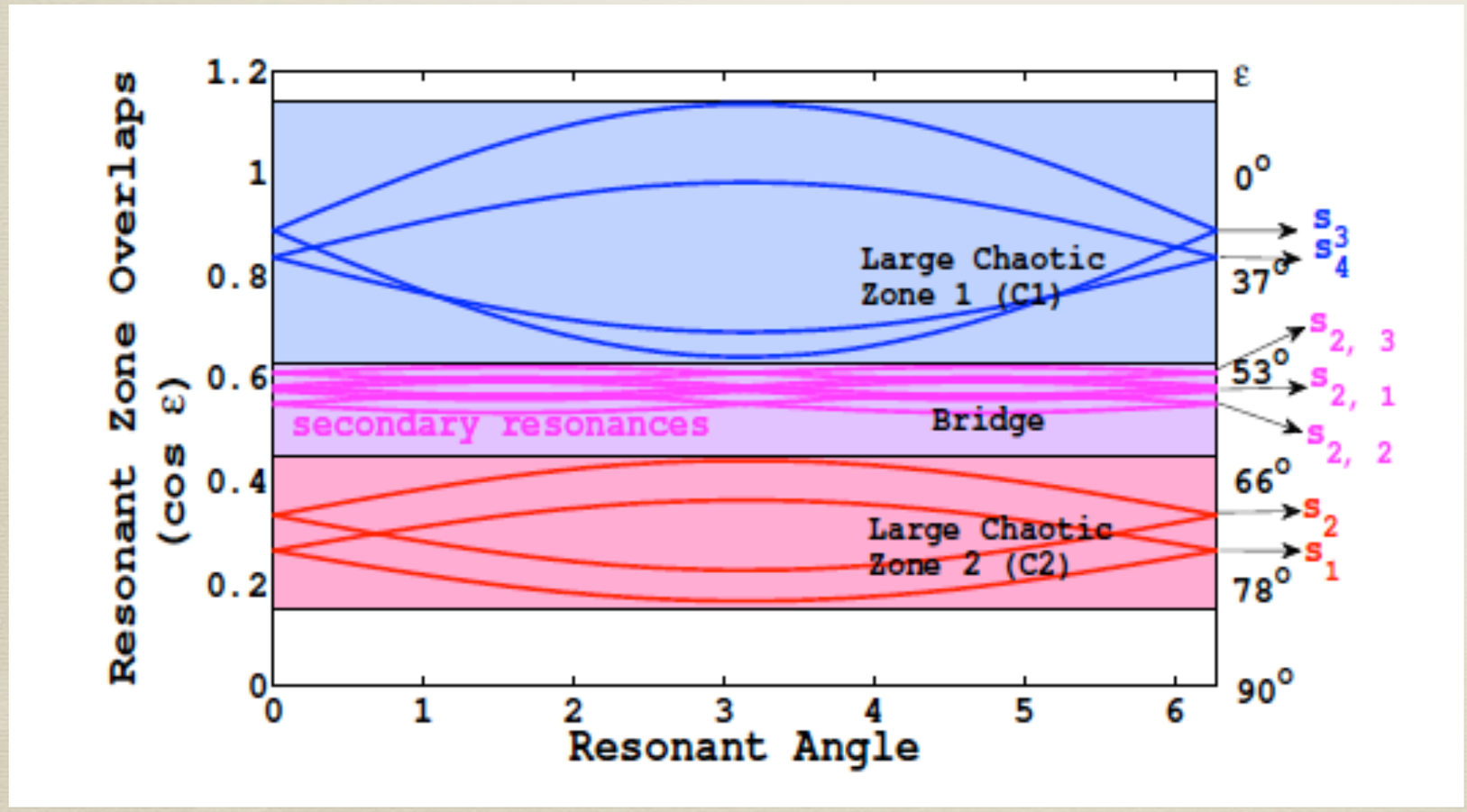

Overlap of the secondary resonances causes the diffusion cross the bridge. (Chirikov 1979).

Li & Batygin, 2014a

Diffusion by Overlap of Resonances

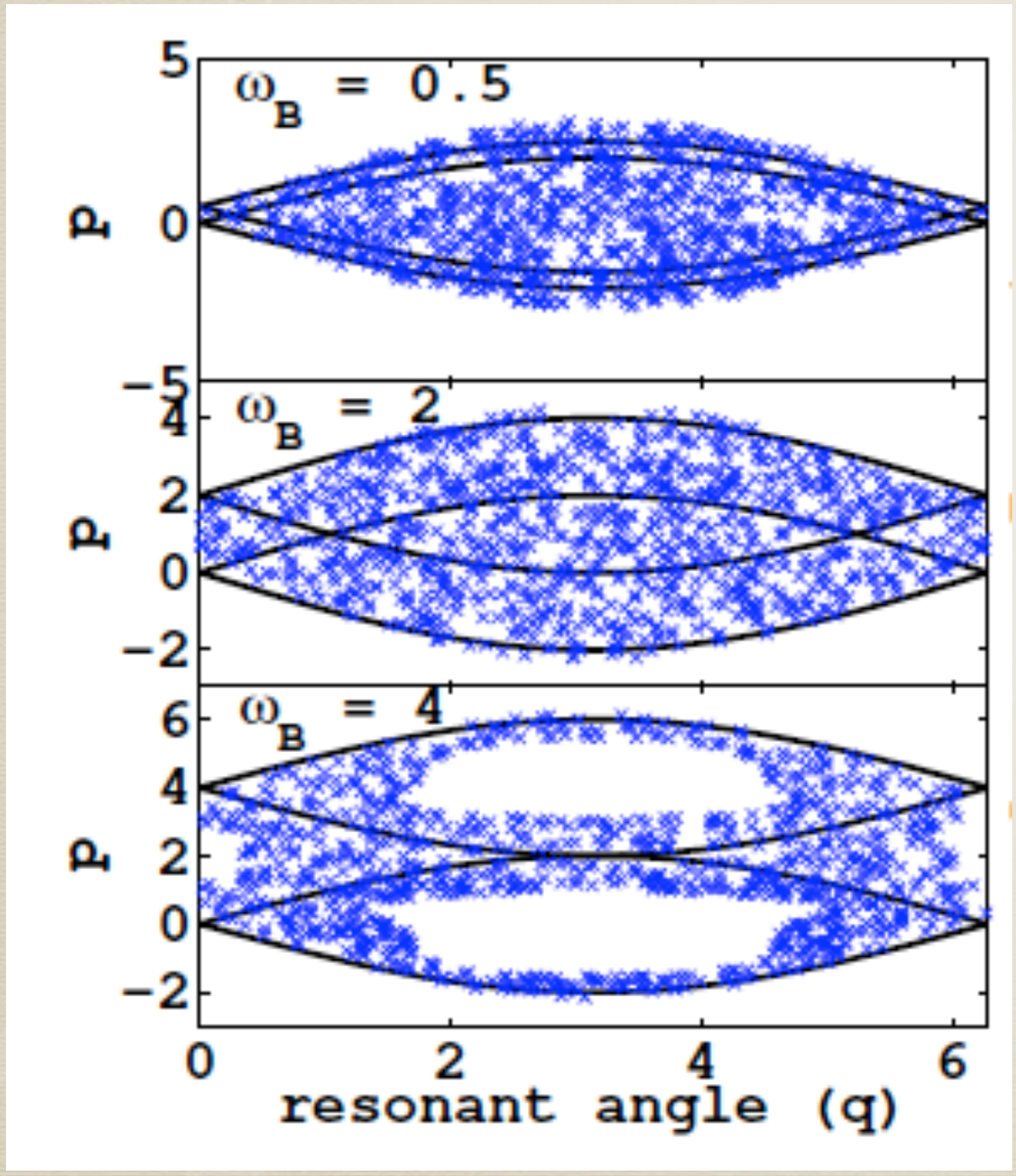

- Overlap of resonances cause chaos.
- Large separation

  Diffusion Coefficient ↓
  Diffusion time ↑,

  Lyapunov Exponent ↓
  Chaos ↓.

Chirikov 1979

Diffusion

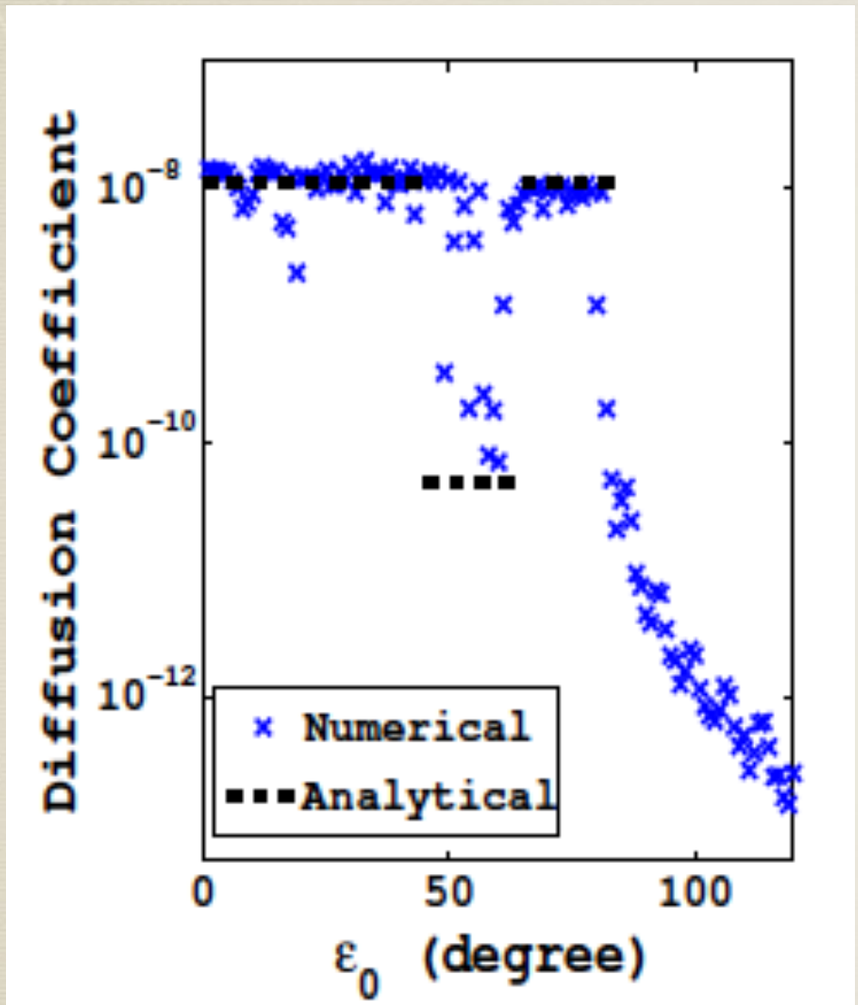

- Diffusion coefficient:

$$\delta\chi^2/\delta t$$

- Diffusion coefficient lower in the bridge.
- Diffusion timescale ~ 2Gyr in the bridge

- Numerical Results consistent with analytical estimations.

Li & Batygin, 2014a

Numerical Runs

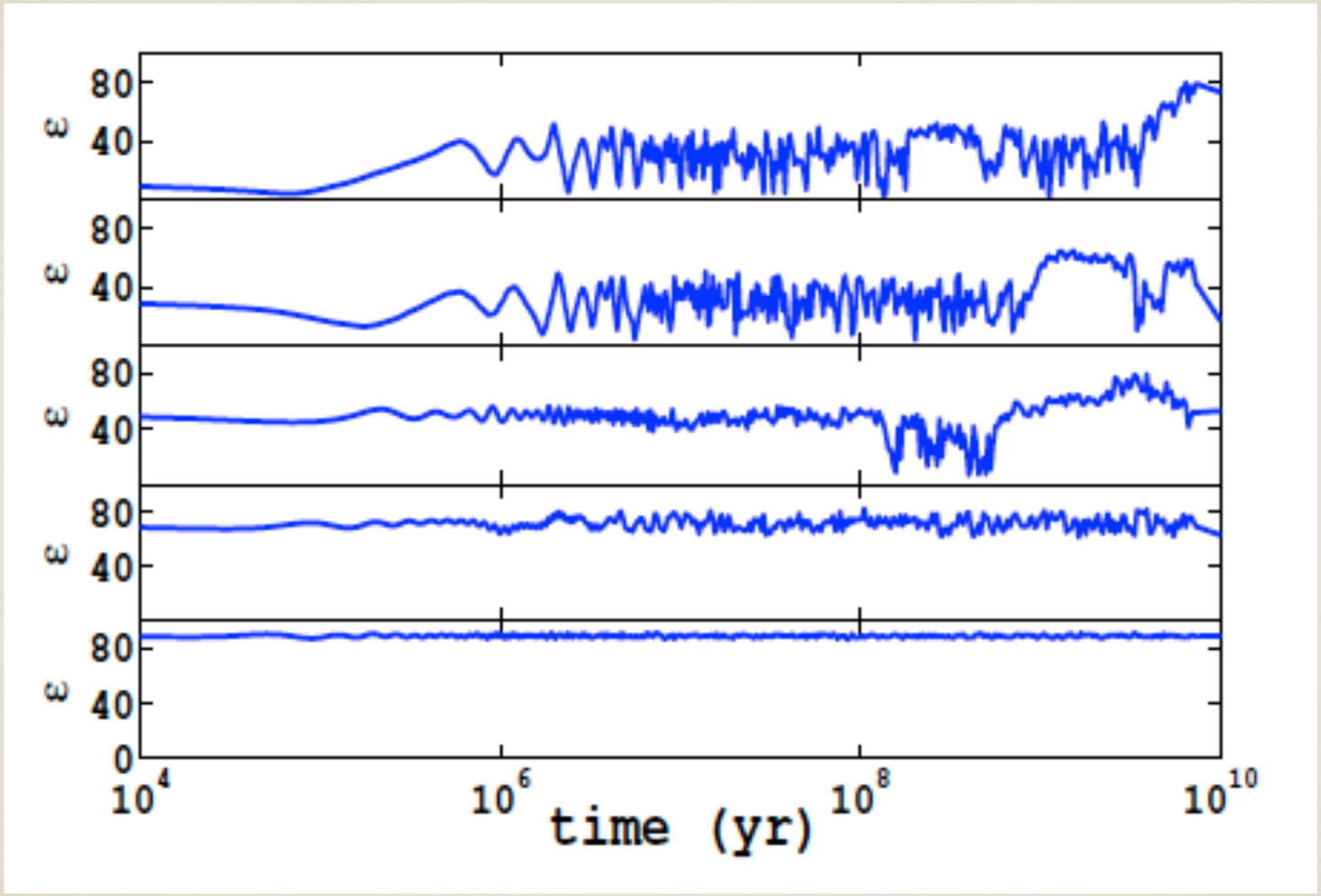

- It takes ≳ Gyrs to cross the bridge.

Li & Batygin 2014

Numerical Runs

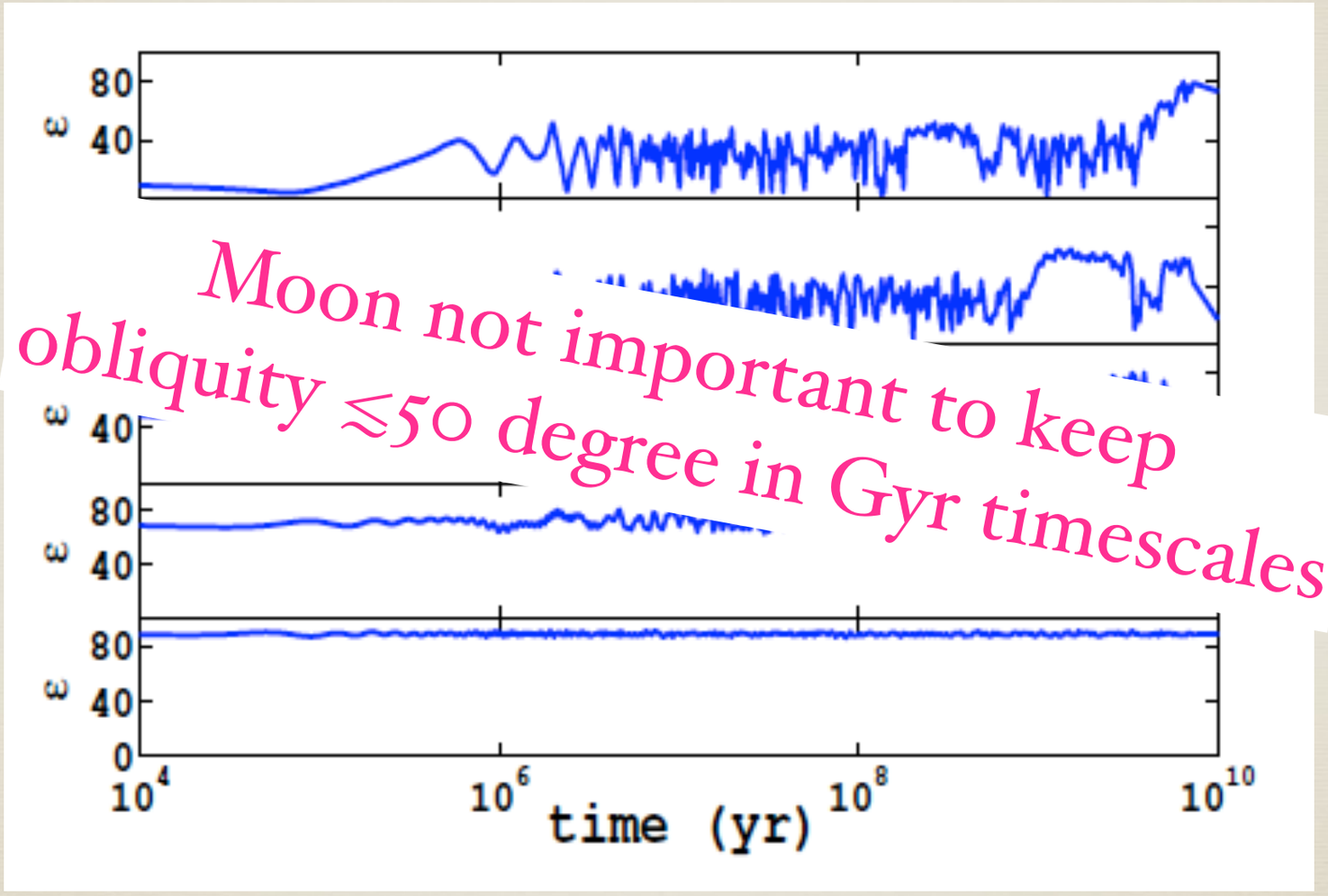

- It takes ≳ Gyrs to cross the bridge.

Li & Batygin 2014

Application to Exoplanetary Systems

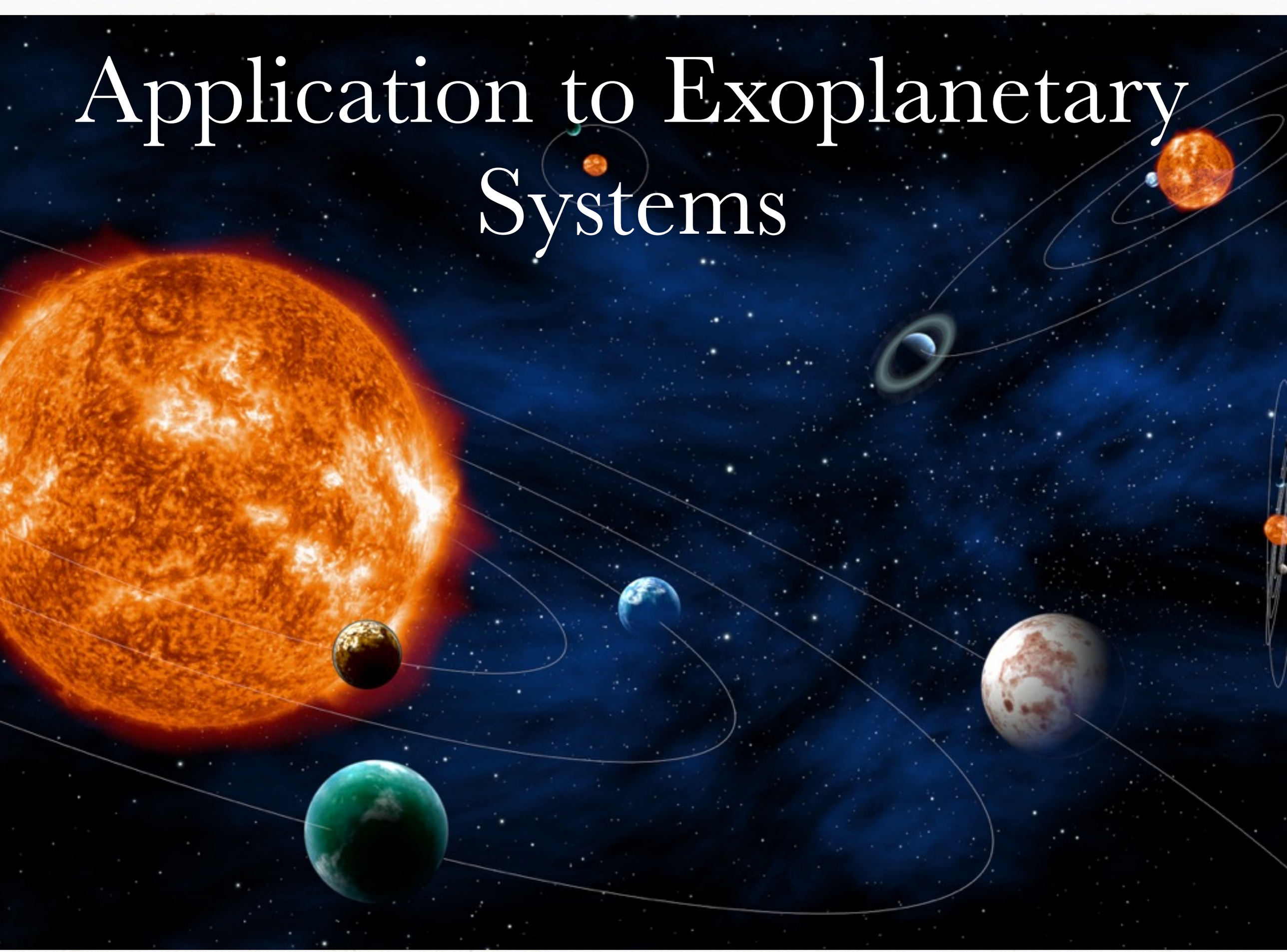

Application to Exoplanetary Systems

* Scale over which biological material may be transmitted via collision ejecta

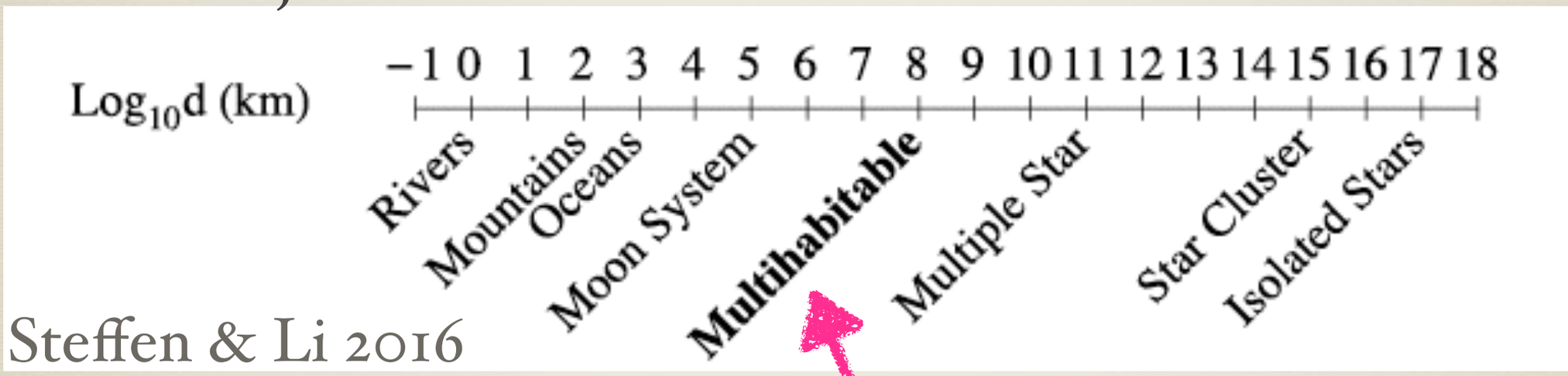

Steffen & Li 2016

Kepler-36: a super-Earth and a mini-Neptune with *a* differ by only 0.013 AU.

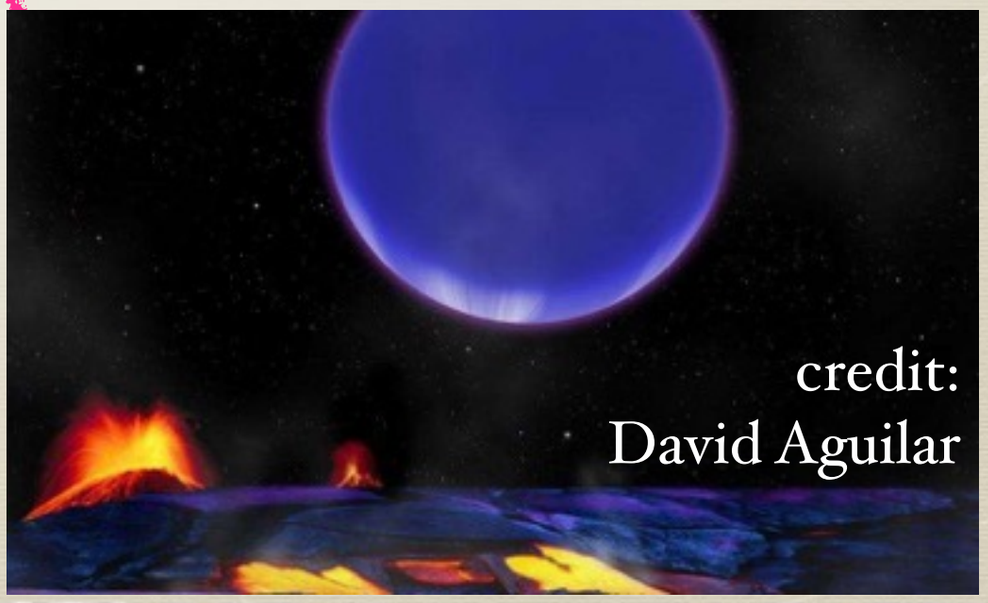

credit:
David Aguilar

Application to Exoplanetary Systems

* Substitute Earth by two closely separated planets

Inner substitute planet →

Outer substitute planet →

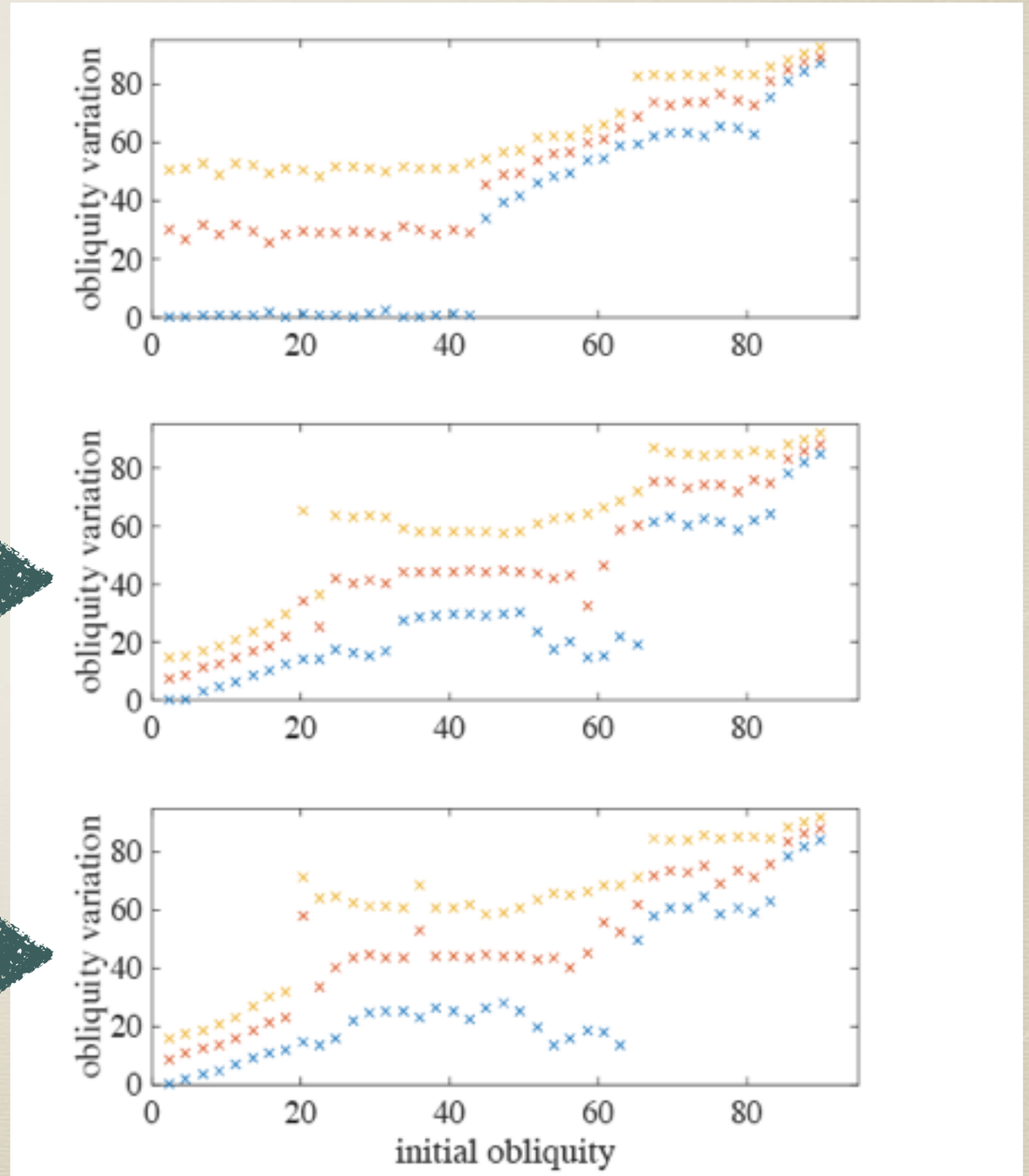

Steffen & Li 2016

Planetary obliquity variations

- Moonless Earth: the secondary resonances are responsible for the obliquity to cross the chaotic bridge (45° ~ 65°). It takes over ~2Gyr to cross the chaotic bridge.

- Extra-solar planets: closely separated planets do not tend to cause significant obliquity variations

Summaries

* Extra solar planetary systems exhibit a large variety of spin-orbit misalignments, including retrograde configurations. Perturbations from a farther object can produce various stellar obliquities and a large fraction of tidal disruption events.

* Tidal re-alignment and other mechanisms together may explain the stellar obliquity features for cool stars.

* Planetary obliquity variations can be caused by the resonance between the planetary spin precession and inclination variations.

Thank you!

Obliquity Of the Sun

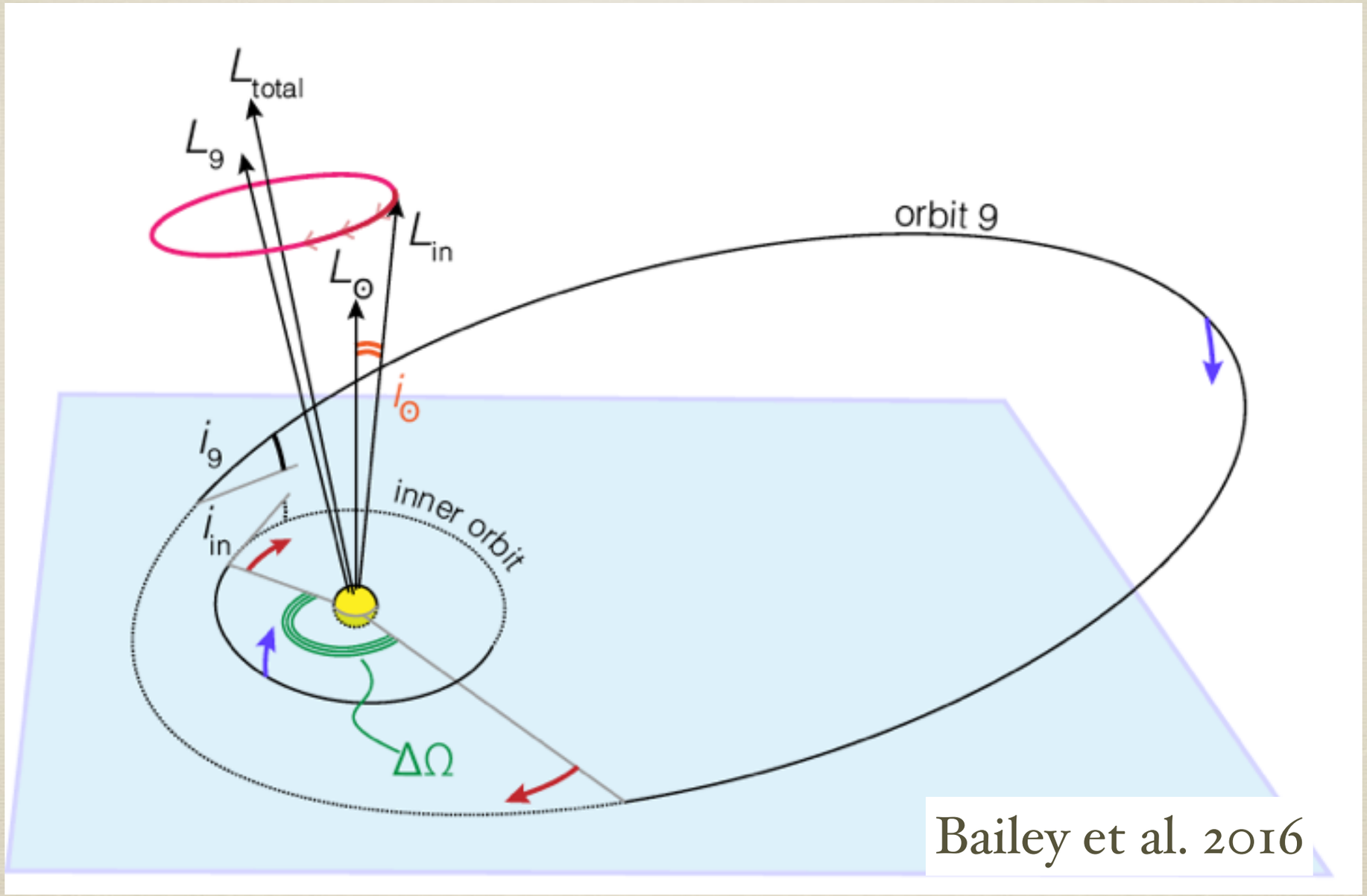

Bailey et al. 2016

Solar Obliquity ~ 6 degrees relative to inner orbits

UNDERLYING RESONANCES

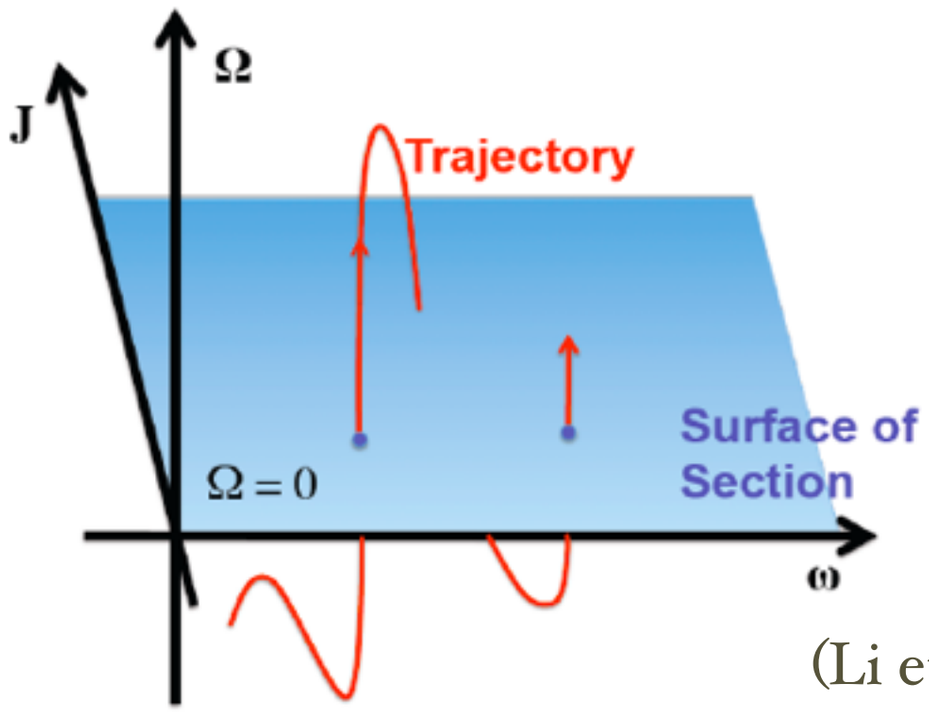

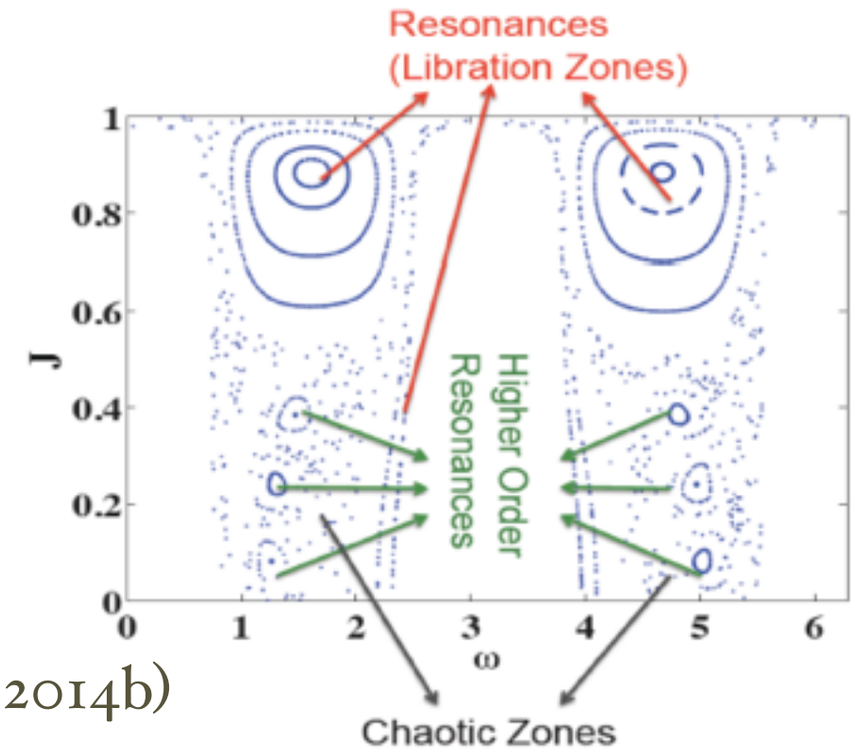

(Li et al. 2014b)

- Resonant zones: points fill 1-D lines.
  trajectories are quasi-periodic.
- Chaotic zones: points fill a higher dimension.

SURFACE OF SECTION

Low i ⟷ High i (40-60°) ⟷ i~90°

Quadrupole order dominates

Octupole order stronger

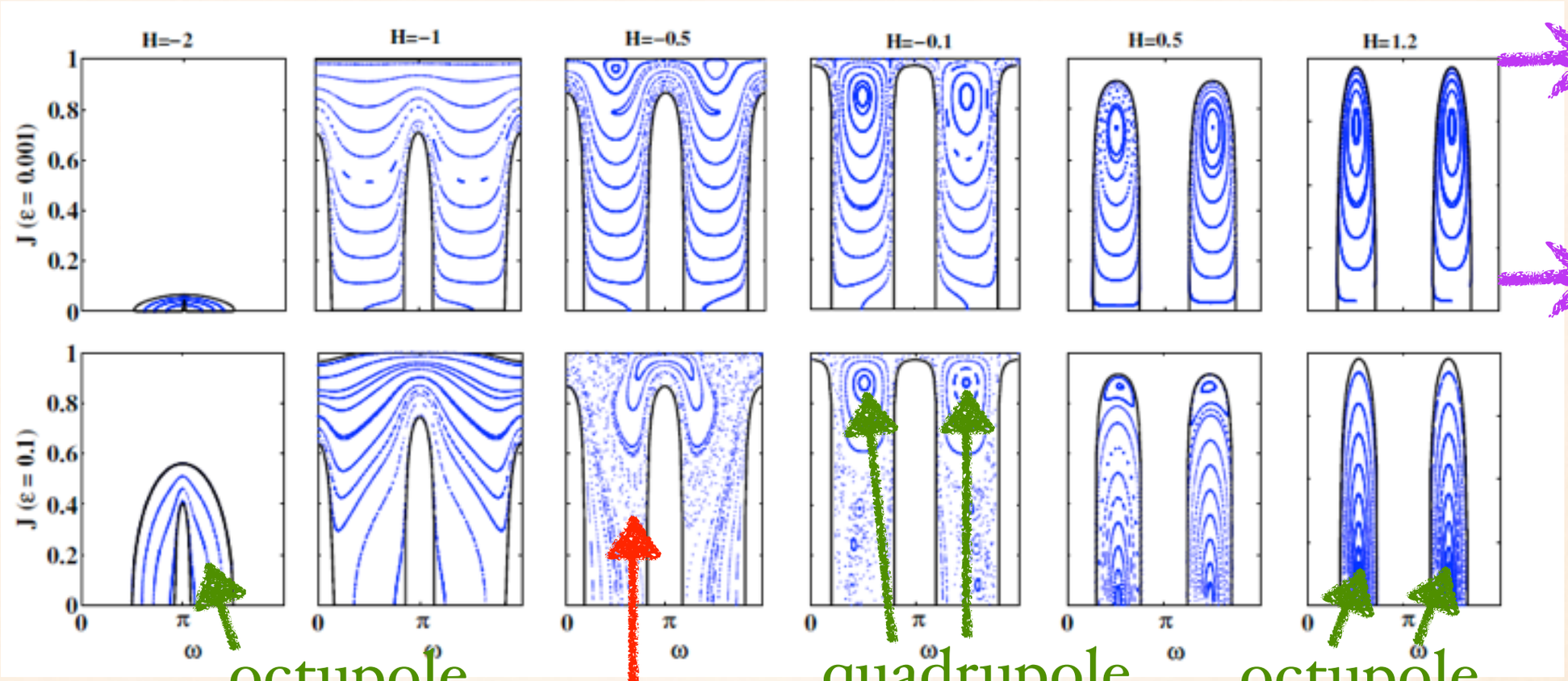

low e

high e

octupole resonances

chaos

quadrupole resonances

octupole resonances

Quadrupole resonances:

centers at low e_1, $\omega=\pi/2$ and $3\pi/2$ (*e.g., Kozai 1962*)

Octupole resonances:

centers at high e_1, $\omega=\pi$ or $\pi/2$ and $3\pi/2$

Li et al. 2014b

ANALYTICAL OVERVIEW

- Hamiltonian has two degrees of freedom in test particle limit:

  $(J = \sqrt{1-e_1^2},\ Jz = \sqrt{1-e_1^2}\cos i_1,\ \omega,\ \Omega\ )$

  2 conjugate pairs: J & ω, Jz & Ω

- The Hamiltonian up to the Octupole order:

$$H = F_{quad}(J, Jz, \omega) + \epsilon F_{oct}(J, Jz, \omega, \Omega)$$

Quadrupole order: Independent of Ω => Jz constant

ϵ : hierarchical parameter: $\epsilon = \frac{a_1}{a_2}\frac{e_2}{1-e_2^2}$

Octupole order: Depend on both Ω & ω => J and Jz not constant

DIFFICULTY IN THE FORMATION OF COUNTER-ORBITING HOT JUPITERS

The analytical flip condition by Li et al. (2014) is also an approximation for the necessary condition for the migration

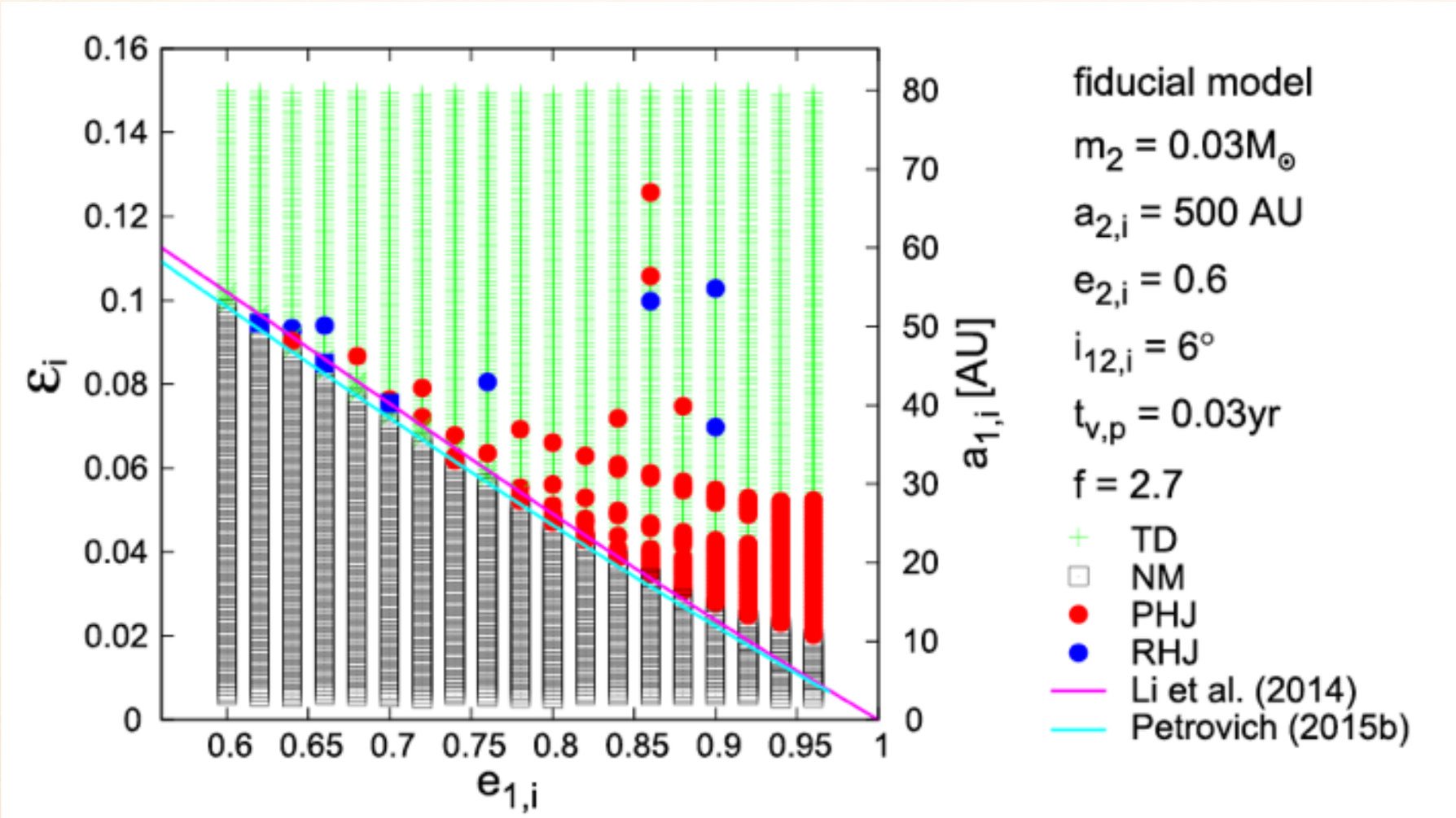

Xue & Suto 2016

FORMATION OF MISALIGNED HOT JUPITERS (KL + TIDE) BY POPULATION SYNTHESIS

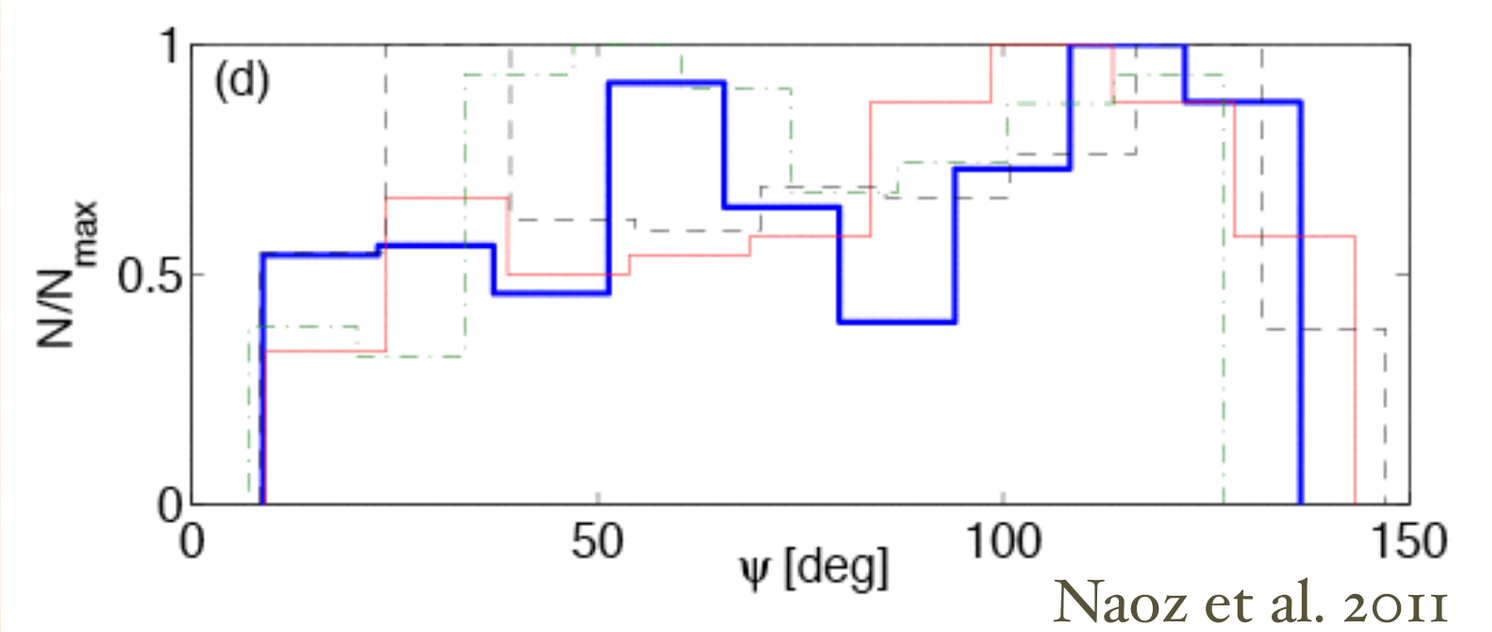

Naoz et al. 2011

- 15% of systems produce hot Jupiters
- EKL may account for about 30% of hot Jupiters

(Naoz et al. 2011)

FORMATION OF MISALIGNED HOT JUPITERS (KL + TIDE) BY POPULATION SYNTHESIS

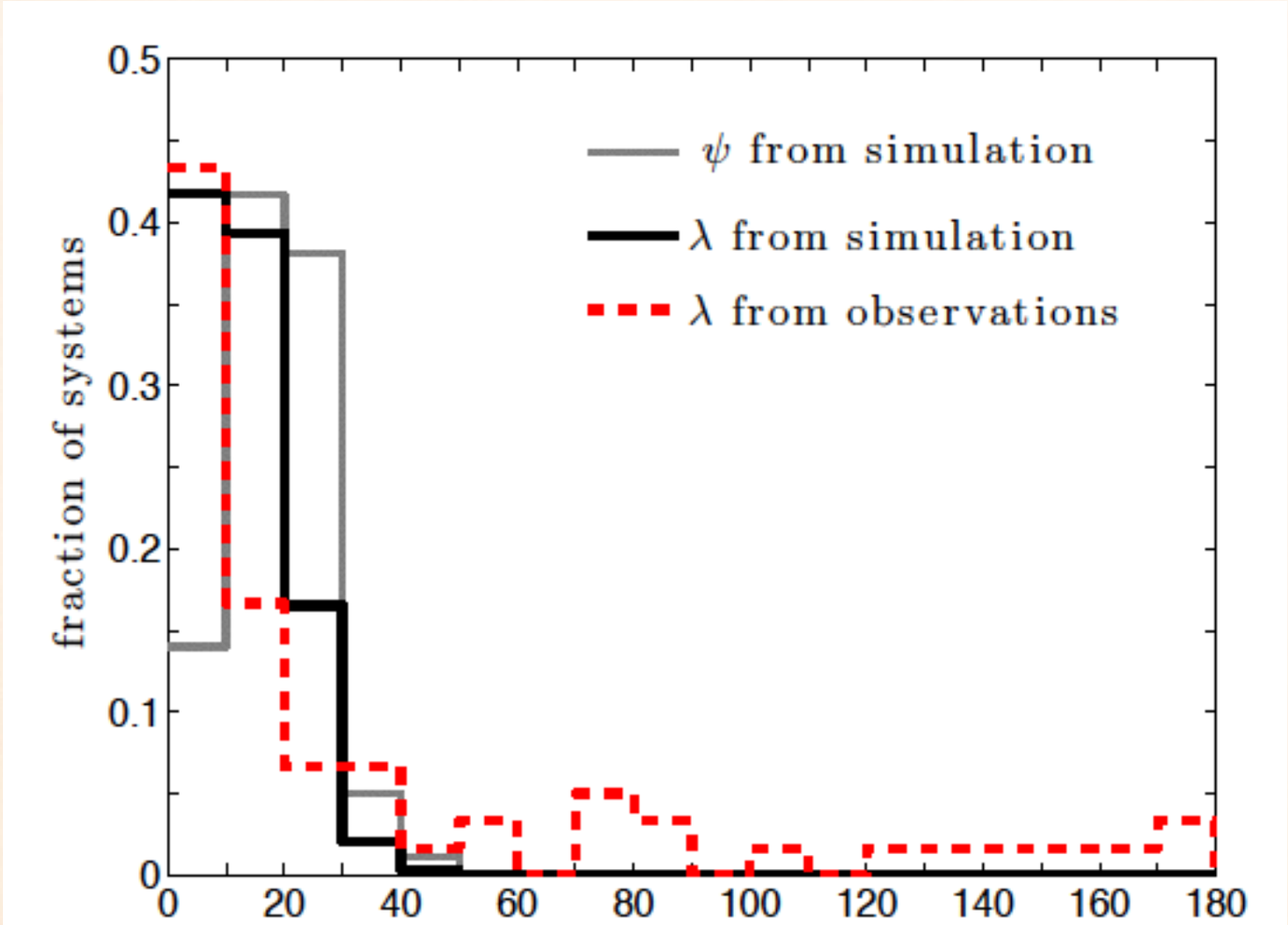

Petrovich 2015

Population synthesis study of interaction of two giant planets.

=> a different mechanism is needed (Petrovich 2015)

FORMATION OF MISALIGNED HOT JUPITERS (KL + STELLAR OBLATENESS + TIDE)

If the host star is spinning and oblate, gravity from the planet makes stellar spin precess around L, and can cause chaos under Kozai-Lidov oscillations (Storch et al. 2014).

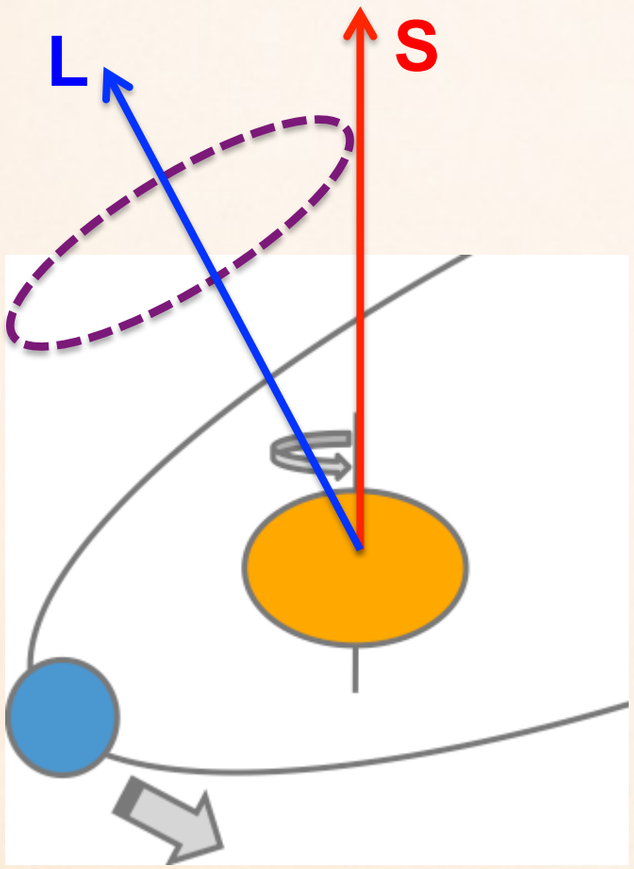

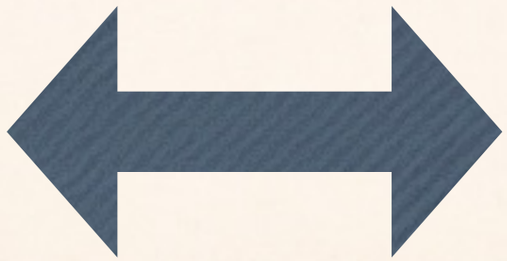

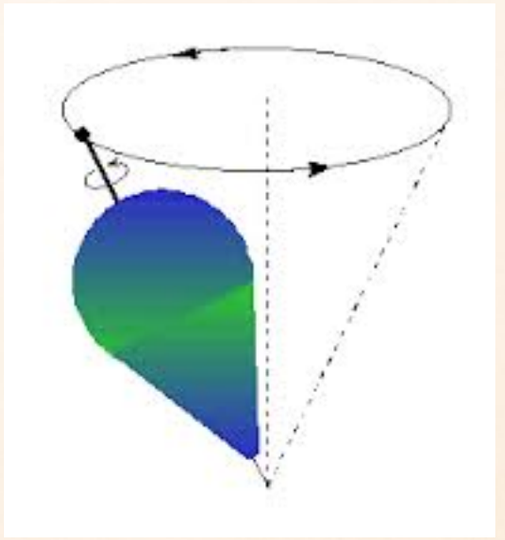

Storch et al. 2014

Chaos: precession period ~ Kozai-Lidov oscillation period

FORMATION OF MISALIGNED HOT JUPITERS (KL + STELLAR OBLATENESS + TIDE)

Anderson et al. 2016:

Mp < 3 M_J

=> bimodal

Mp ~ 5M_J

=> low misalignment (solar-type stars)

=> higher misalignment (more massive stars)

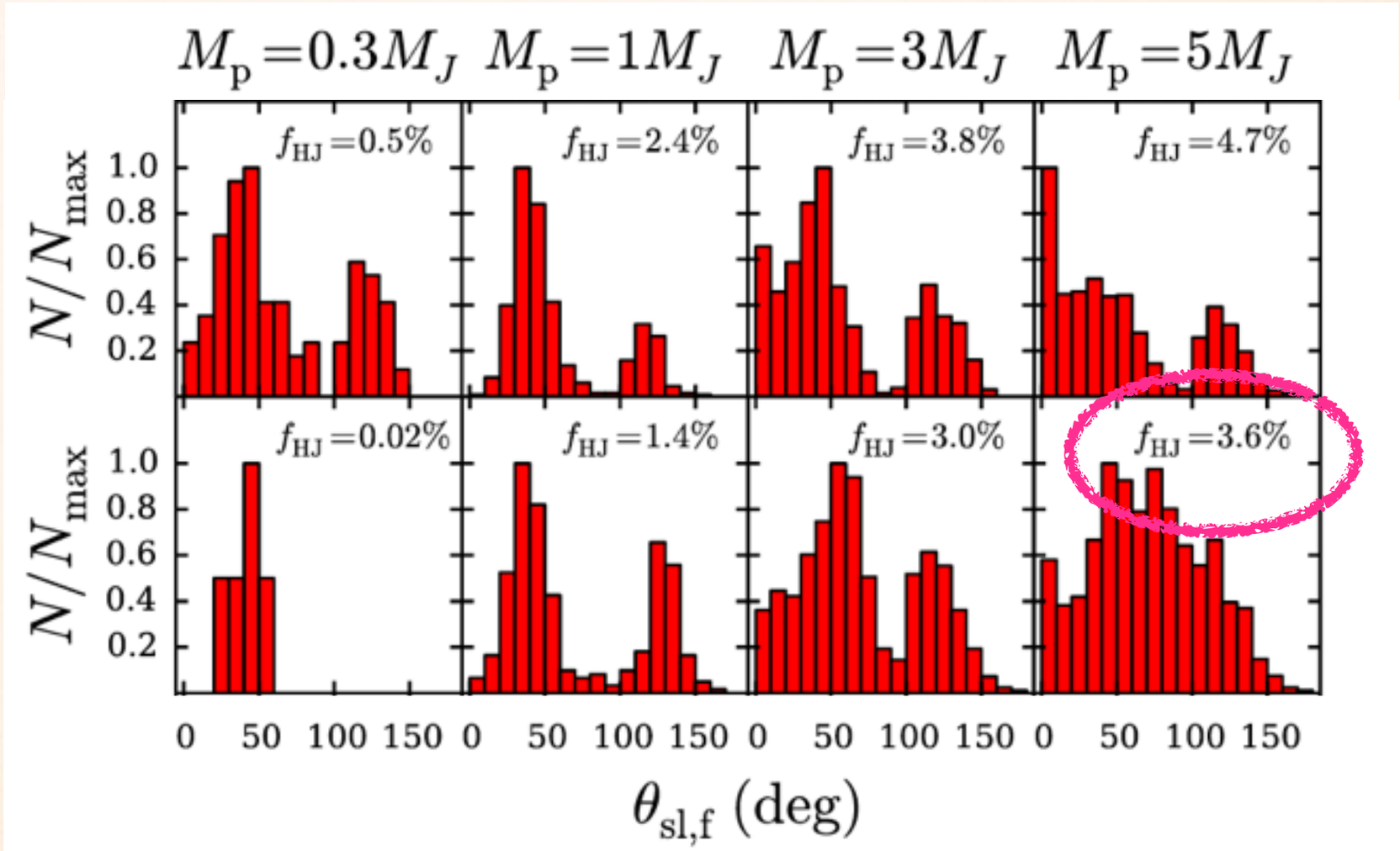

Anderson et al. 2016

Period Dependence of R_{var}?

* Mazeh et al. 2015 find that R_{var} shows no significant difference between P_{orb} =1-5 days & P_{orb} =5-50 days

* R_{var} doesn't depend on planetary orbital period.

→ Inconsistent with alignment involving tidal effects.

Period Dependence — Selection Effect ?

* Selection effect: low R_{var} may be required to observe long P_{orb} planets

* Compare long period R_{var} with simulated long period $R_{var,s}$, which is only affected by selection effect

(method introduced by Mazeh et al. 2015)

* *P:* long period KOIs; *R*: short period KOIs.

R_i: Simulated long period sample:

We associate with each planet from *P* with a randomly-selected star from *R* that has S/N >10, and include the chosen stellar R_{var} in R_i.

$$S/N \propto \frac{1}{\bar{\sigma}_{\mathrm{CDPP}} R_\star^{3/2}}$$

Li & Winn, 2015

Period Dependence — Selection Effect ?

* Selection effect: low R_{var} may be required to observe long P_{orb} planets

* Simulate long period R_{var} requiring s/n > 10.

* It's unlikely that the low value of long period R_{var} is due to purely selection effects.

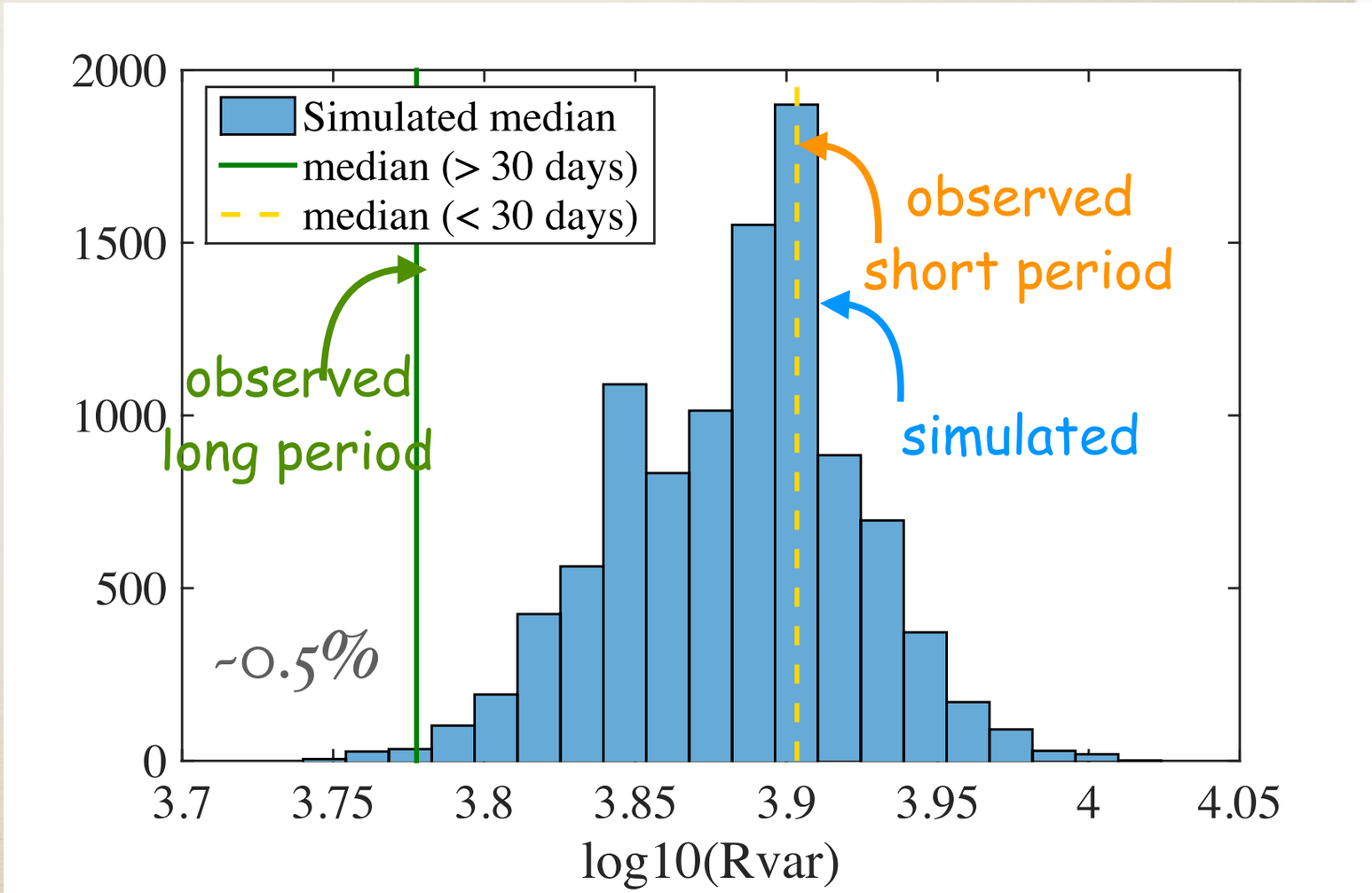

Li & Winn, 2015

Reexamine Period Dependence

* No significant difference b.t. long period (≳20 days) KOIs & non-KOIs
* Significant difference b.t. long period (≳30 days) & short period (≲2 days) KOIs

* R_{var} ↑ when P_{orb} ↓

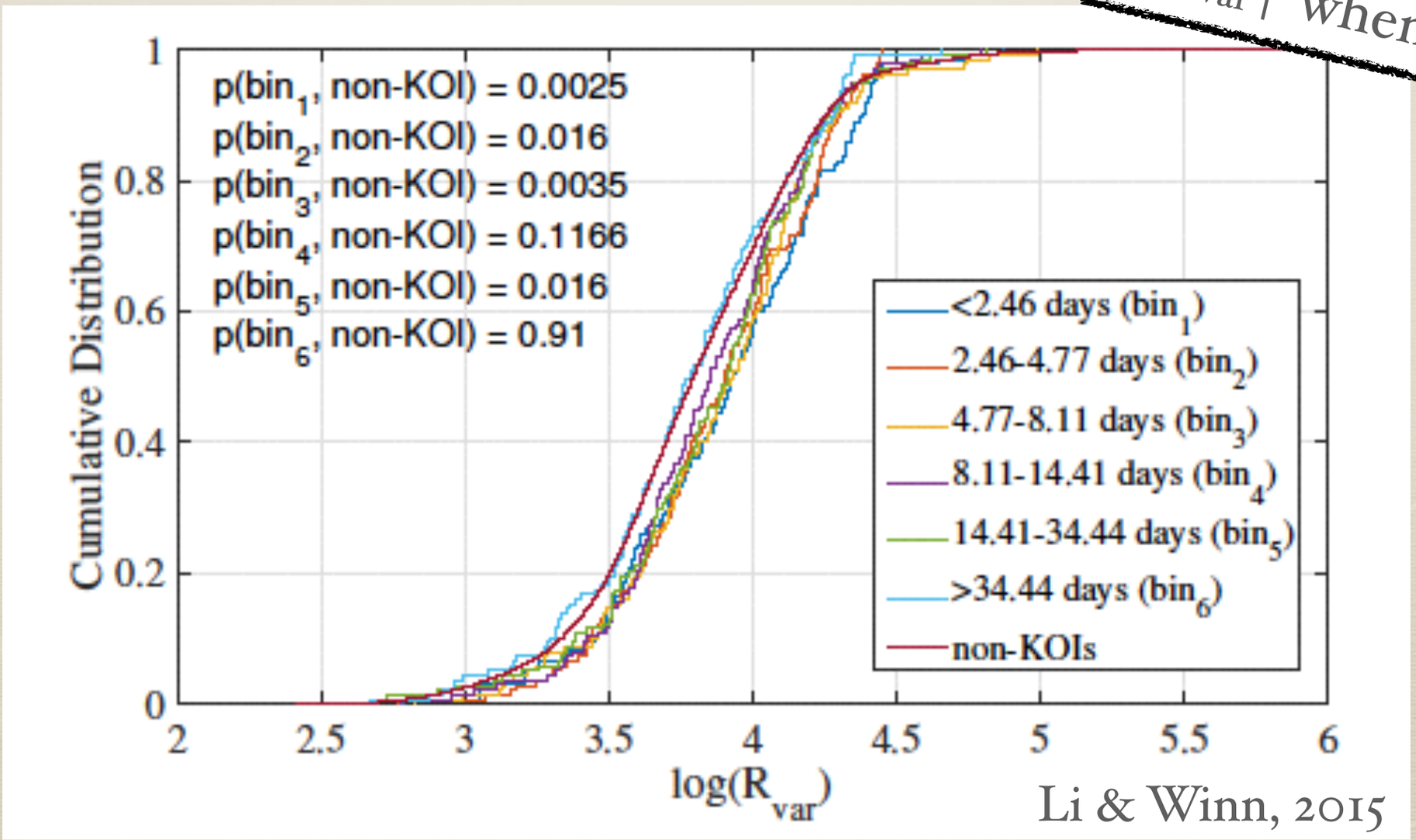

Li & Winn, 2015

Resonances and Chaotic Regions

- The Hamiltonian H_{res} takes form of a pendulum.
  - Two dynamical regions: libration region and circulation region.

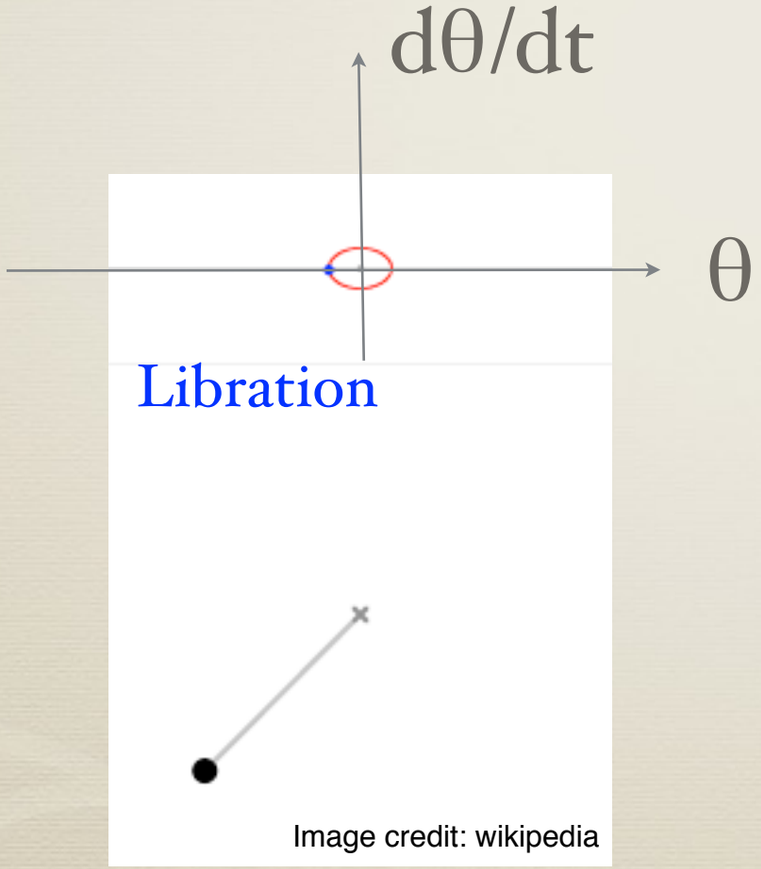

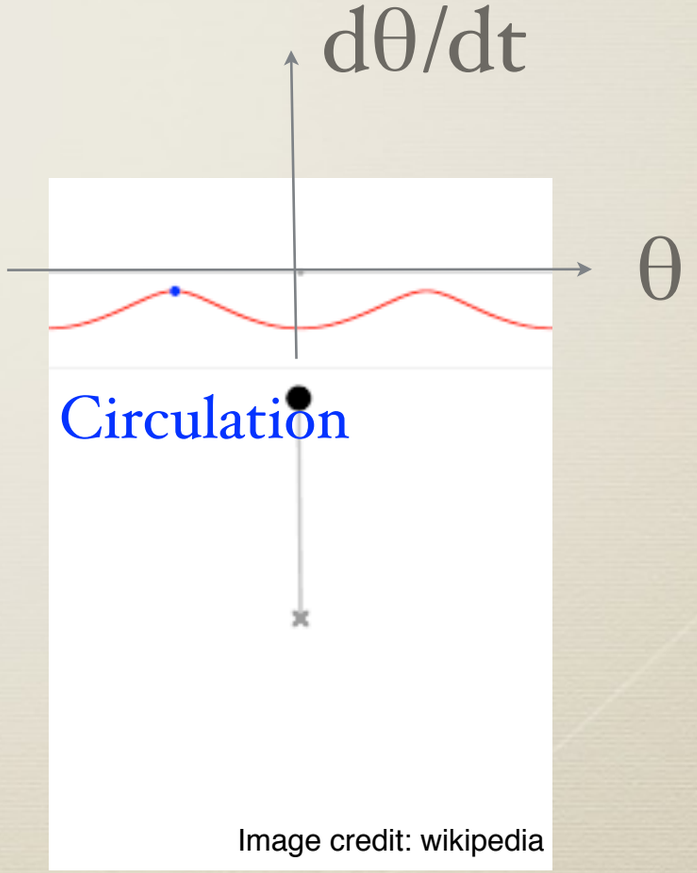

Resonances and Chaotic Regions

- The Hamiltonian H_{res} takes form of a pendulum.
- Two dynamical regions: libration region and circulation region, separated by separatrix.

Phase Diagram:

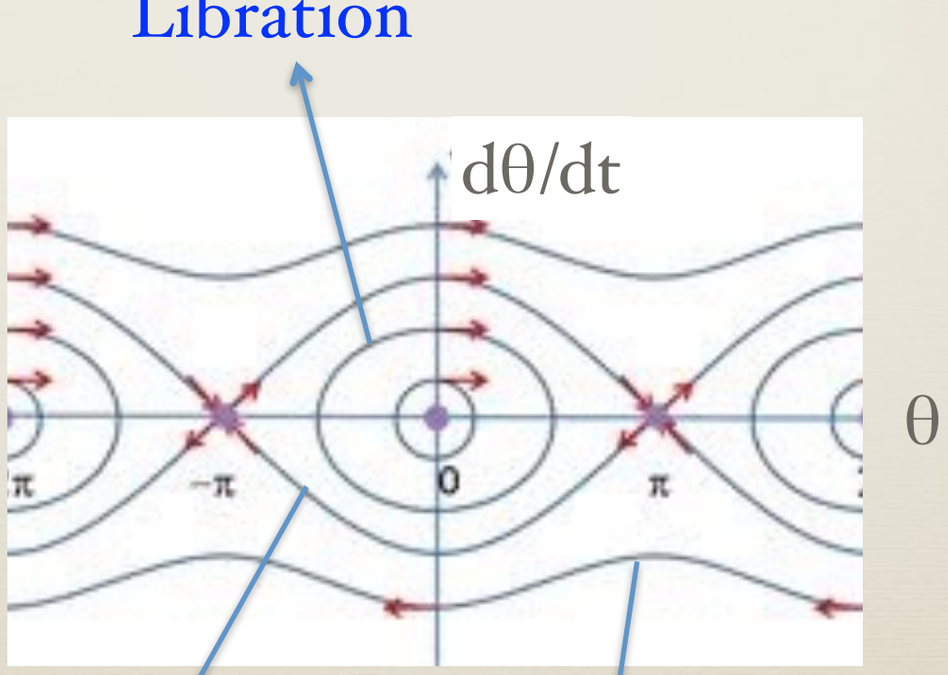

Resonances and Chaotic Regions

- The Hamiltonian H_{res} takes form of a pendulum.
- Two dynamical regions: libration region and circulation region, separated by separatrix.

Libration

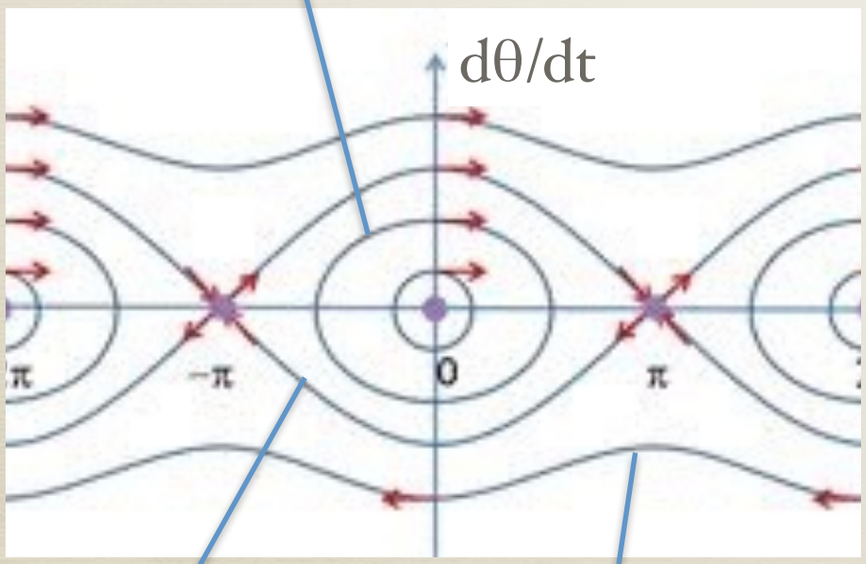

Separatrix

Circulation

Overlap of resonances can cause chaos

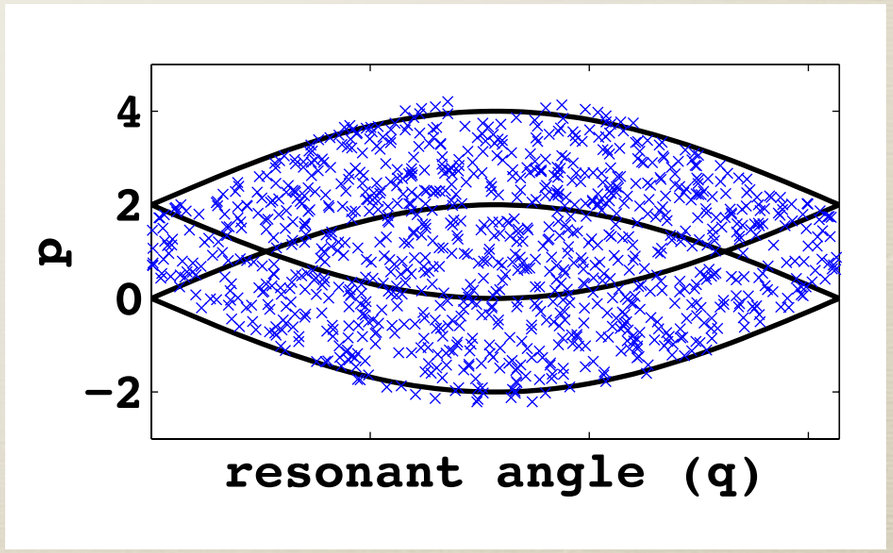

Diffusion by Overlap of Resonances

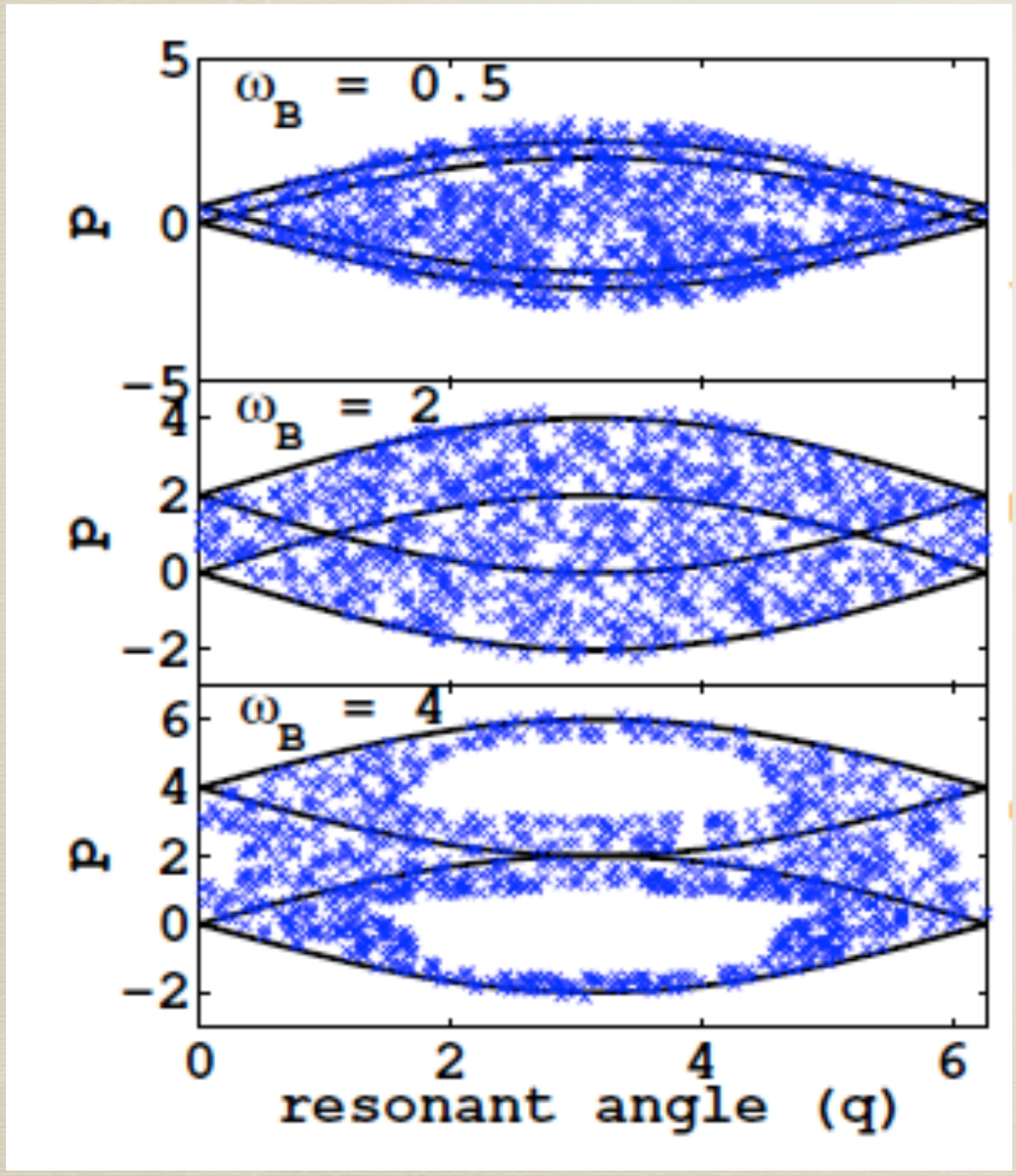

- Overlap of resonances cause chaos.
- Large separation

  Diffusion Coefficient ↓
  Diffusion time ↑,

  Lyapunov Exponent ↓
  Chaos ↓.

Chirikov 1979

Diffusion by Overlap of Resonances

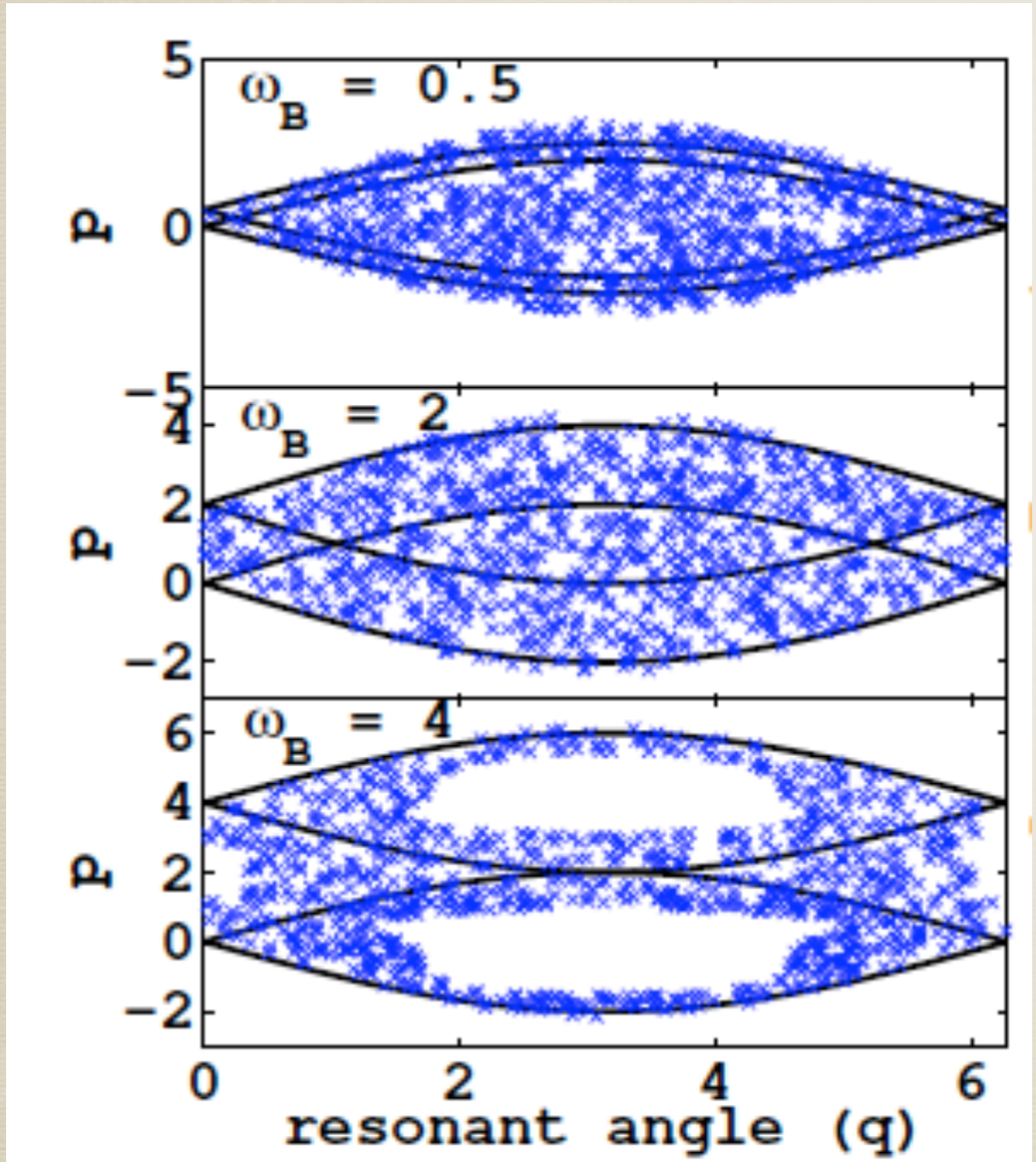

Lyapunov Exponent:

$$\lambda \sim \frac{1}{K}\frac{\omega_L}{2\pi} \sim \begin{cases} \nu_B \\ 2\nu_L \end{cases}$$

Closely overlapped

Marginally overlapped

$$K = 2\frac{\omega_L}{\omega_B}$$

Difusion coefficient:

$$D \sim \Delta^2\lambda \sim \begin{cases} \Delta^2\nu_B \\ \Delta^2\nu_L \end{cases}$$

Closely overlapped

Marginally overlapped

Chirikov 1979

Chaotic Features

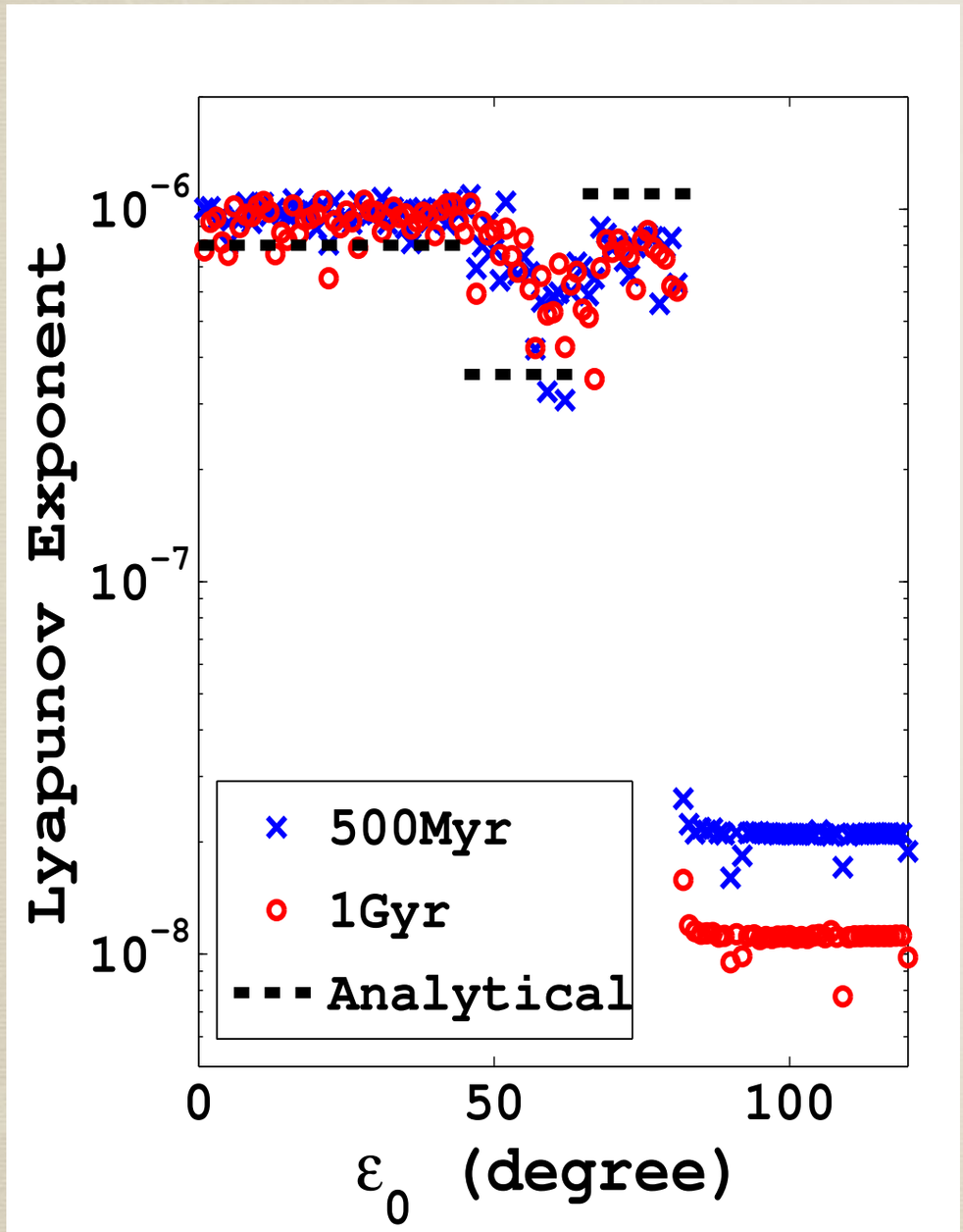

- Lyapunov exponent (λ):

  λ↑, more chaotic.

- C1,C2: λ∼ 10-6

  Bridge: λ∼5×10-7

  ≥85° Regular

- Analytical results consistent with numerical results.

Li & Batygin, 2014a

Application to Exoplanetary Systems

* Relative fraction of successful panspermia transfer

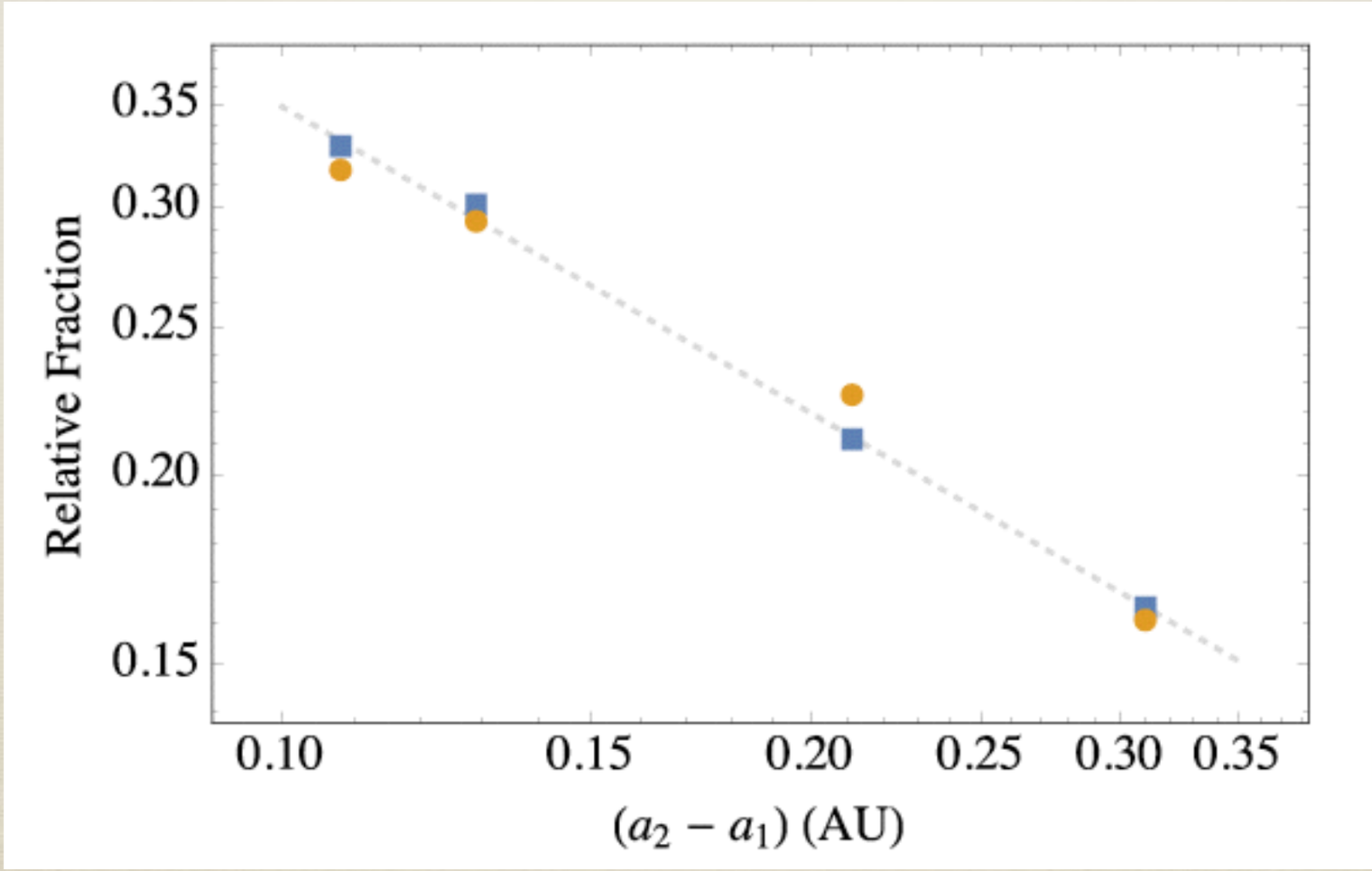

Steffen & Li 2016

Application to Exoplanetary Systems

* Inclination variation modes in first order resonant v.s. non-resonant systems

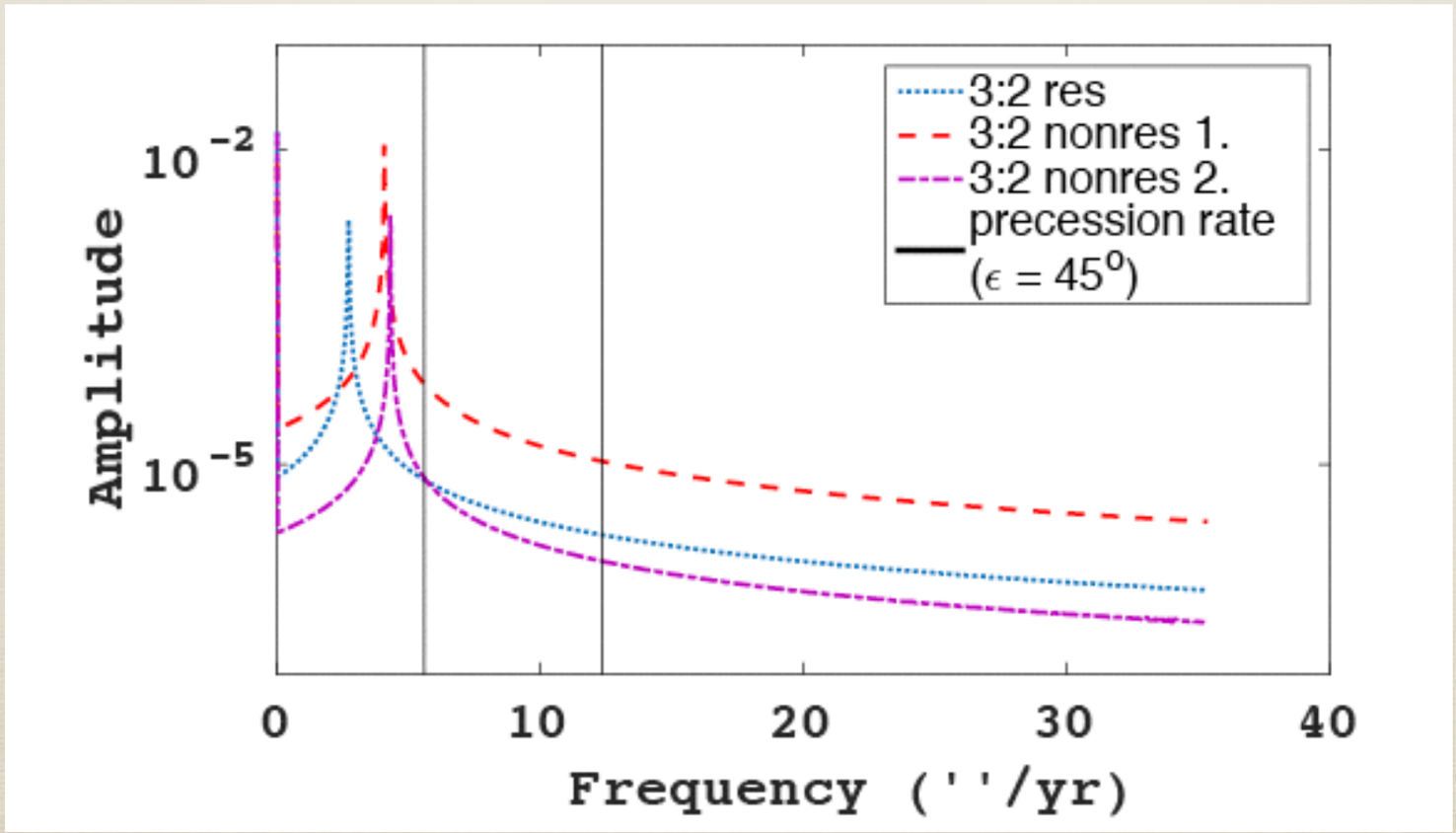

Steffen & Li 2016

Application to Exoplanetary Systems

* Obliquity variation in 3:2 resonant systems

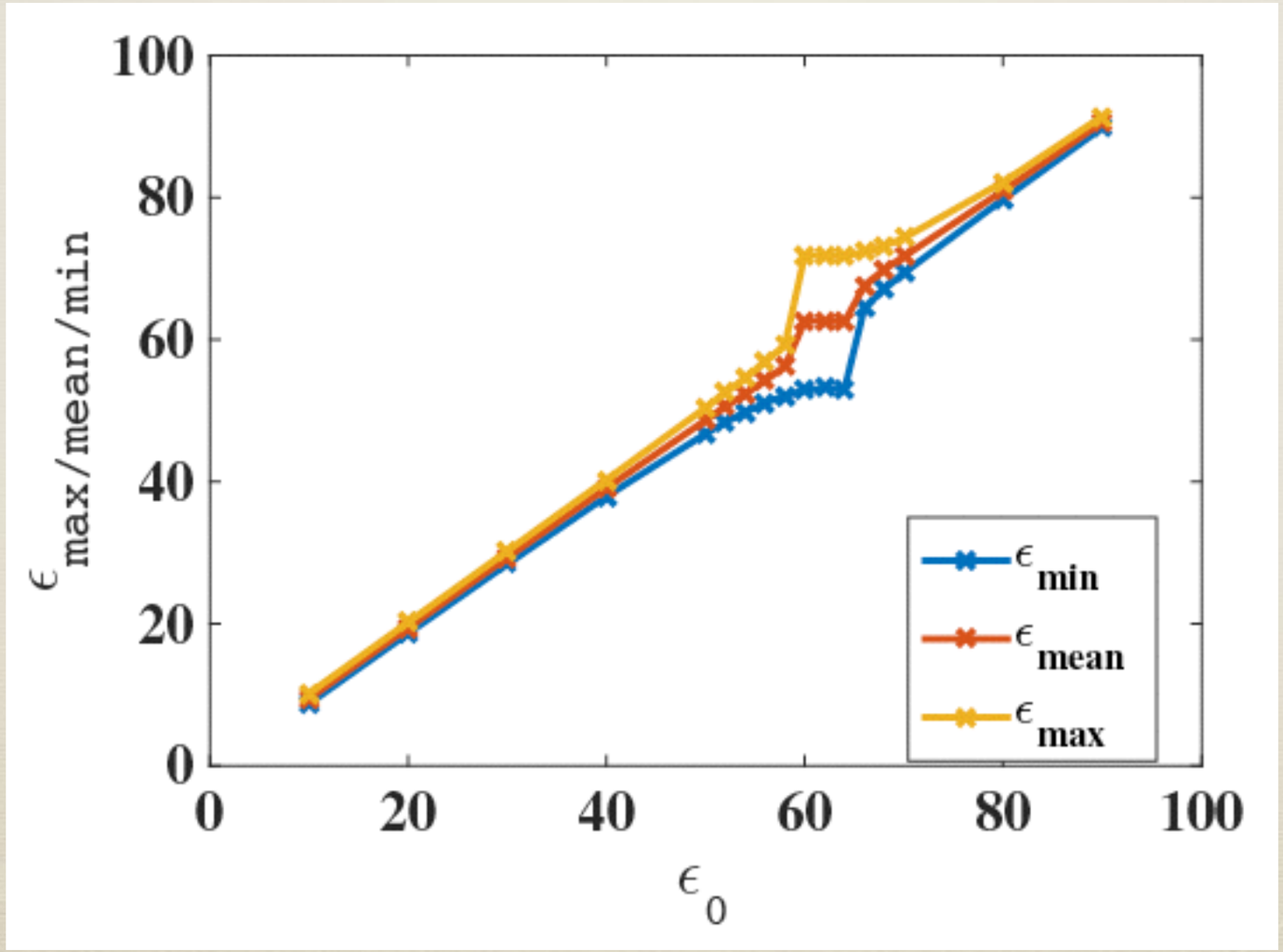

Steffen & Li 2016

How Primordial is Earth's Obliquity?

Pre-late Heavy Bombardment Evolution of the Earth's Obliquity

Nice Model:

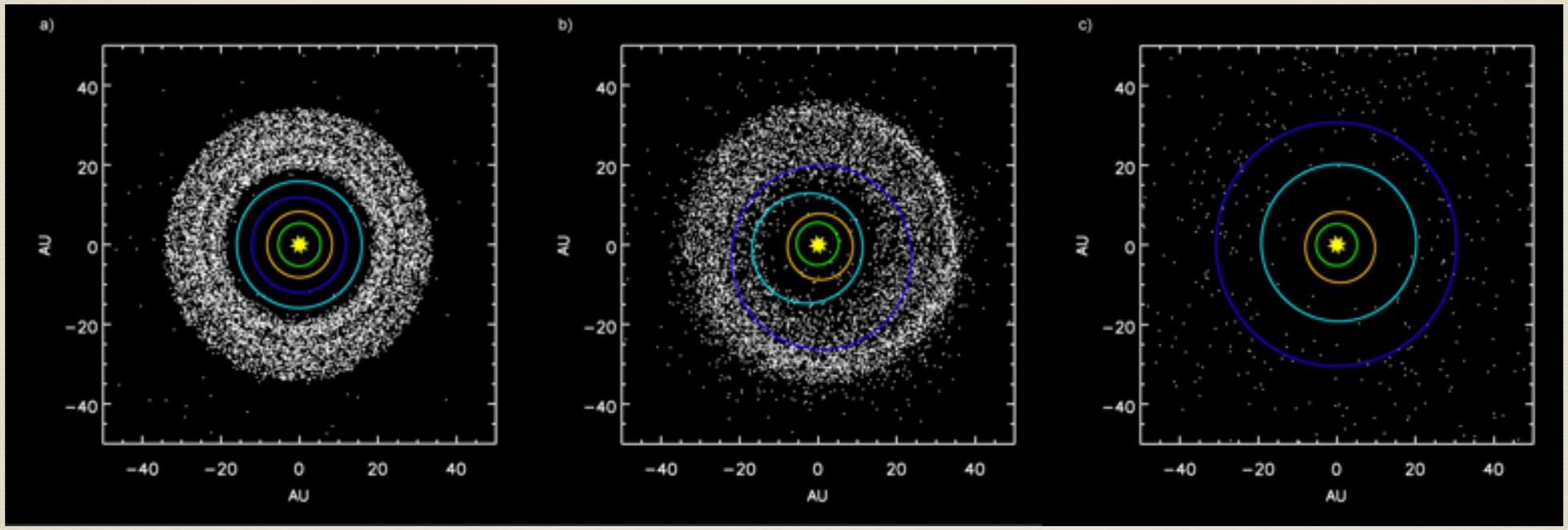

- Formation of the Kuiper belt

(Levison et al. 2008; Batygin et al. 2011),

- Chaotic capture of Jupiter and Neptune trojan populations

(Morbidelli et al. 2005; Nesvorny et al. 2007)

- Triggering LHB

(Gomes et al. 2005).

Pre-late Heavy Bombardment Evolution of the Earth's Obliquity

Nice Model:

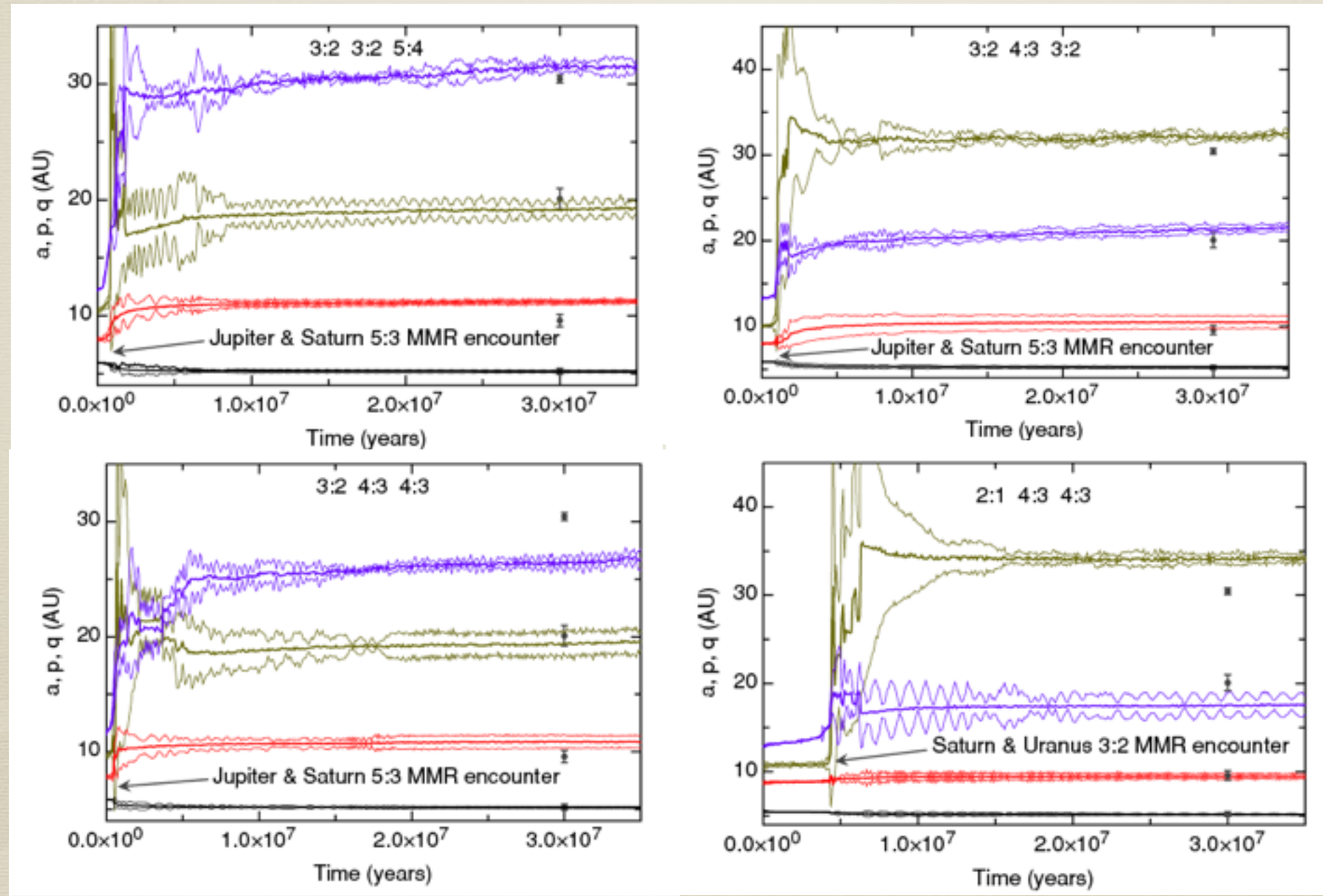

Batygin & Brown 2010

Pre-late Heavy Bombardment Evolution of the Earth's Obliquity

- Solar system starts more compact

  (Nice model).

=>

  Changes in mode frequencies.

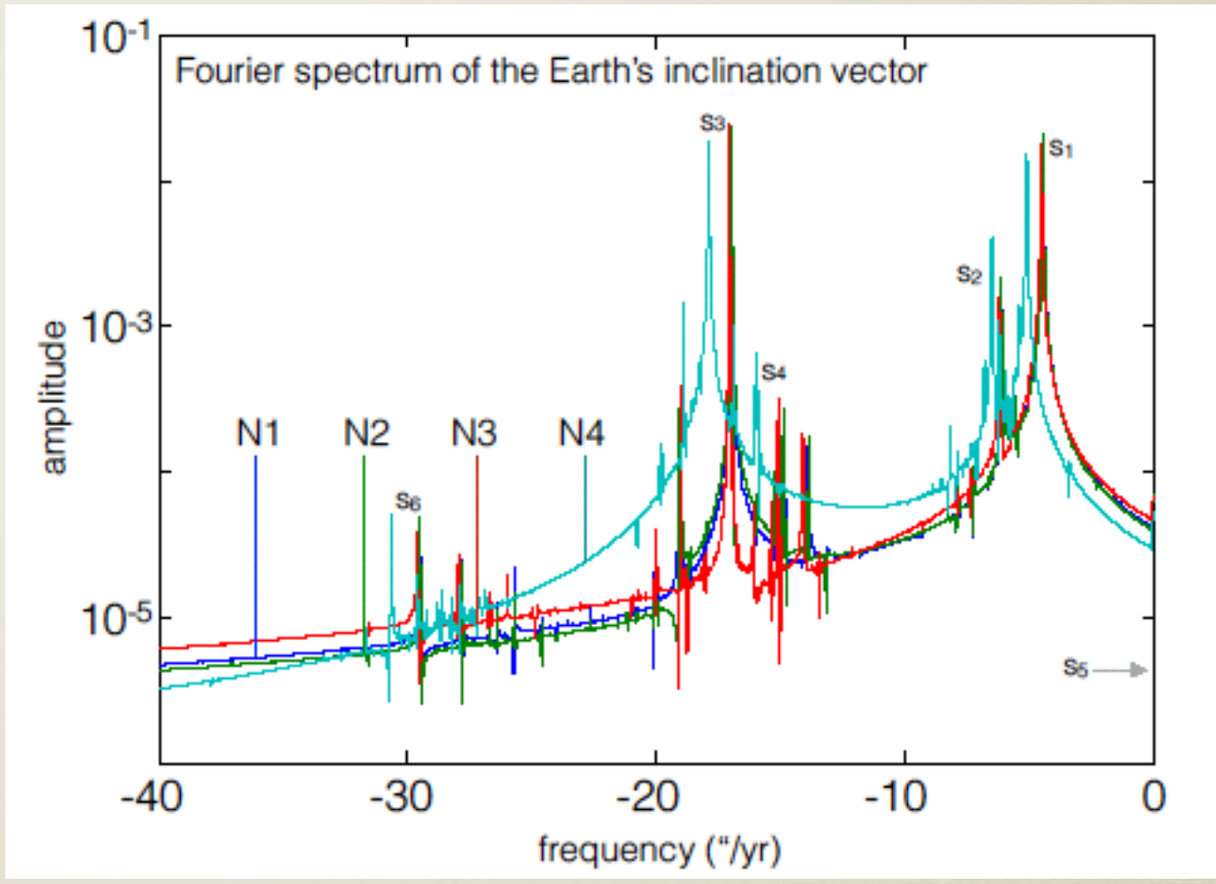

Li & Batygin, 2014b

Pre-late Heavy Bombardment Evolution of the Earth's Obliquity

- Frequencies can slightly shift

  e.g., s_3 ~ 18 arcsec/yr

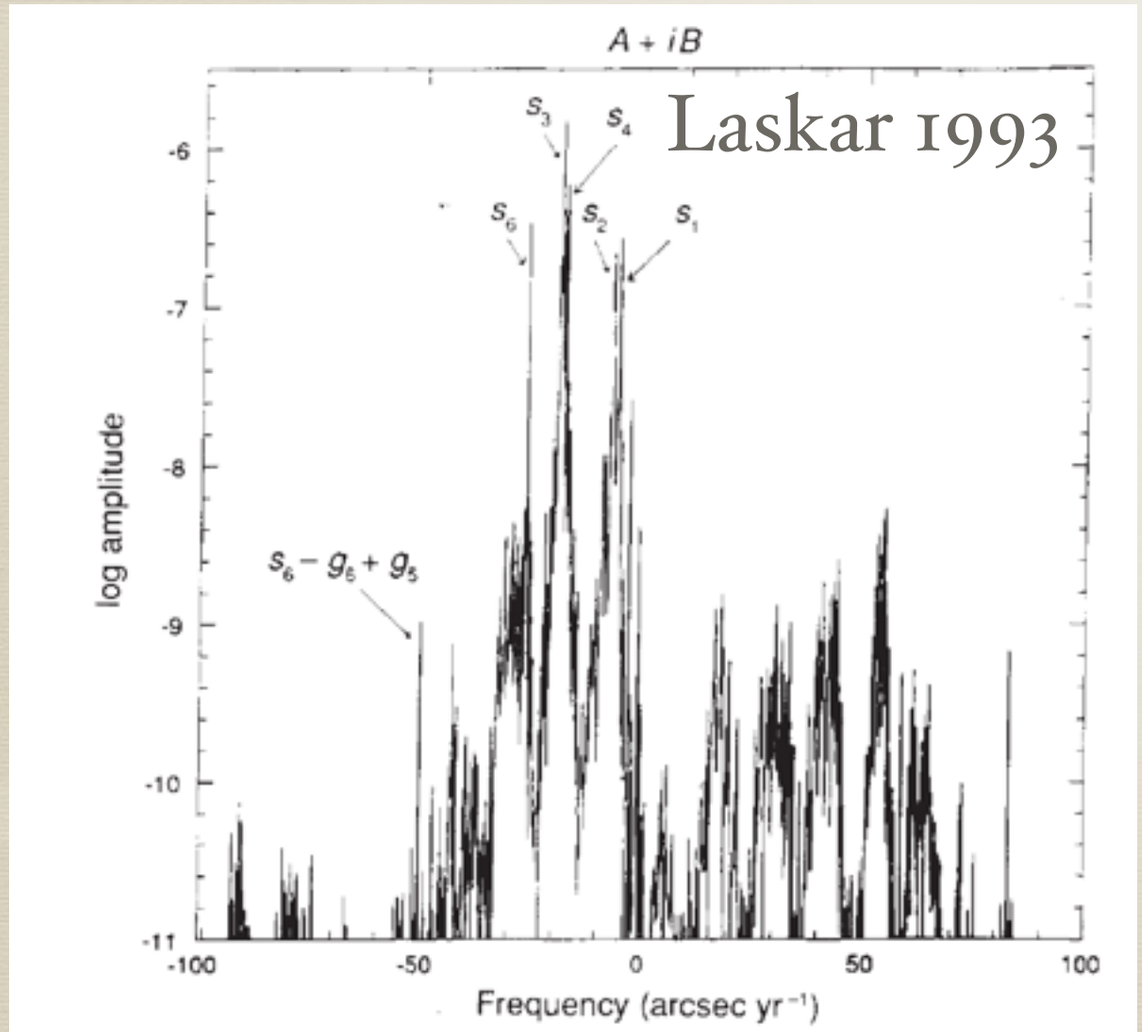

Laskar 1993

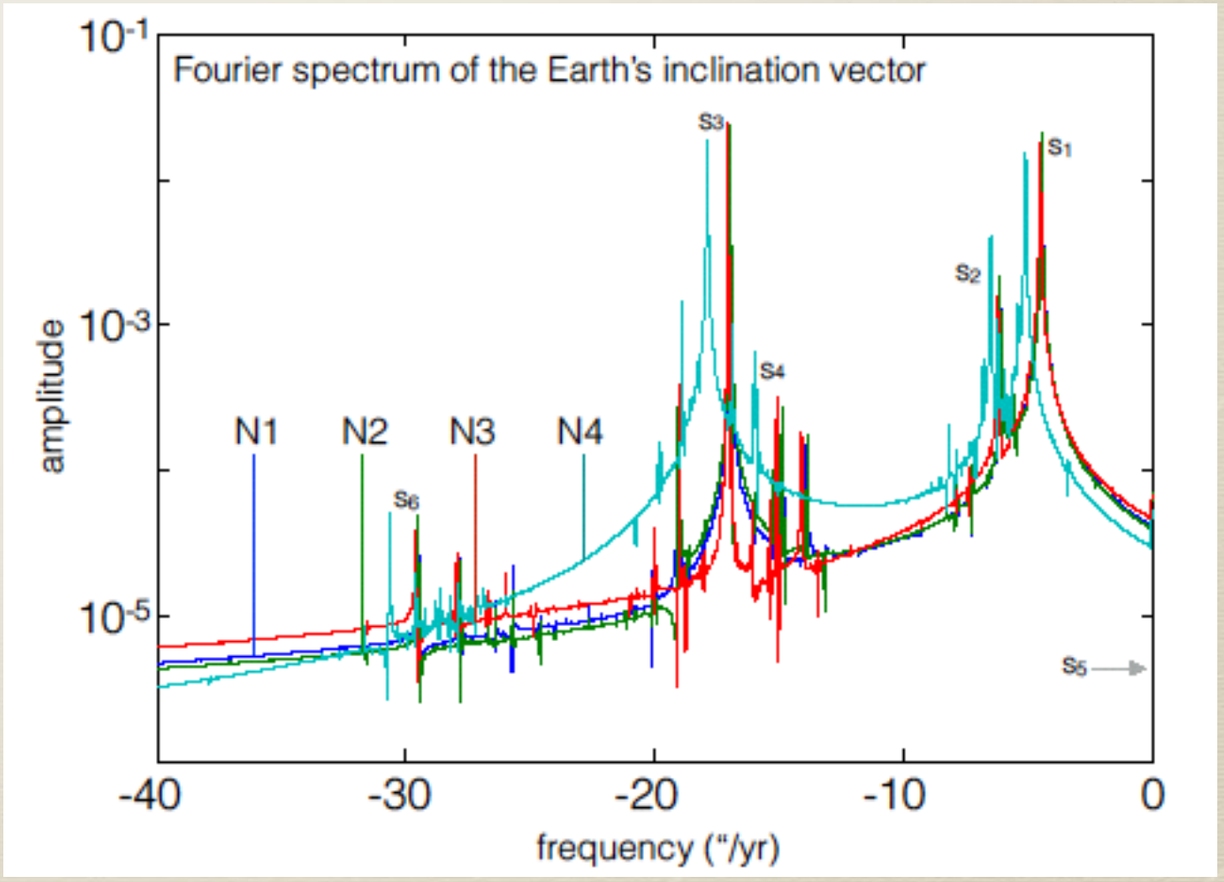

Li & Batygin, 2014b

Pre-late Heavy Bombardment Evolution of the Earth's Obliquity

- Moon was closer

=> Change in precession frequency

- Two frequencies do not match prior to LHB except at high obliquity (~85°)

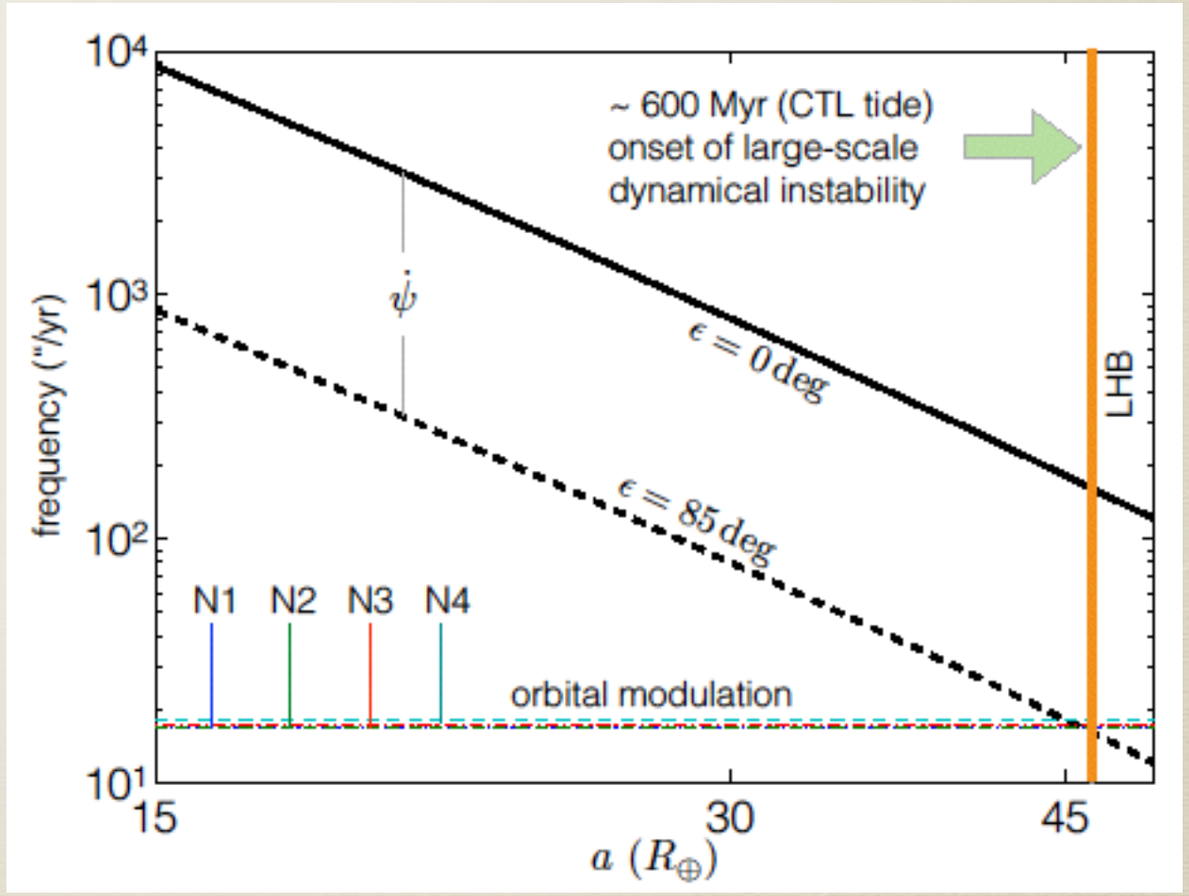

Li & Batygin, 2014b

Pre-late Heavy Bombardment Evolution of the Earth's Obliquity

Direct Integration

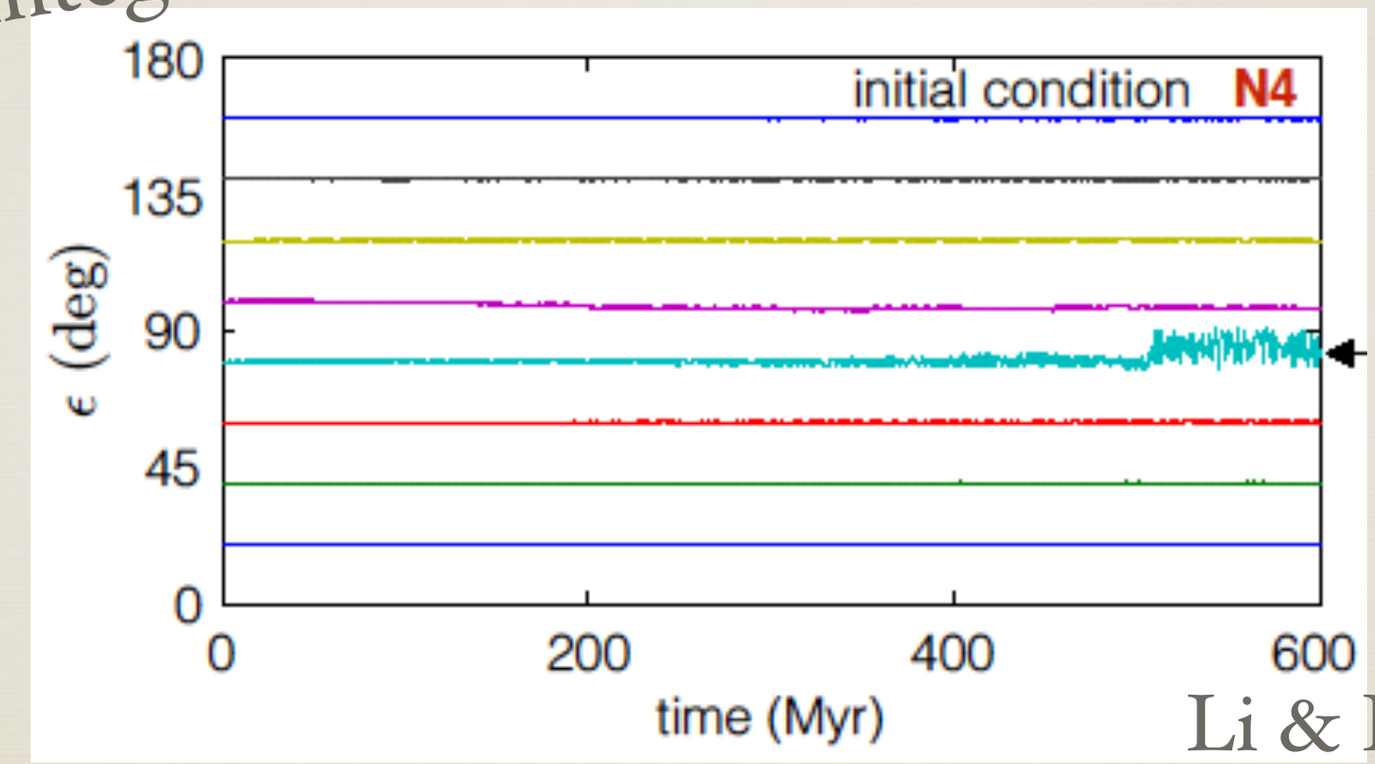

Li & Batygin, 2014b

- Obliquity varies only in the high obliquity regime prior to LHB.
- Earth obtained its obliquity during the formation of the Moon.

Application to Exoplanetary Systems

* Inclination variation modes in first order resonant v.s. non-resonant systems

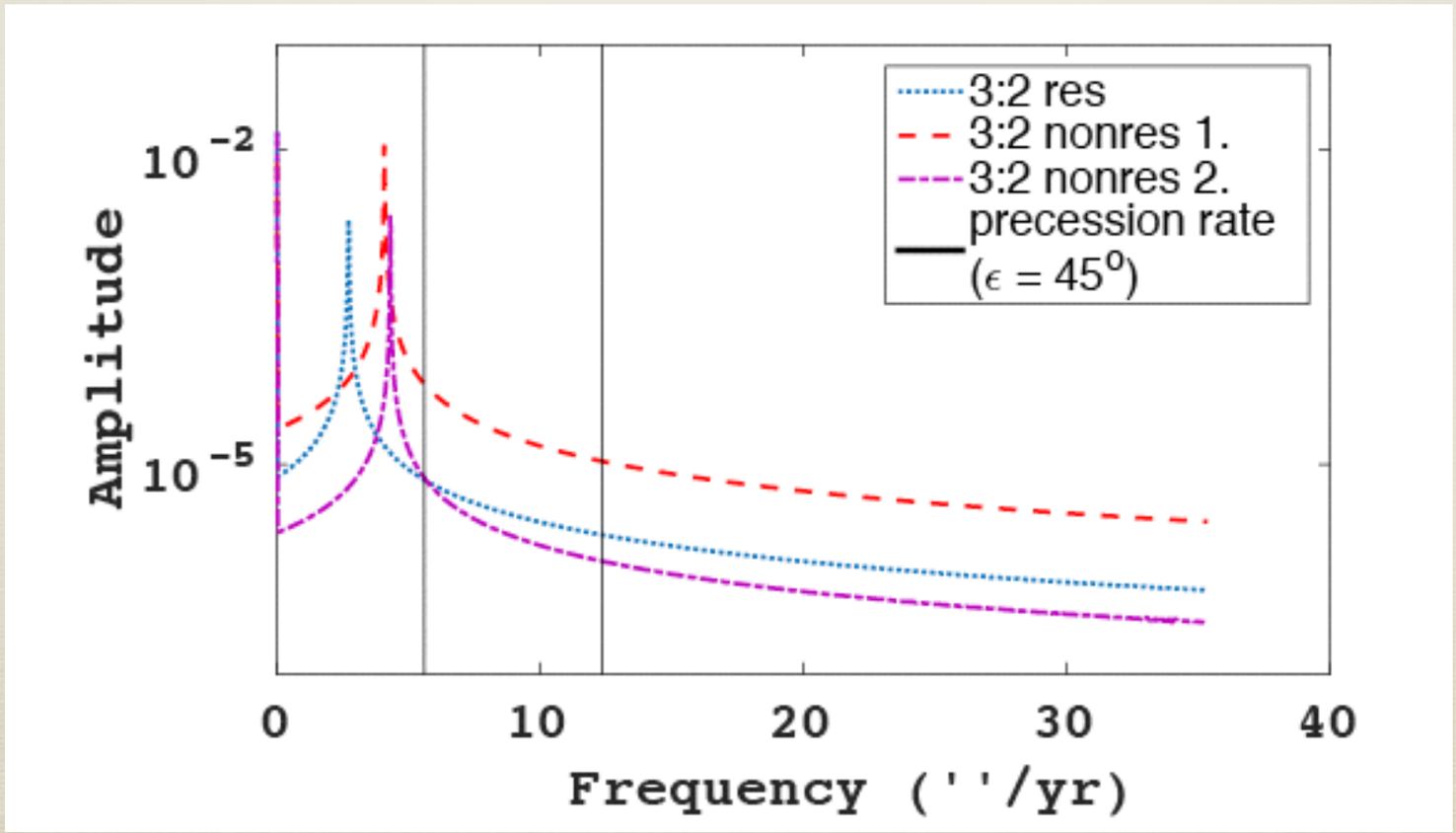

Steffen & Li 2016

Application to Exoplanetary Systems

* Obliquity variation in 3:2 resonant systems

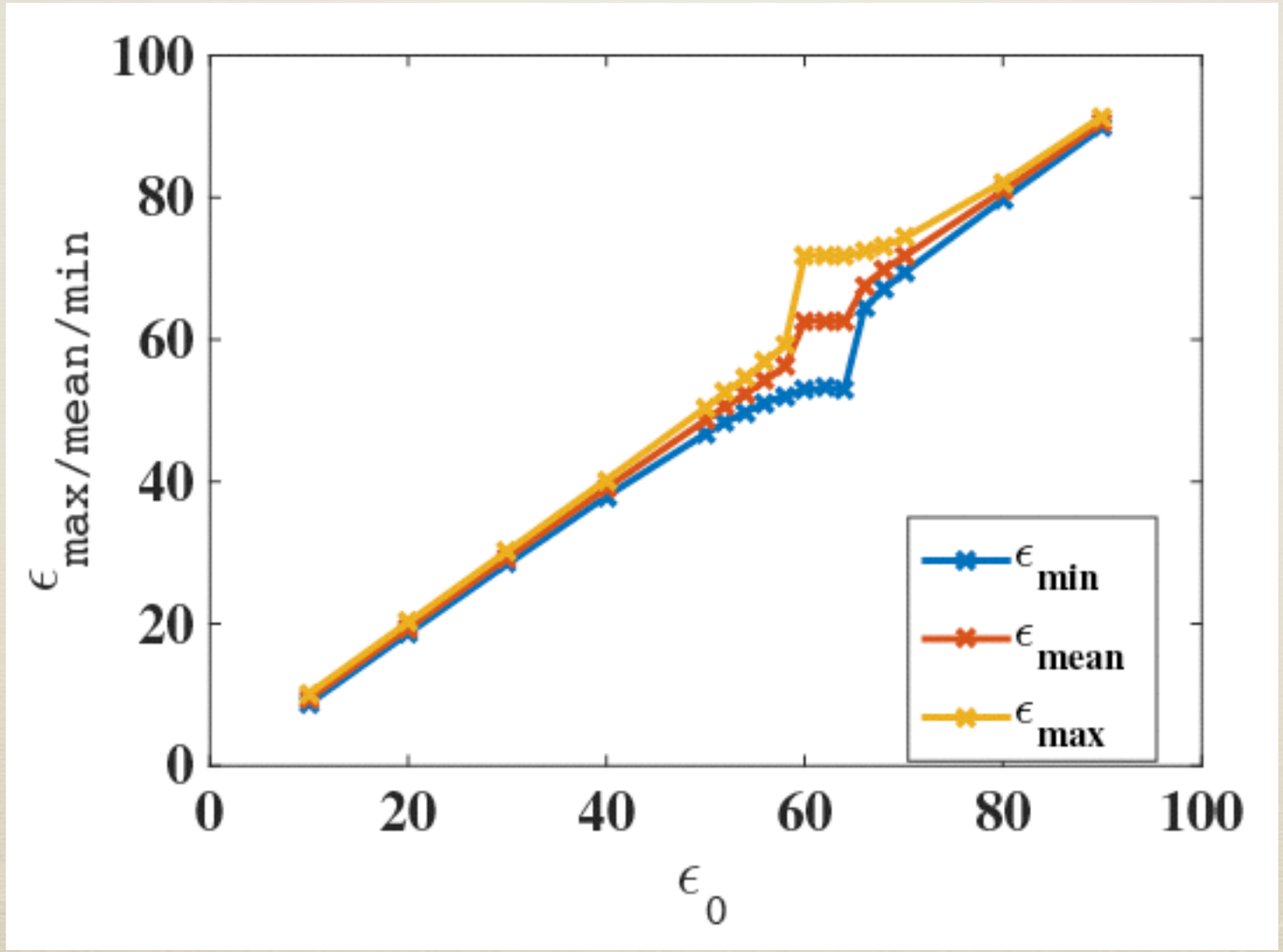

Steffen & Li 2016